Star-forming galaxies at cosmic noon

Förster Schreiber & Wuyts 2020, ARA&A, 58, 661

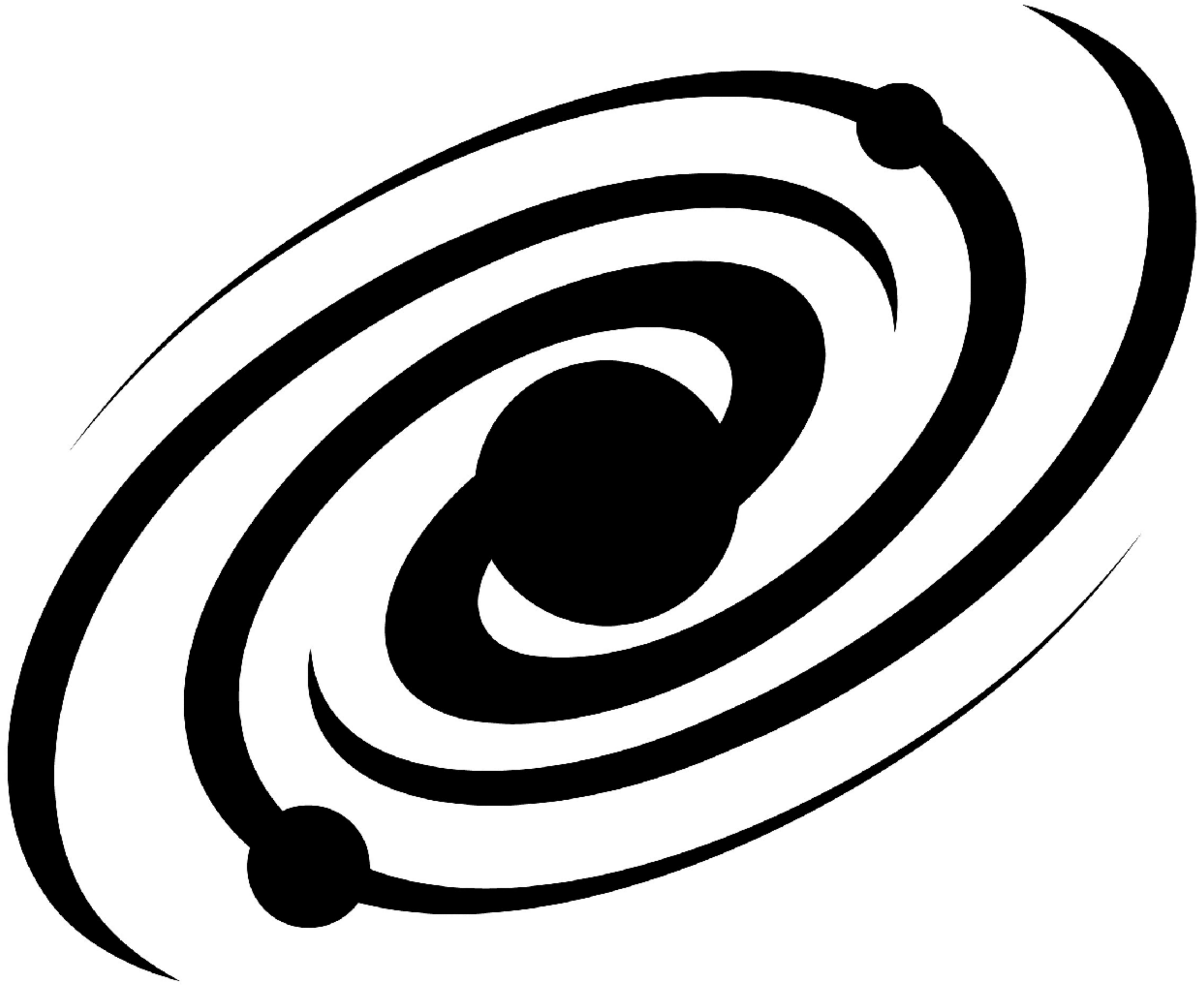

Stijn Wuyts

UNIVERSITY OF BATH

Star-forming galaxies at cosmic noon

Förster Schreiber & Wuyts 2020, ARA&A, 58, 661

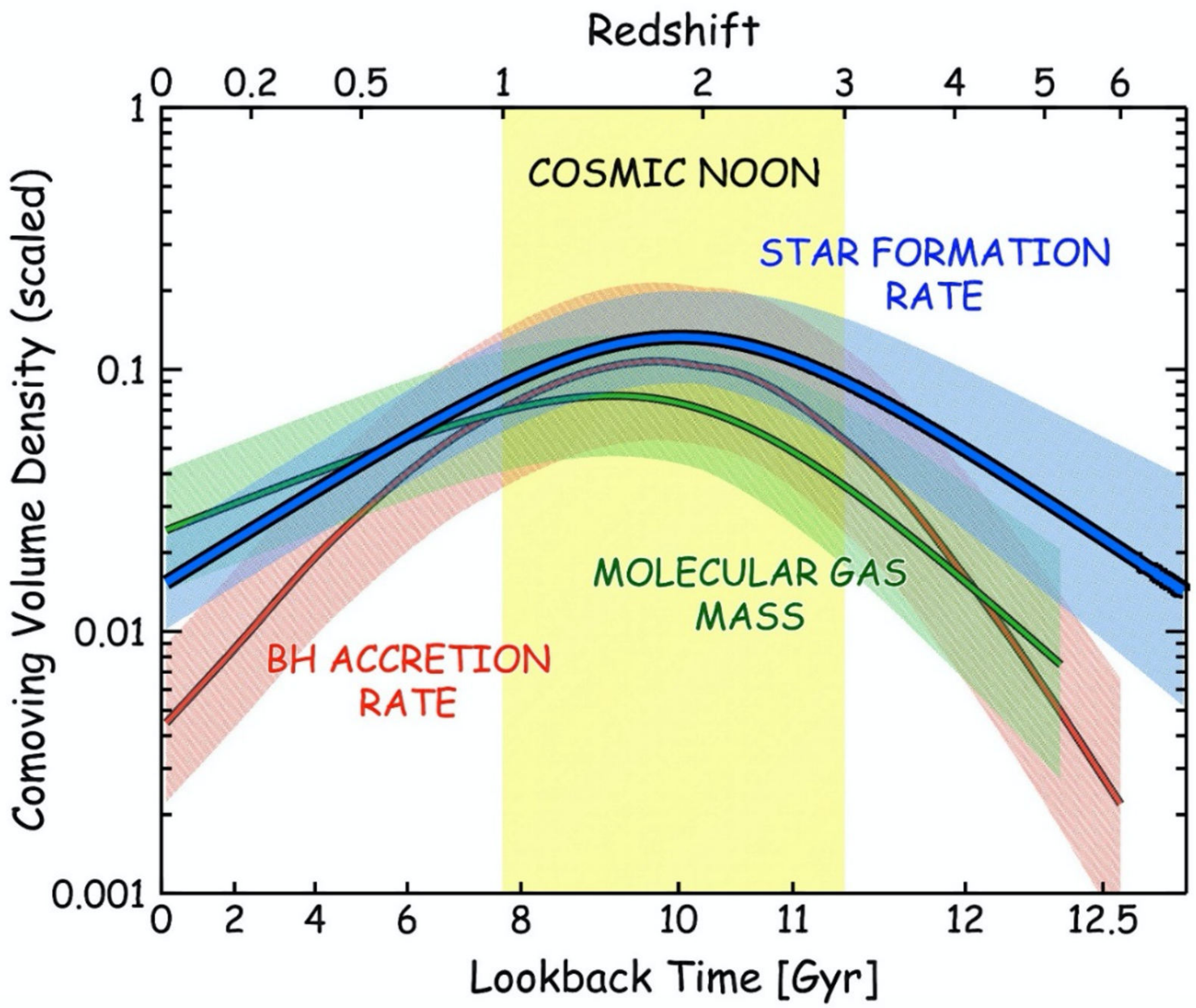

- z ~ 6 — end Epoch of Reionization
- z > 3 — pre-JWST/ALMA/NOEMA census mostly UV-based
- 1 < z < 3 — half of all stars in present-day Universe formed
- z < 0.8 — last half of cosmic history: star formation activity declines, cold gas reservoirs deplete

Madau & Dickinson 2014; Tacconi+2020
Image credit: Natascha Förster Schreiber

Stijn Wuyts

UNIVERSITY OF BATH

Star-forming galaxies at cosmic noon

Förster Schreiber & Wuyts 2020, ARA&A, 58, 661

Observational landscape

Axes of progress

Lookback survey design

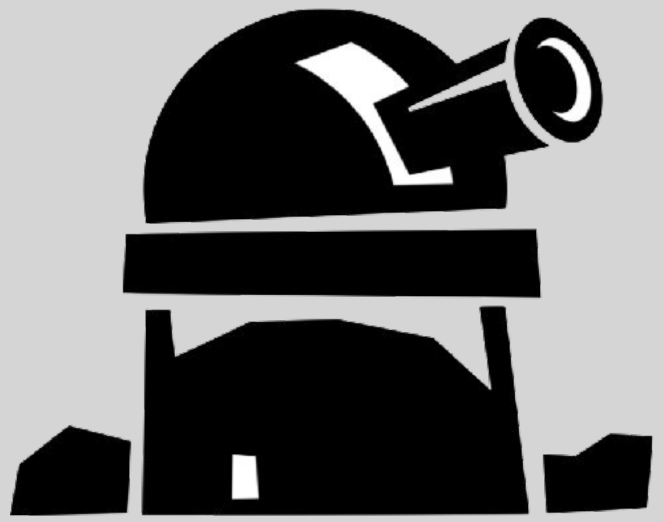

Global

Census

Scaling relations

Evolution

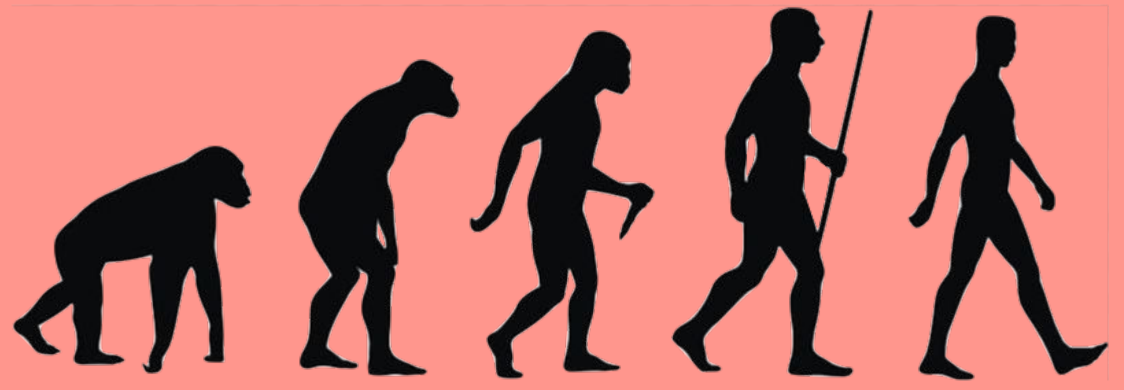

Resolved

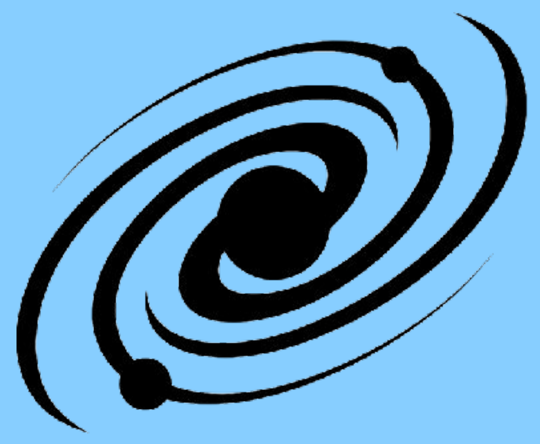

Galaxy sizes

Morphology, shapes & substructure

Disk settling

Kinematics - circular motions

Kinematics - non-circular motions

Kinematics - feedback

Stijn Wuyts

UNIVERSITY OF BATH

Pre-JWST optical/NIR observational landscape

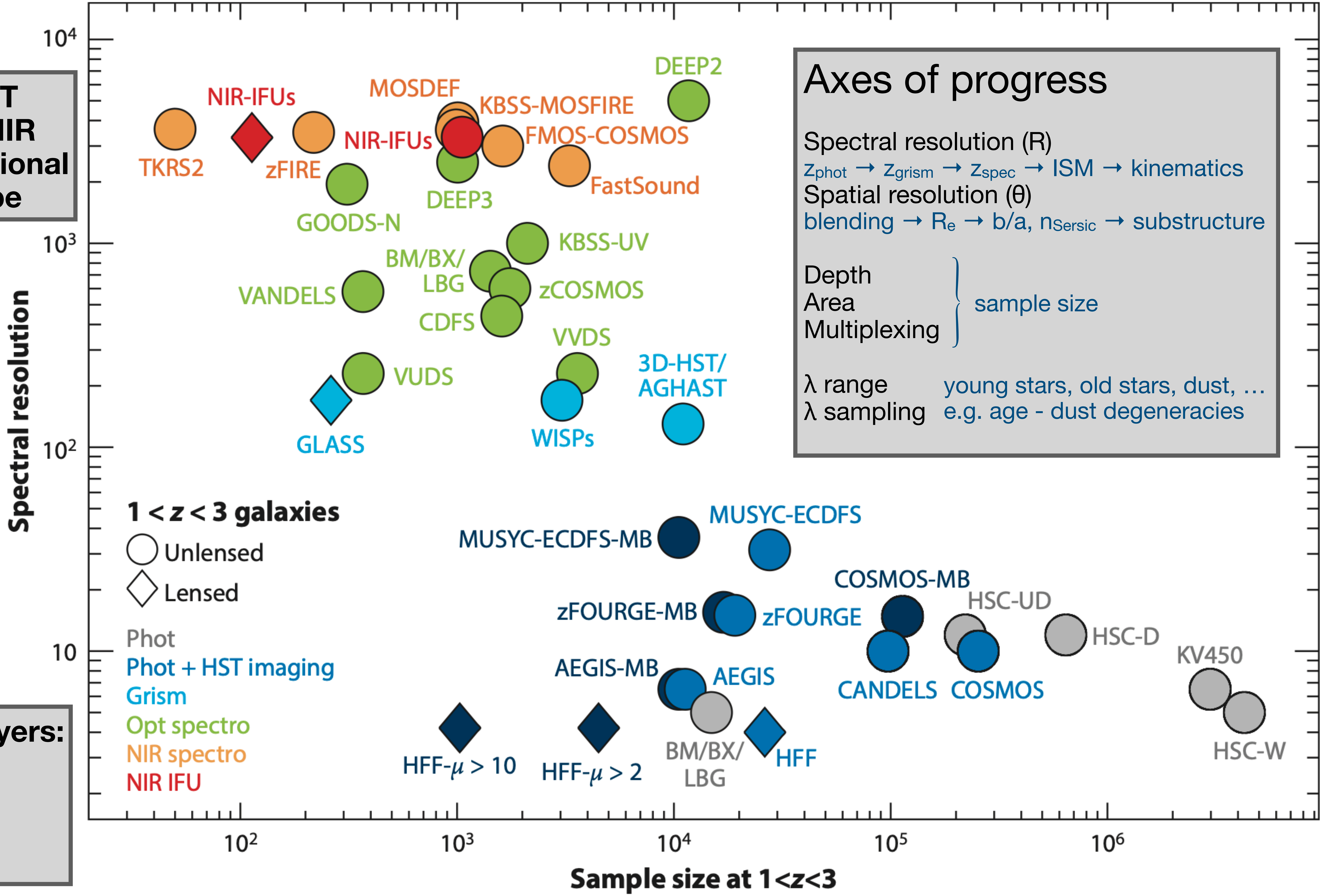

New players:
JWST
Euclid
VRO
Roman

Other λ:
ALMA
NOEMA
Herschel
Chandra

Census and scaling relations

Förster Schreiber & Wuyts, ARAA, 2020; Tomczak+14,16; van der Wel+2014; Barro+2017; Wuyts+2016; Sanders+2018; Simons+2017; Turner+2017; Wisnioski+2019

Evolution

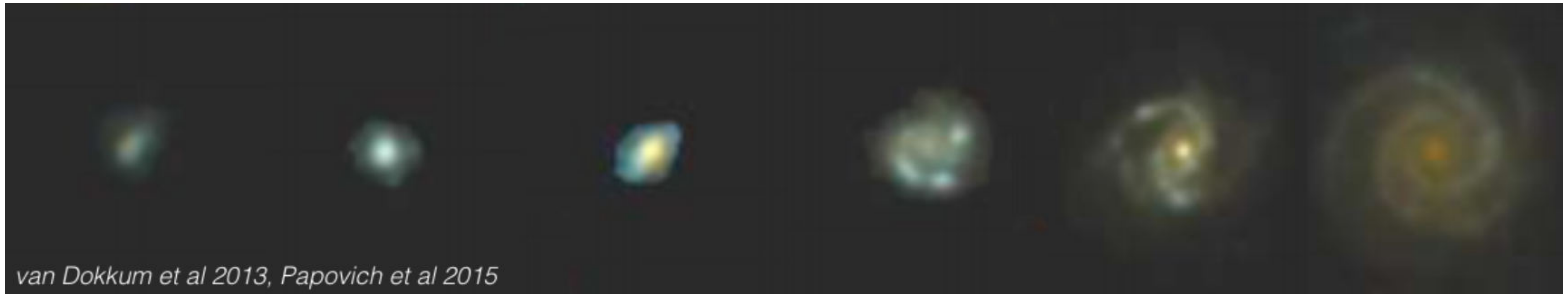

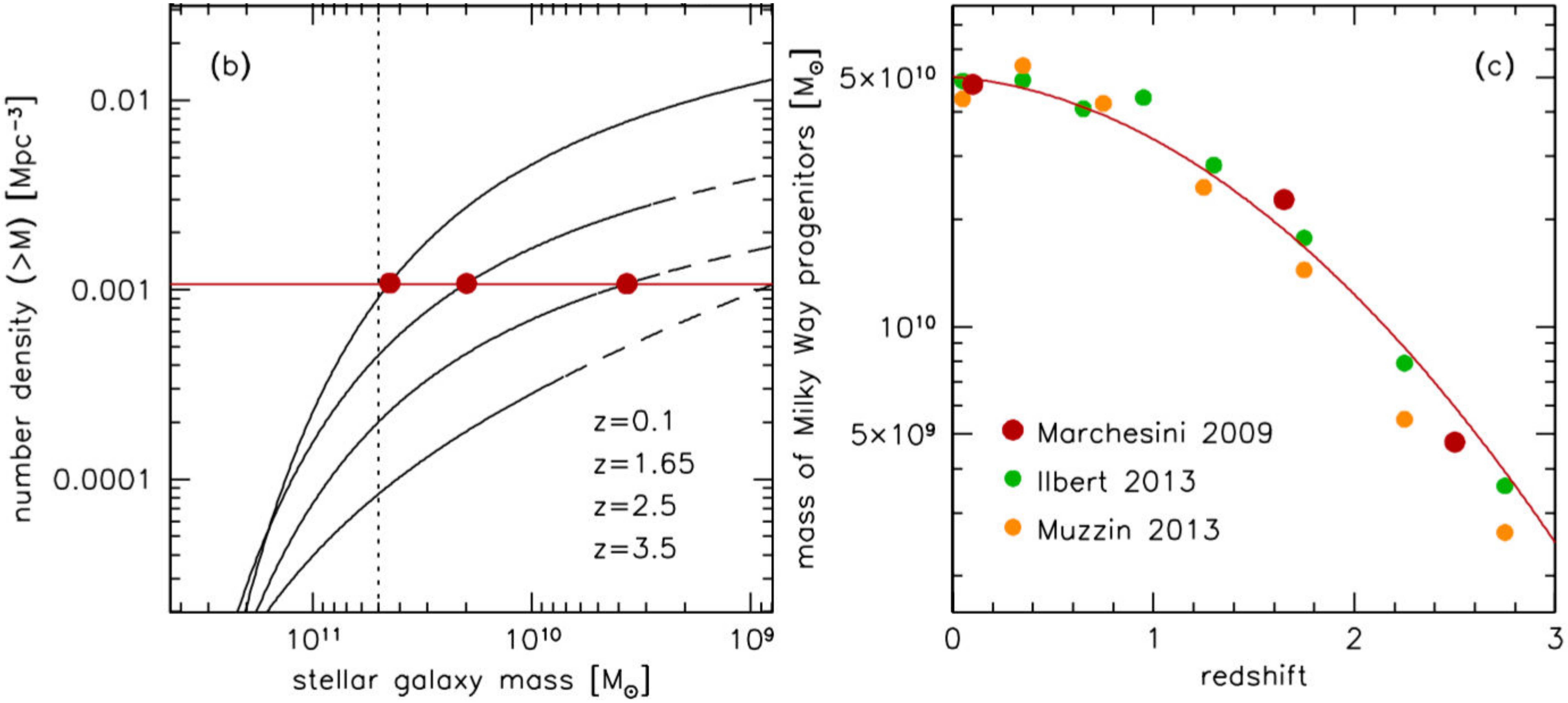

Evolution of population (at fixed M_{star}) vs individual galaxy

Select progenitor - descendants via fixed co-moving number density

Refinements to account for mergers and variance in growth rates

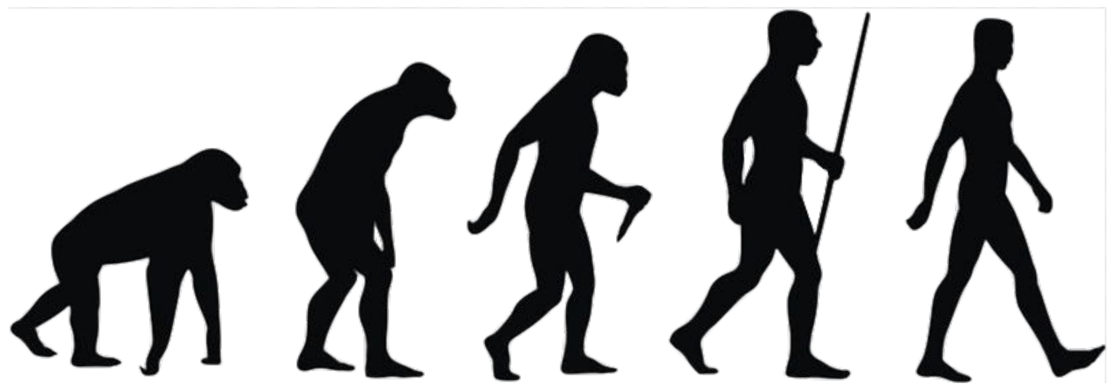

van Dokkum+2013; see also Papovich+2015; van de Voort+2016; Wellons+2017; Torrey+2017; Clauwens+2017

Evolution

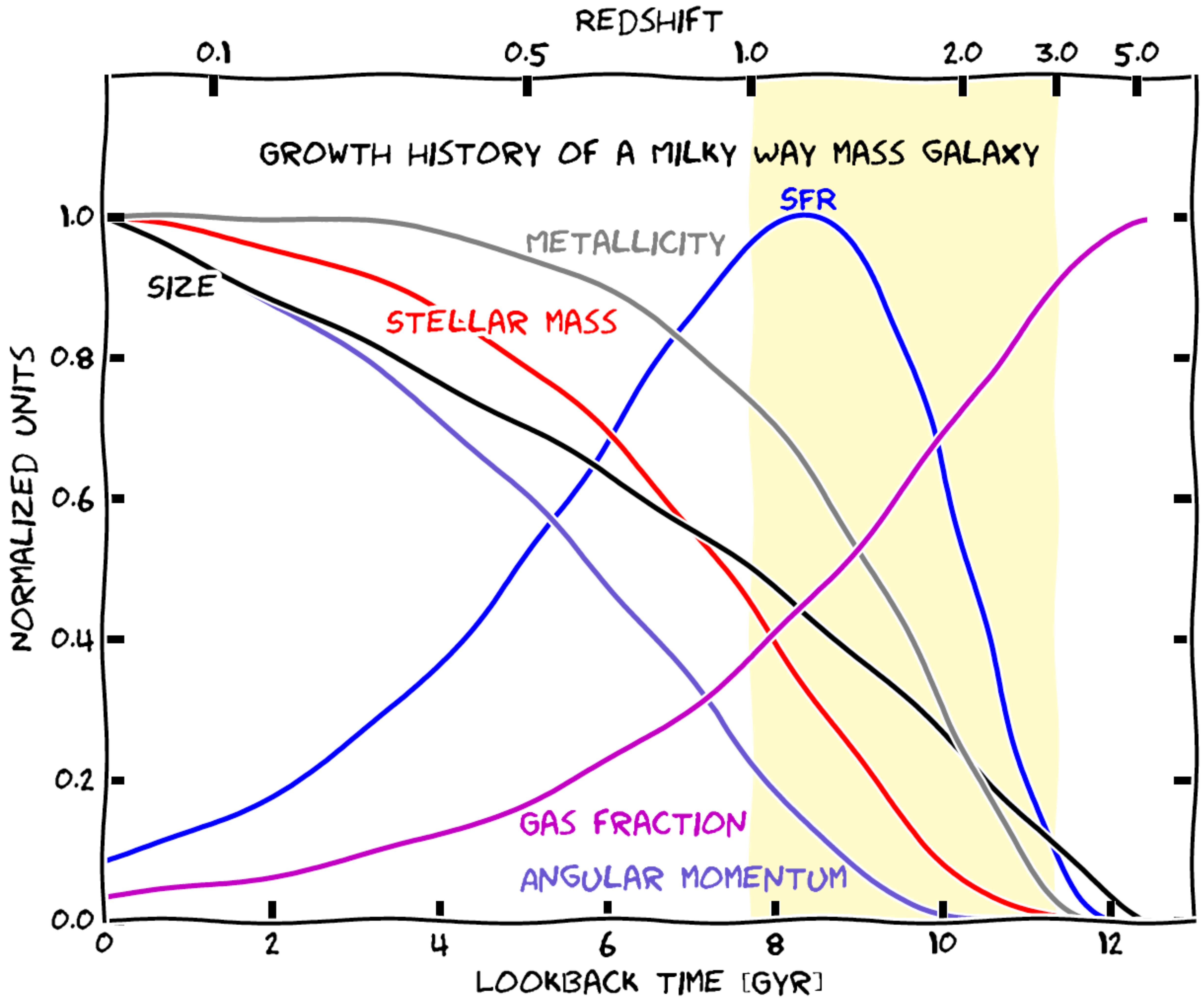

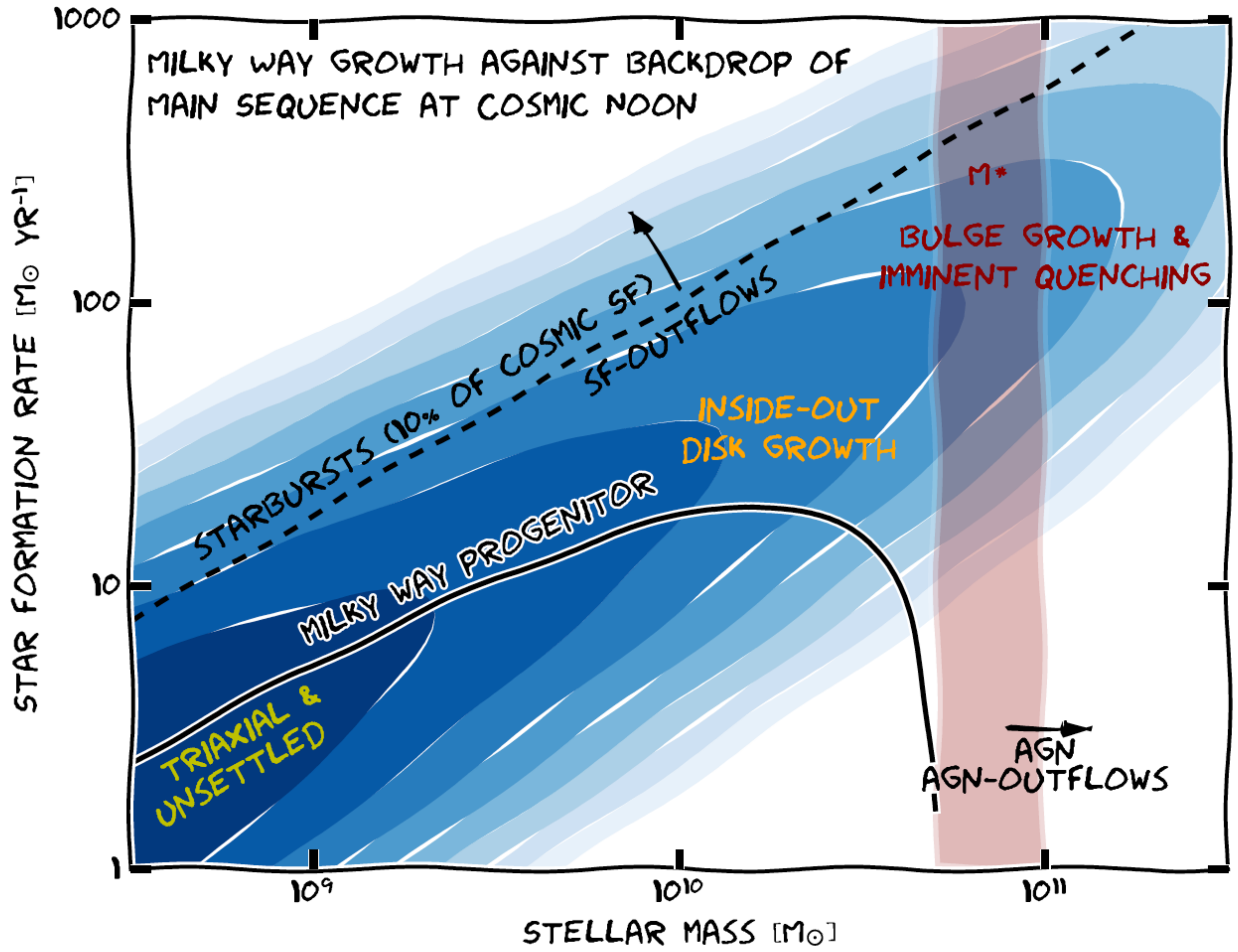

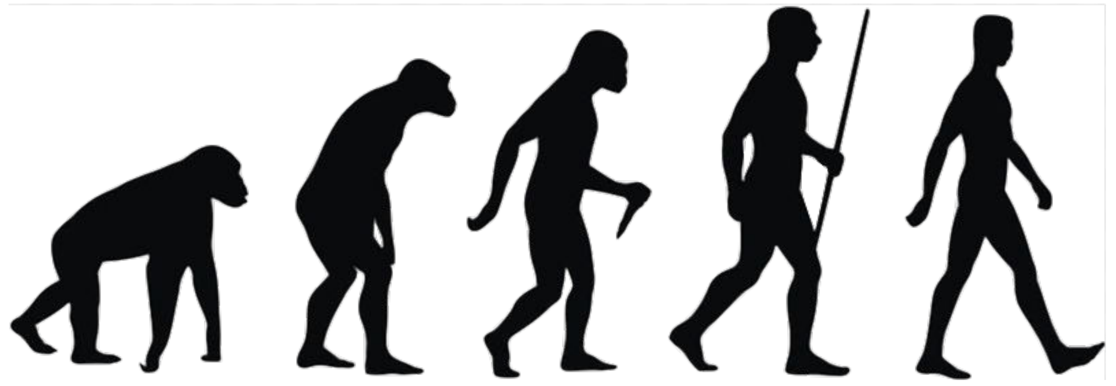

Förster Schreiber & Wuyts, ARAA, 2020 (using stellar mass growth from abundance matching following Hill+2017)

Resolved studies of cosmic noon SFGs

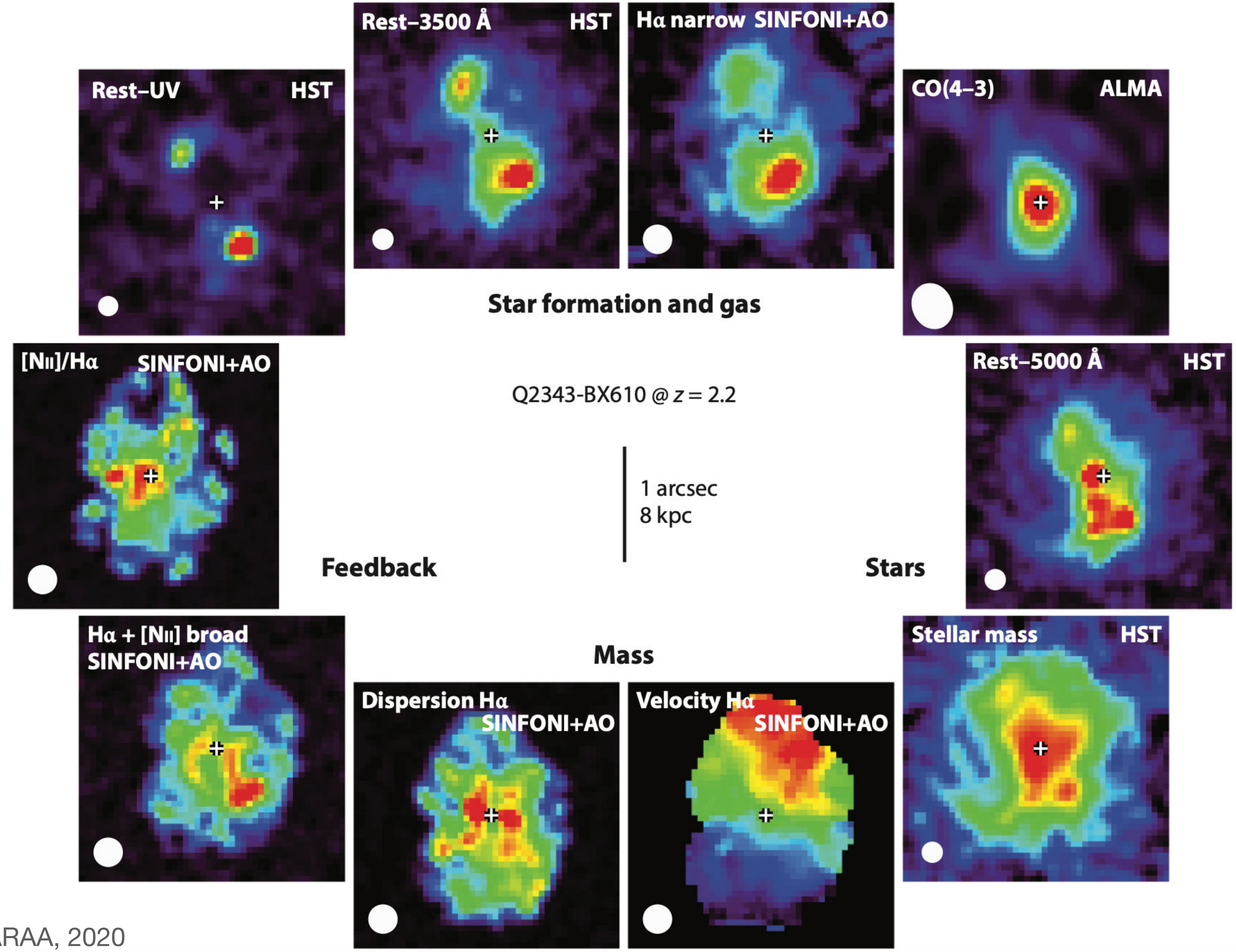

Förster Schreiber & Wuyts, ARAA, 2020

0th order structure - galaxy sizes

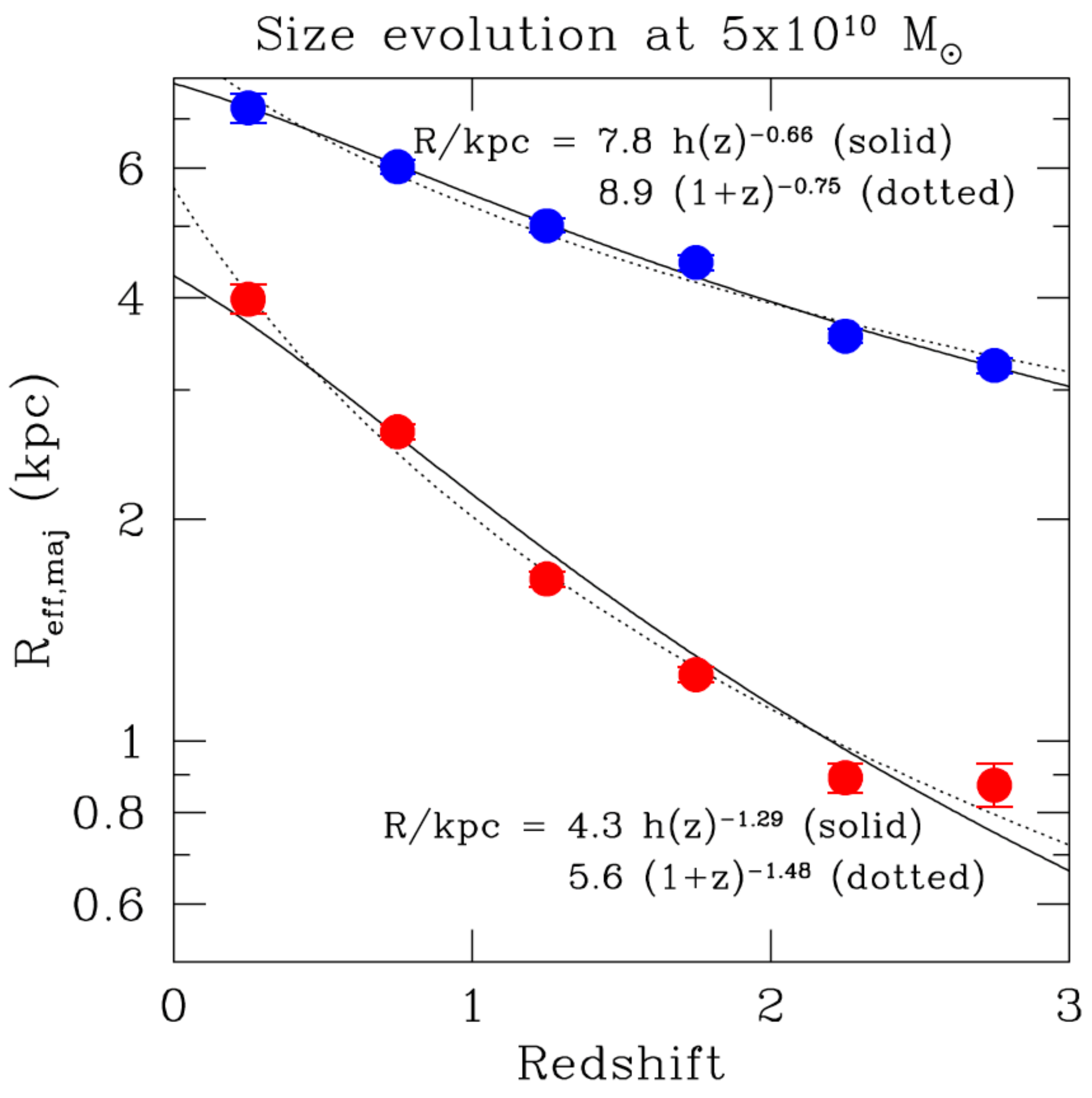

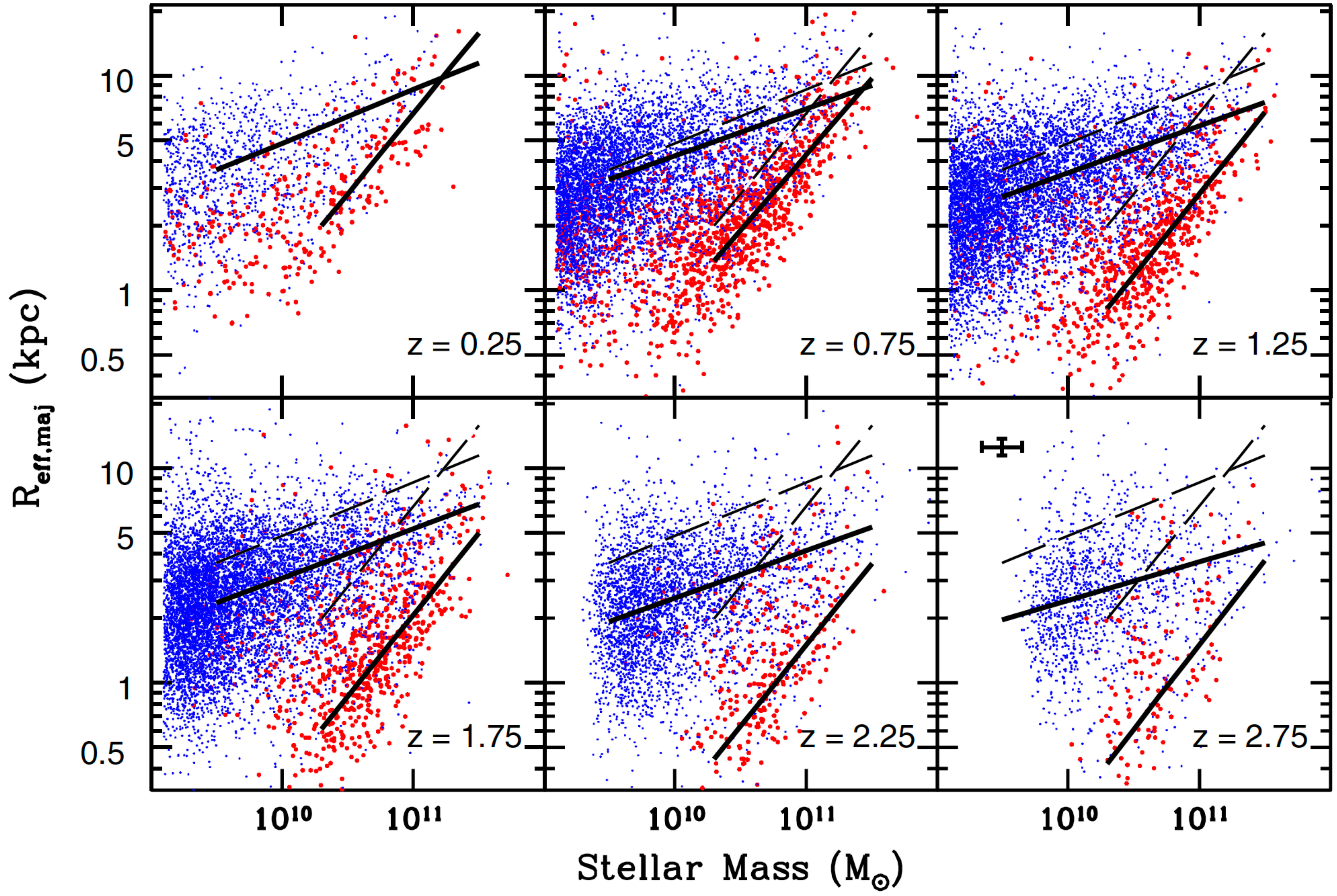

Notes:

$R_{e,major}$ vs $R_{e,circ} = \mathrm{sqrt}(b/a)\ R_{e,major}$

$R_e = R_{50}$ vs R_{80} Mowla+2019

$R_{e,light}$ vs $R_{e,mass}$ Wuyts+2012, Suess+2019

$R_{e,star}$ vs $R_{e,SFR}$ vs $R_{e,dust}$ vs $R_{e,gas}$

van der Wel et al. 2014 (based on HST CANDELS survey, rest-optical)

Star formation profiles

NIR-IFUs reveal **extended Hα disks** ⟷ ALMA reveals **compact dust cores** in massive z~2 SFGs
in massive z~2 SFGs
Even after best-effort dust correction

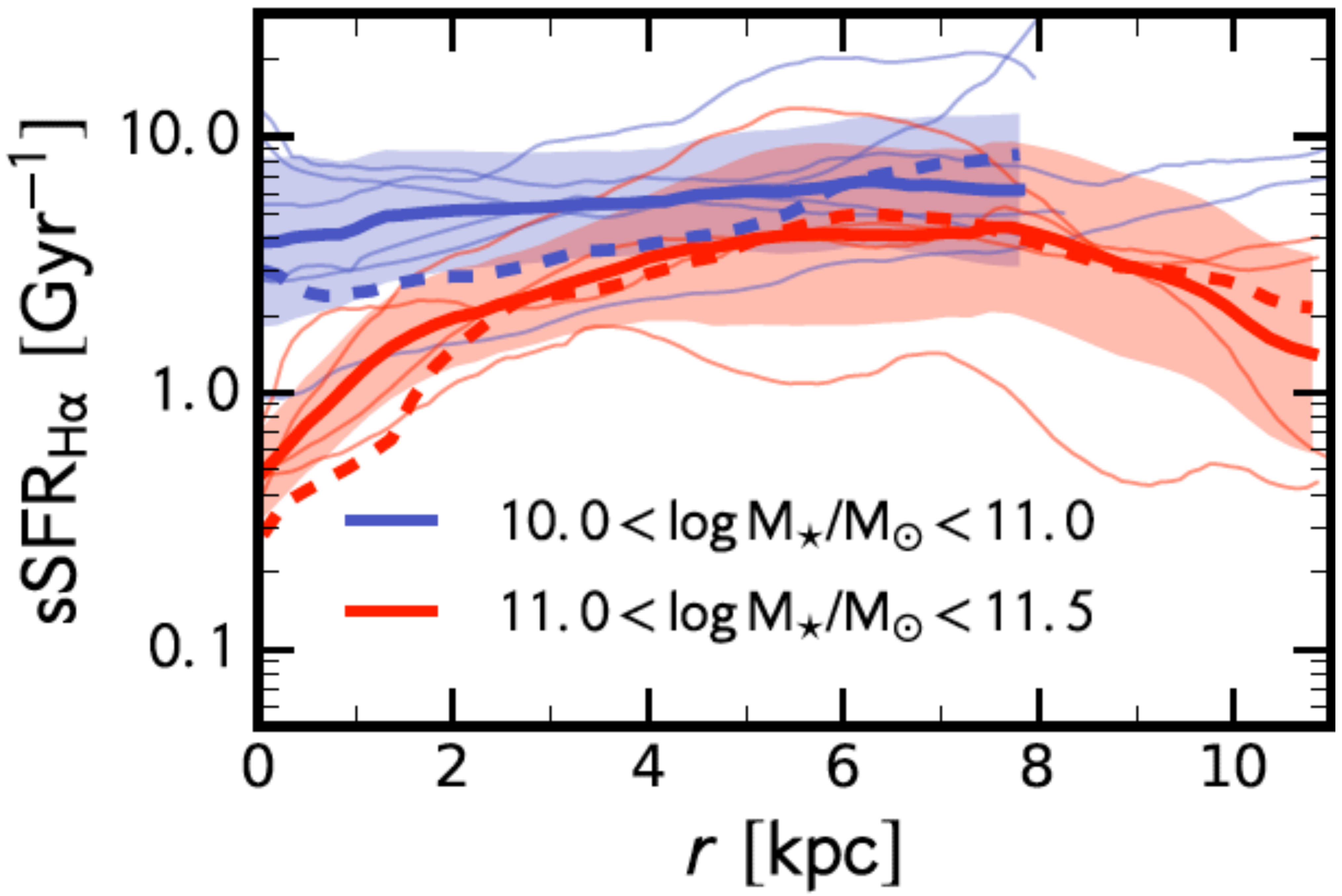

Tacchella+2018 (also Nelson+2021 @ z~1)

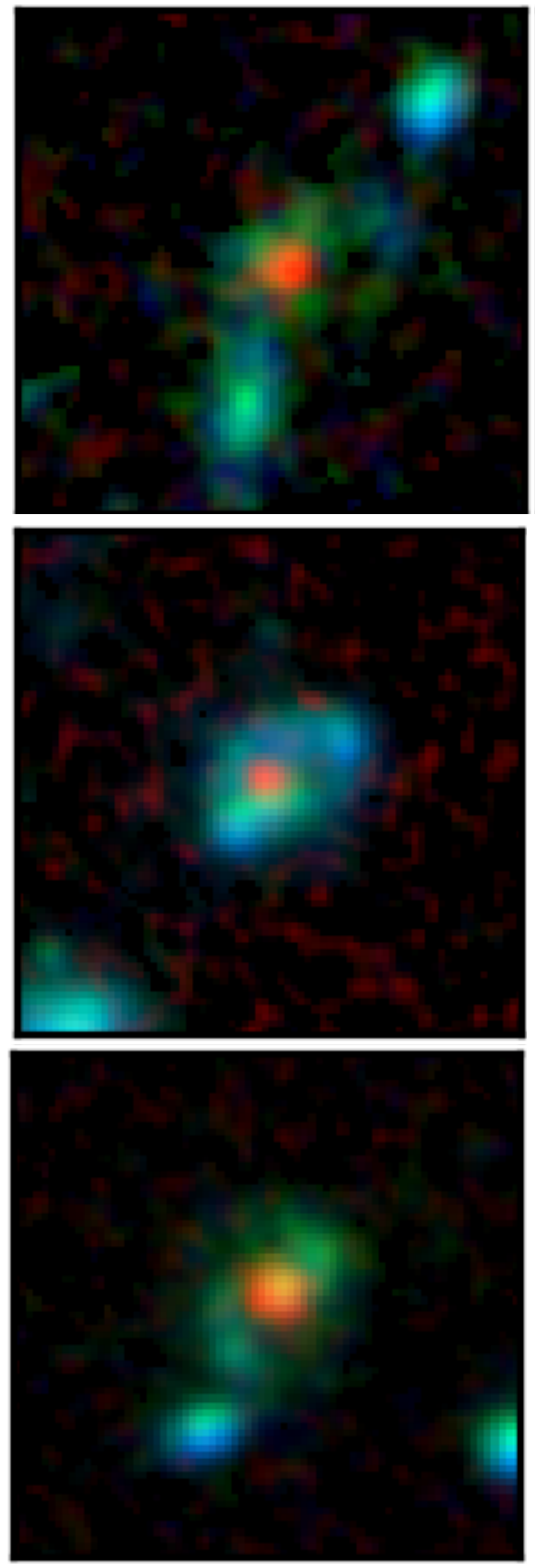

$J_{125}H_{160}$870μm

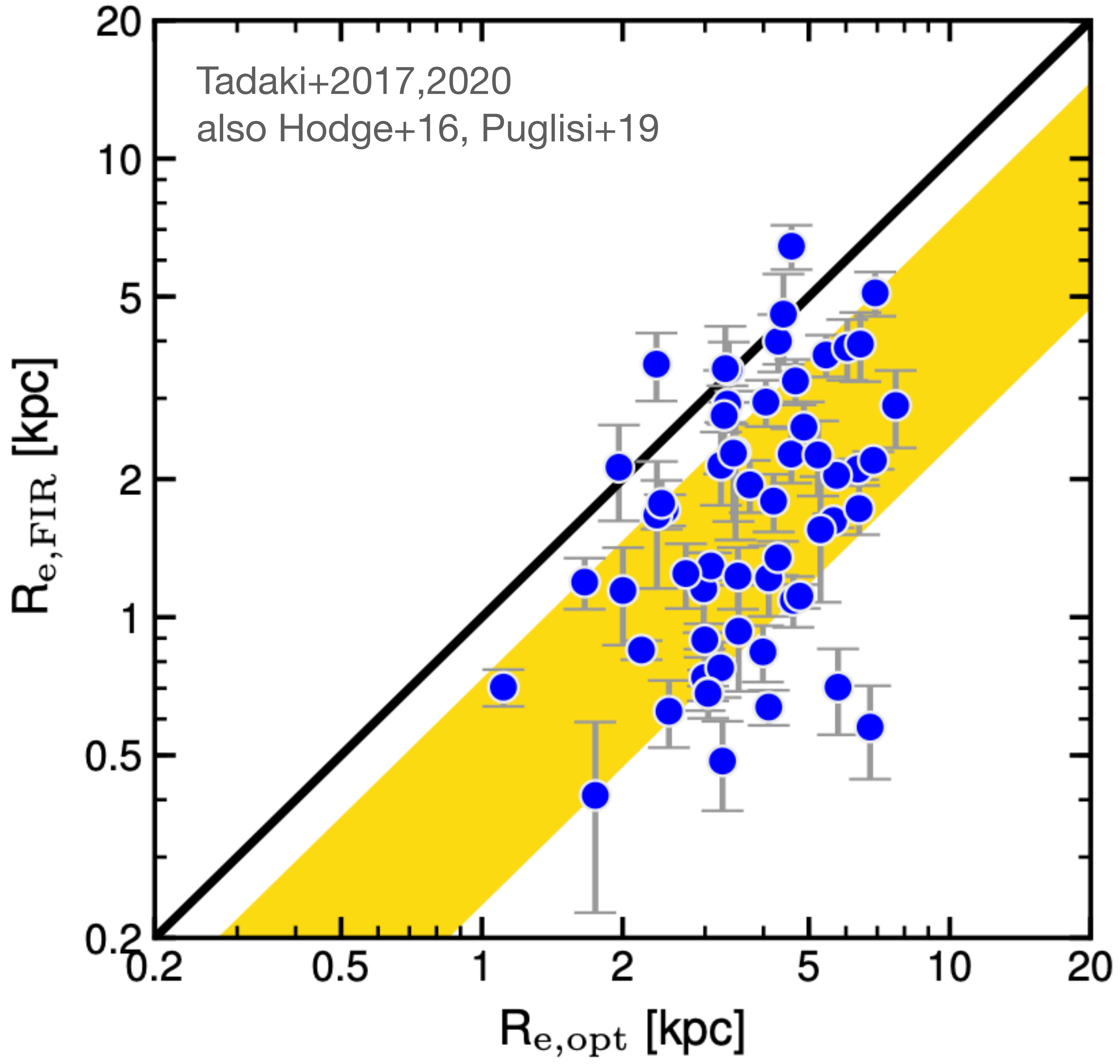

Also new JWST/CEERS PAH 6.2 & 7.7μm sizes of obscured star formation using MIRI (Shen+2023; Magnelli+2023)

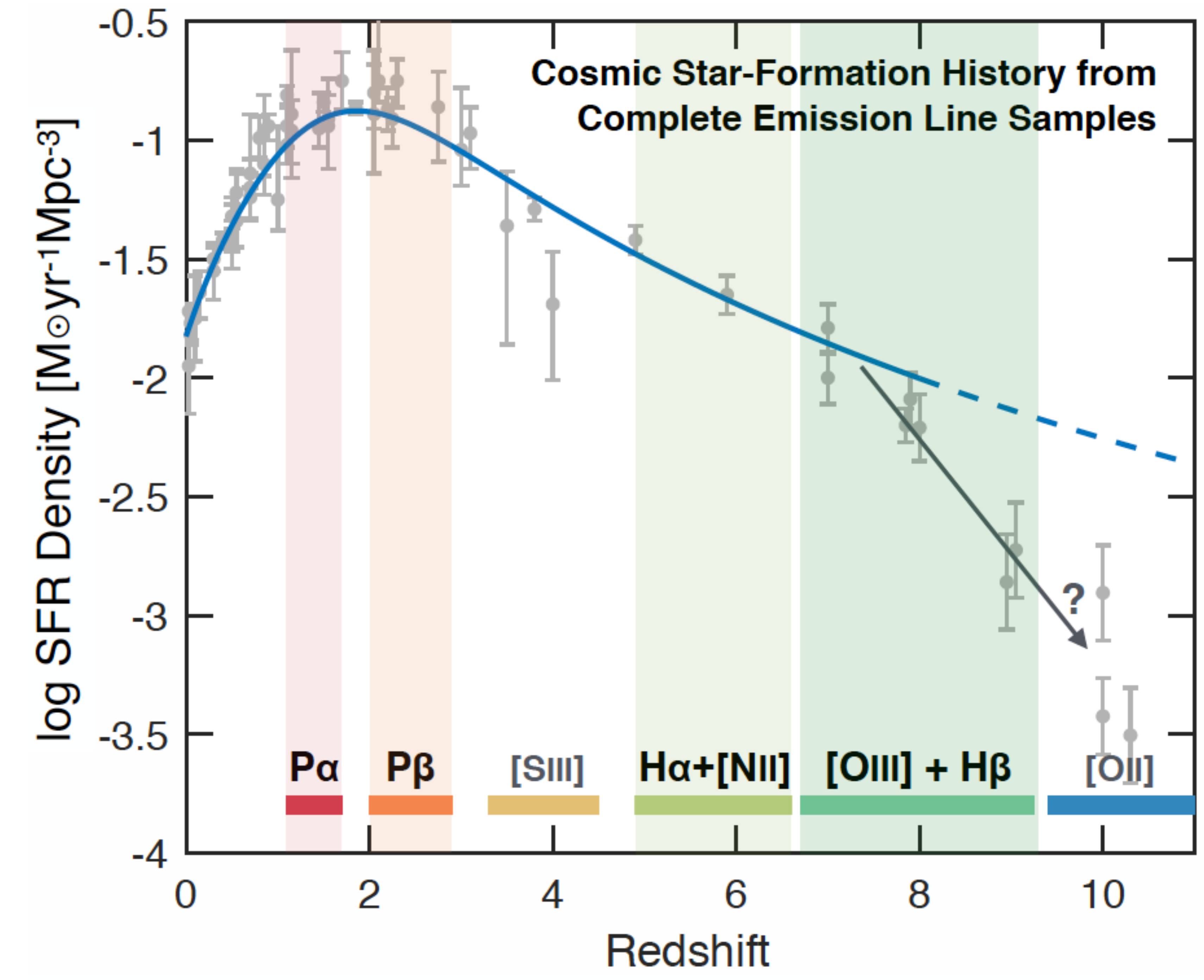

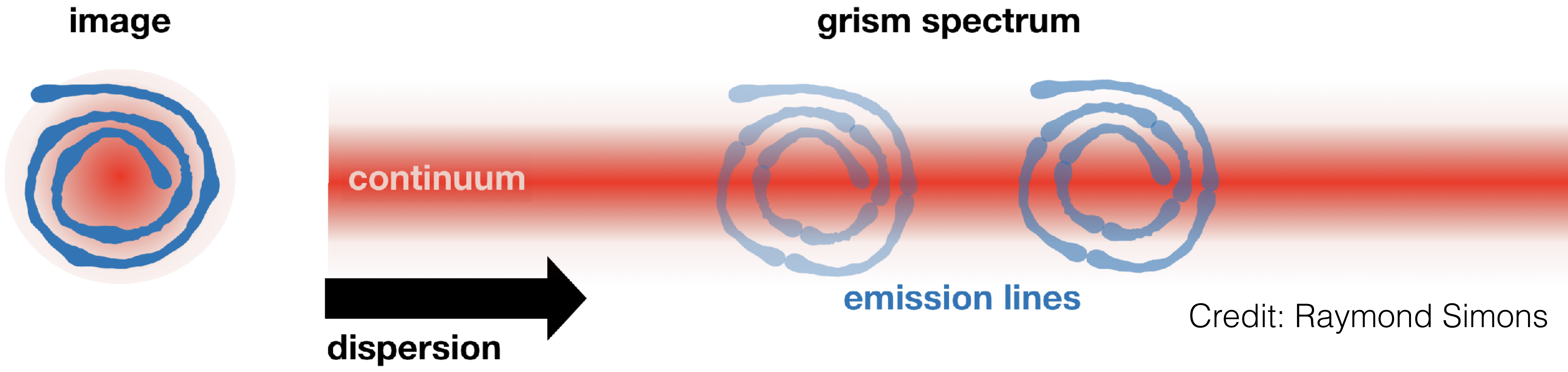

PI P.Oesch **FRESCO JWST/NIRCam grism** targeting CANDELS-DEEP (GOODS-S & -N)

3.3×10^{-18} erg/s/cm^2 (6σ); 164 arcmin^2

Stellar mass maps

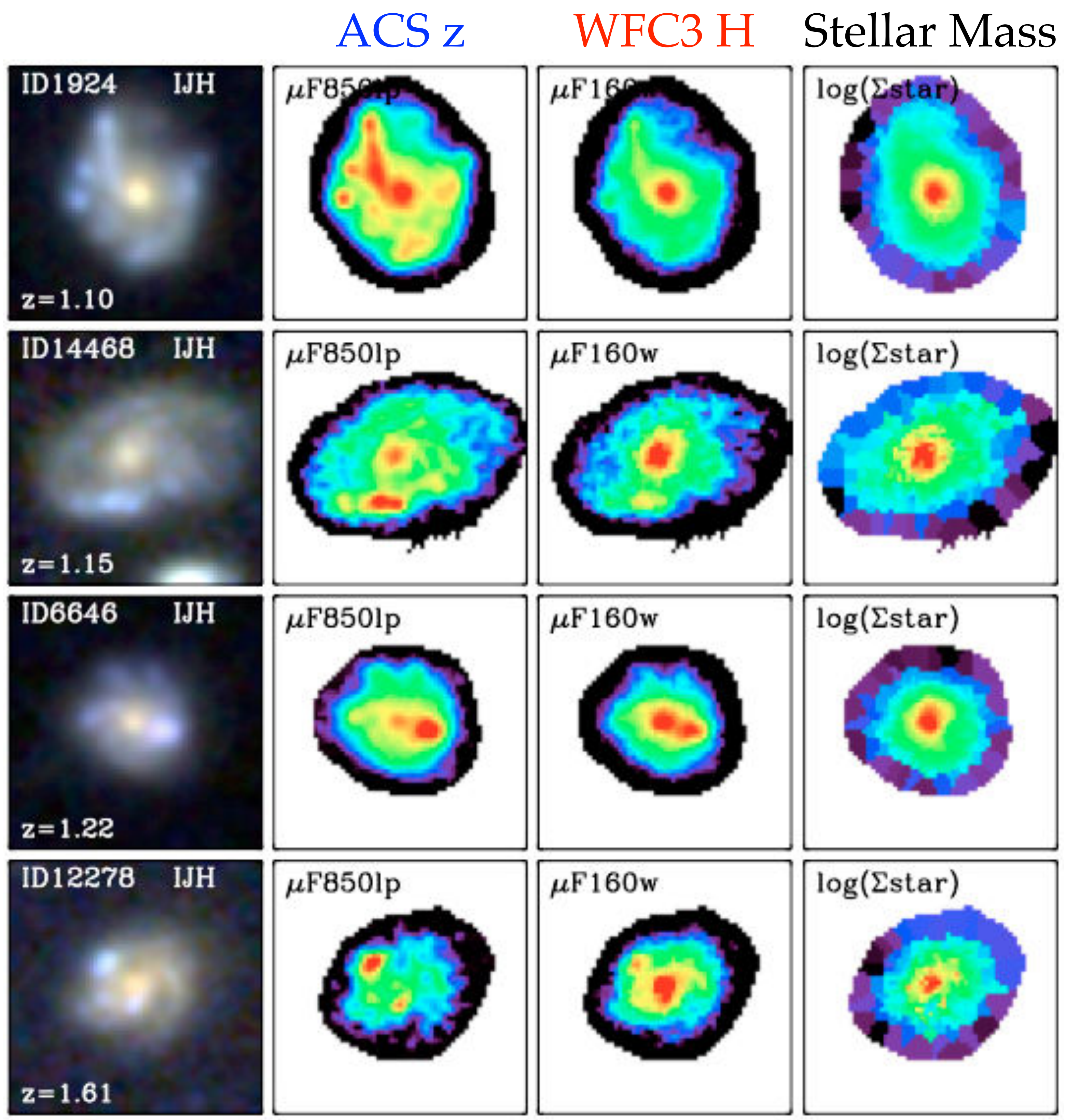

Wuyts+2012
also Guo+2012; Szomoru+2013; Tacchella+2015; Cibinel+2015; Mosley+2017,2020

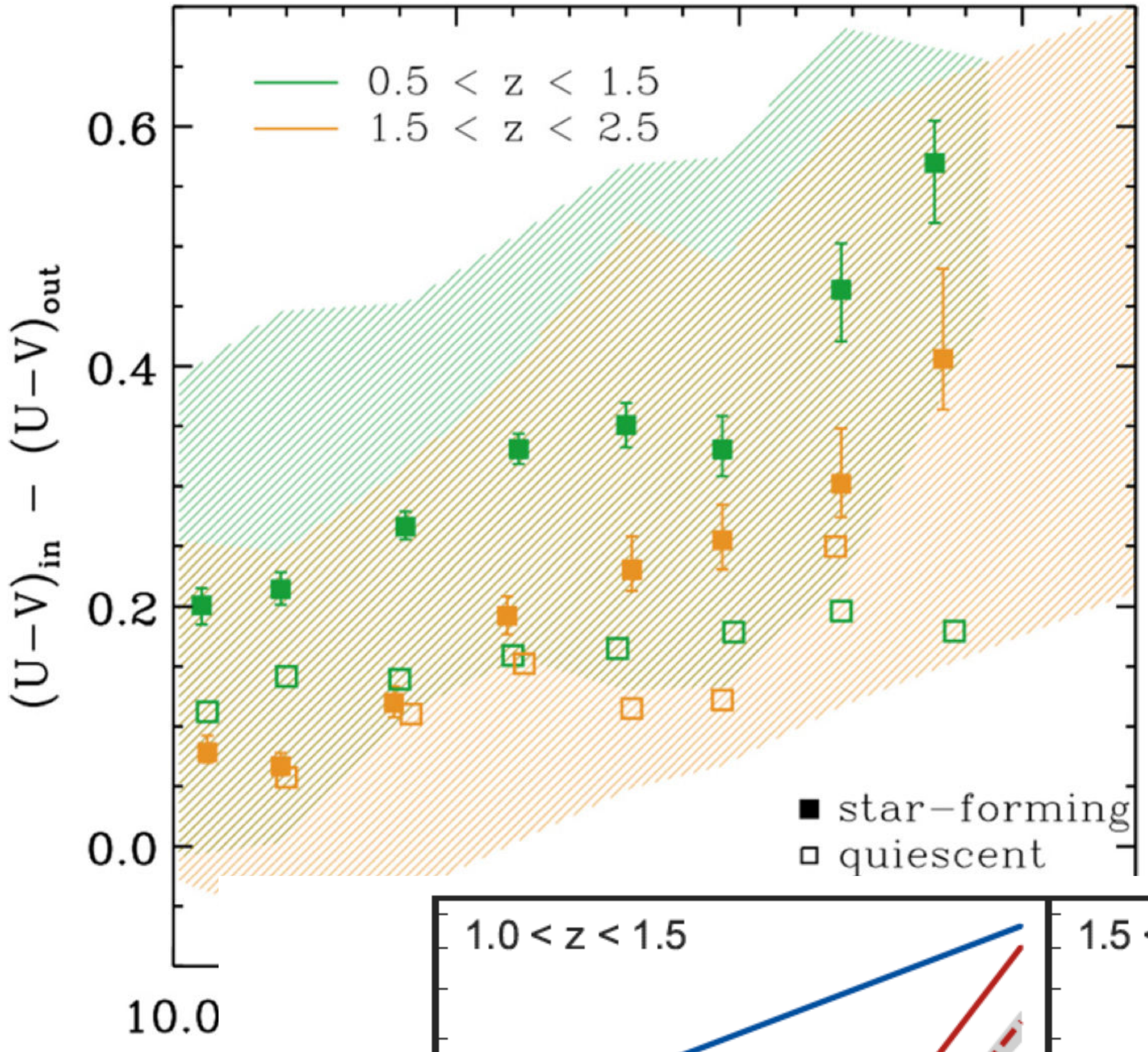

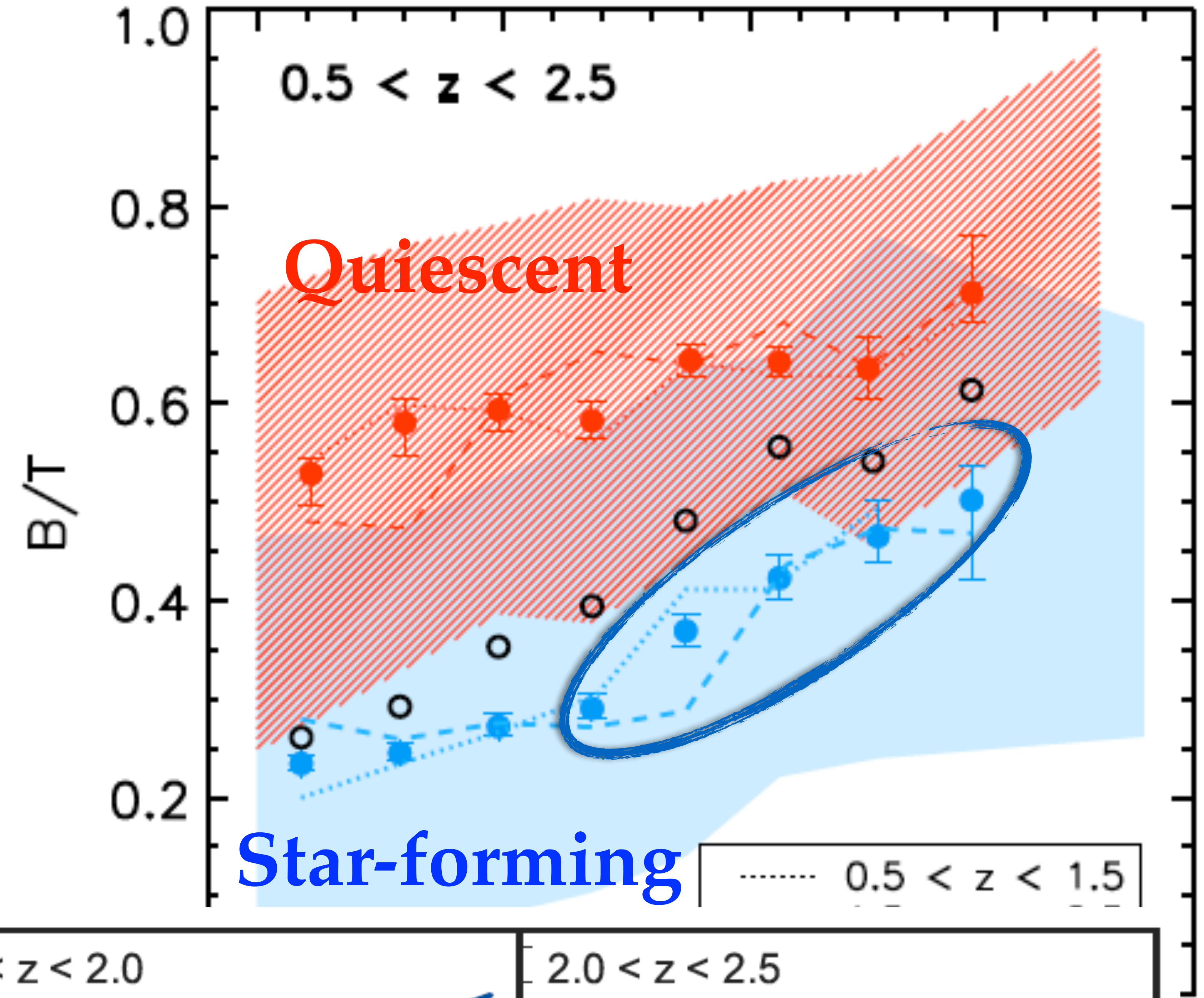

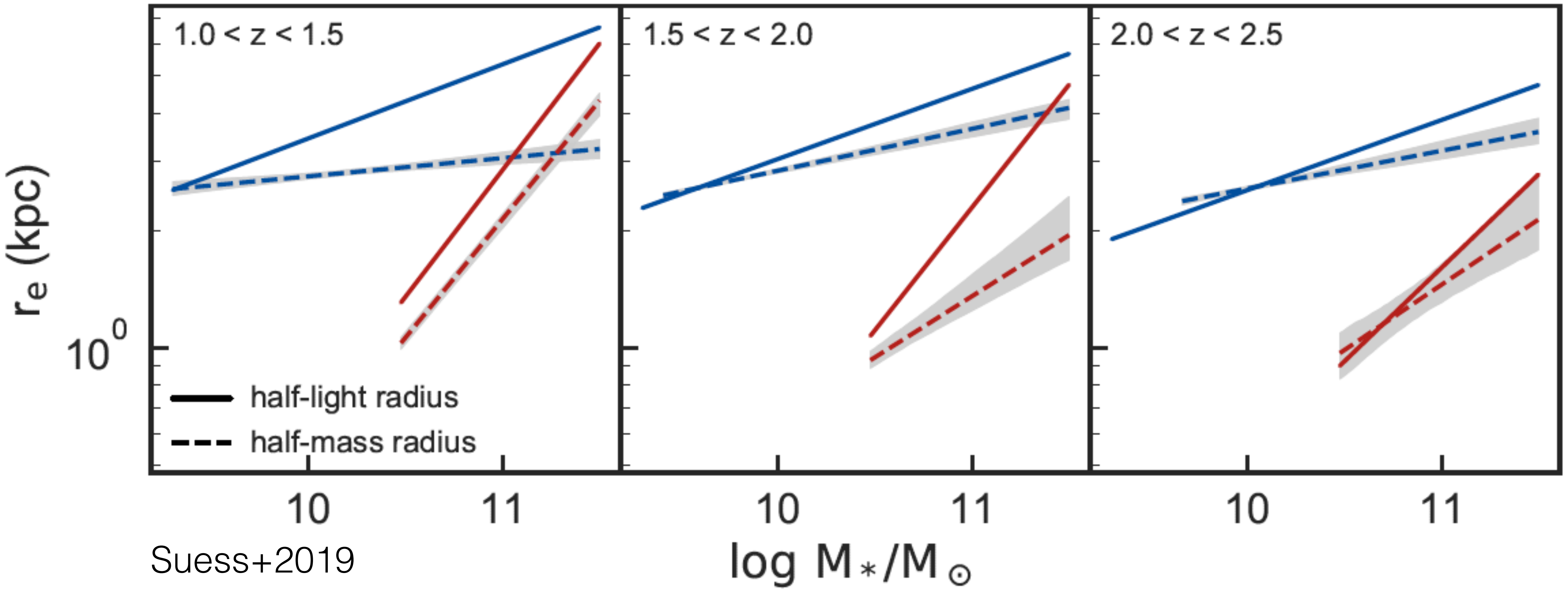

Suess+2019

Stellar mass distributions smoother and more centrally concentrated than light

Implications for size-mass relation and galaxy size evolution!

1st order structure - galaxy light profiles

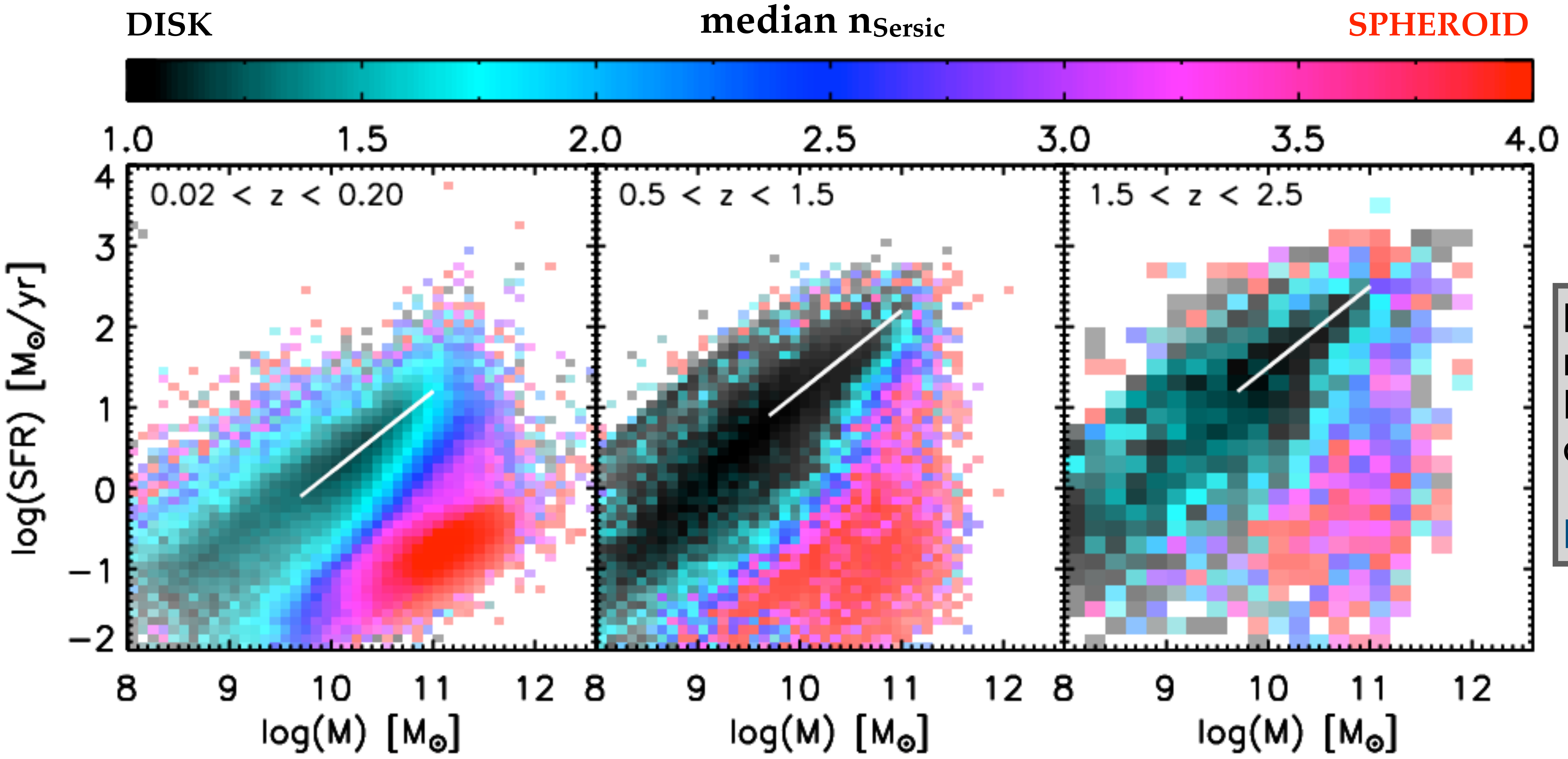

Predictors of quiescence:

n_{Sersic}

B/T

$\sigma_\star \sim M/R_e$

Proxies for M_{BH}?

Wuyts et al. 2011 (also e.g. Bluck et al. 2014; Lang et al. 2014; Whitaker et al. 2015)

1st order structure - 3D intrinsic shapes

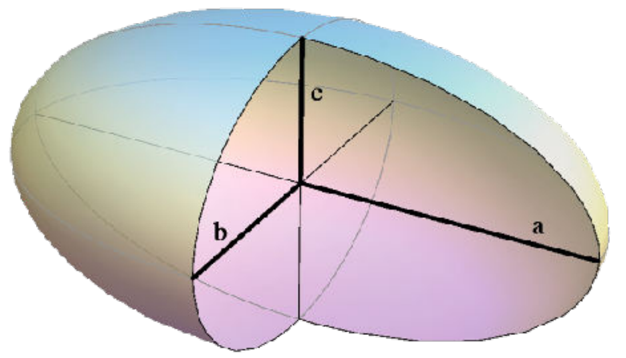

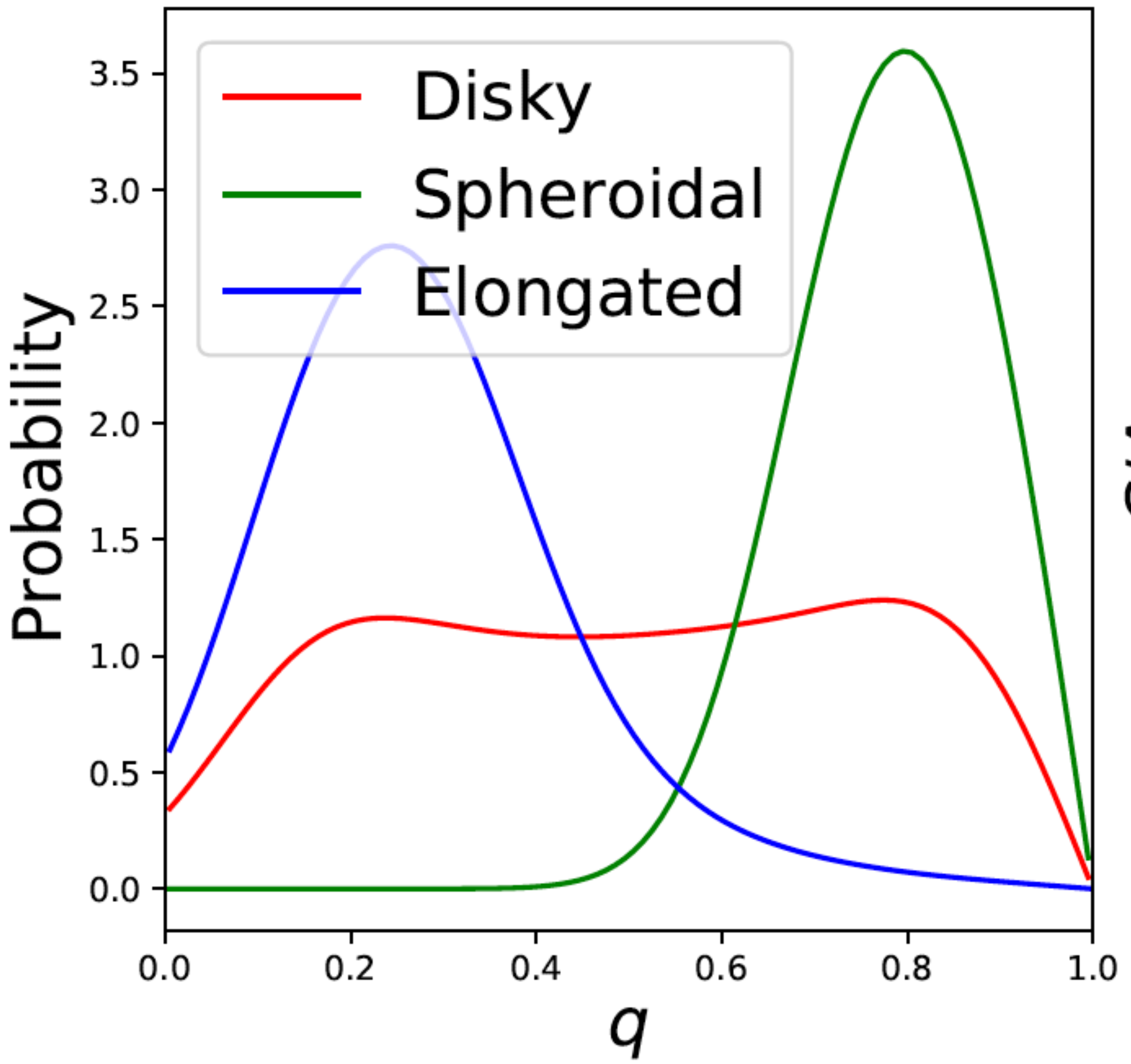

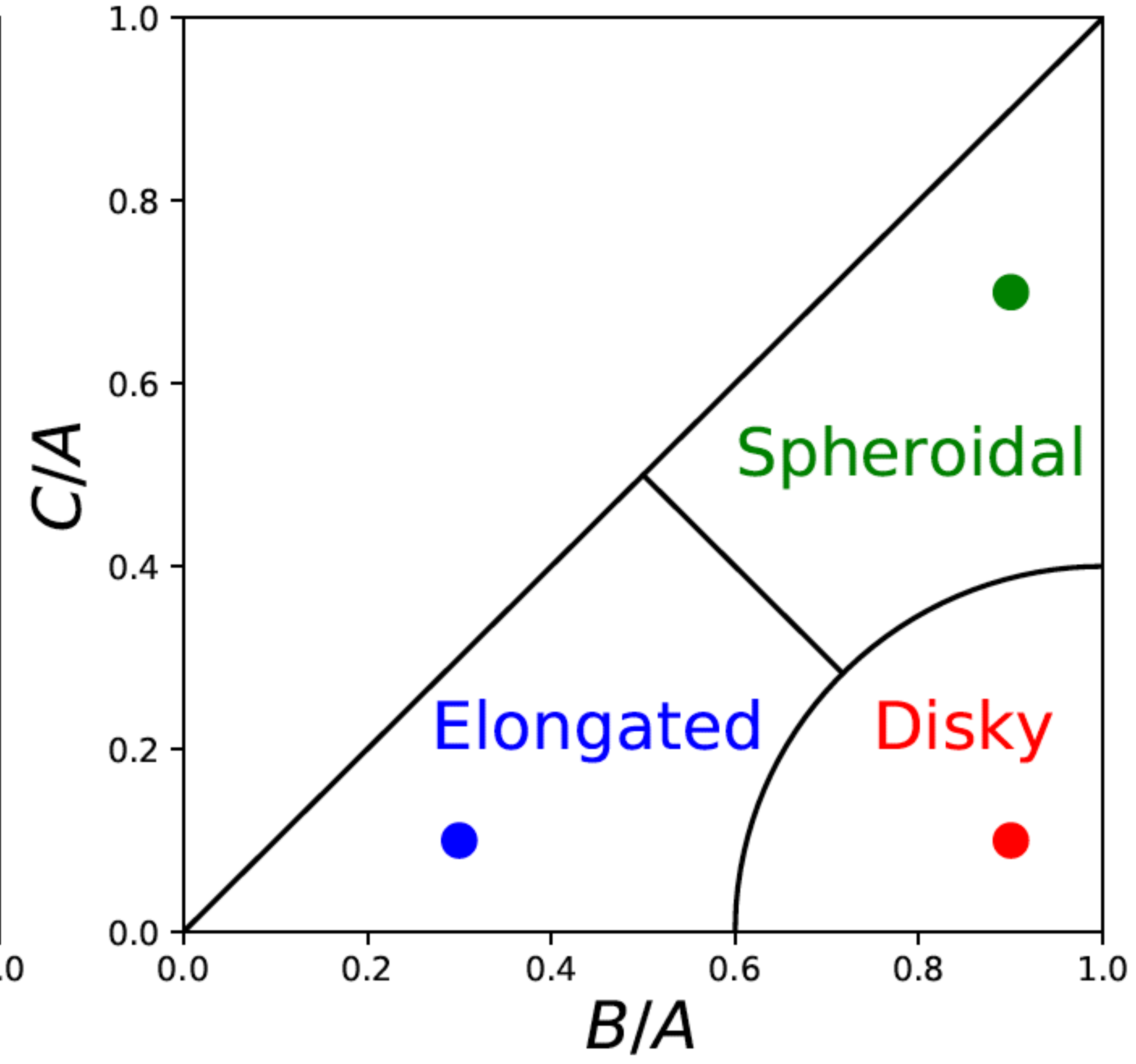

Projected axis ratio

Intrinsic axis ratios

Zhang et al. 2022 (also e.g. van der Wel. 2014; Zhang et al. 2019; Zhang et al. 2023)

3D intrinsic shapes - quiescent galaxies

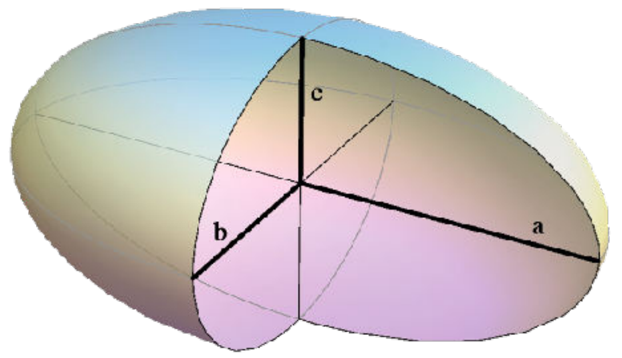

Projected axis ratio

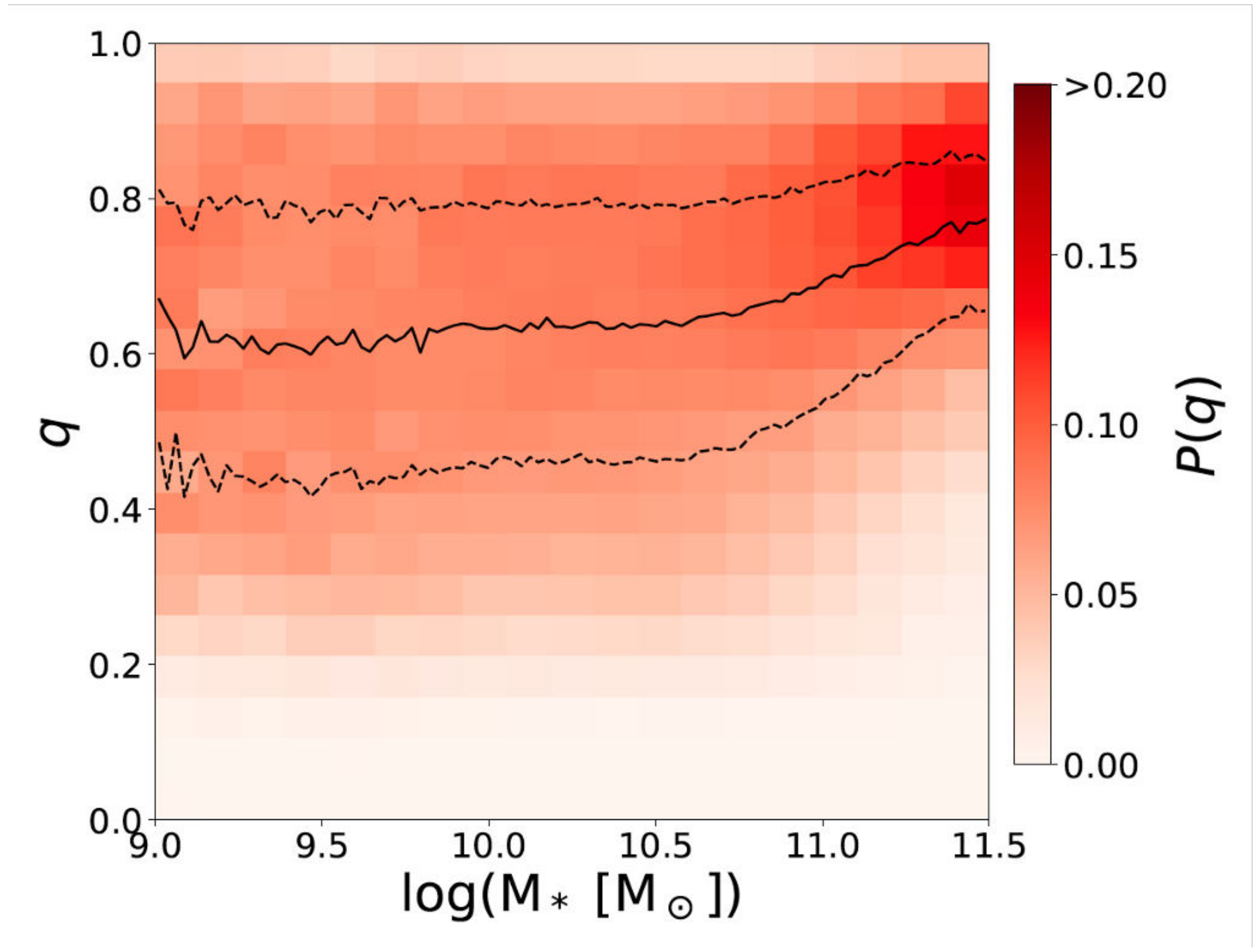

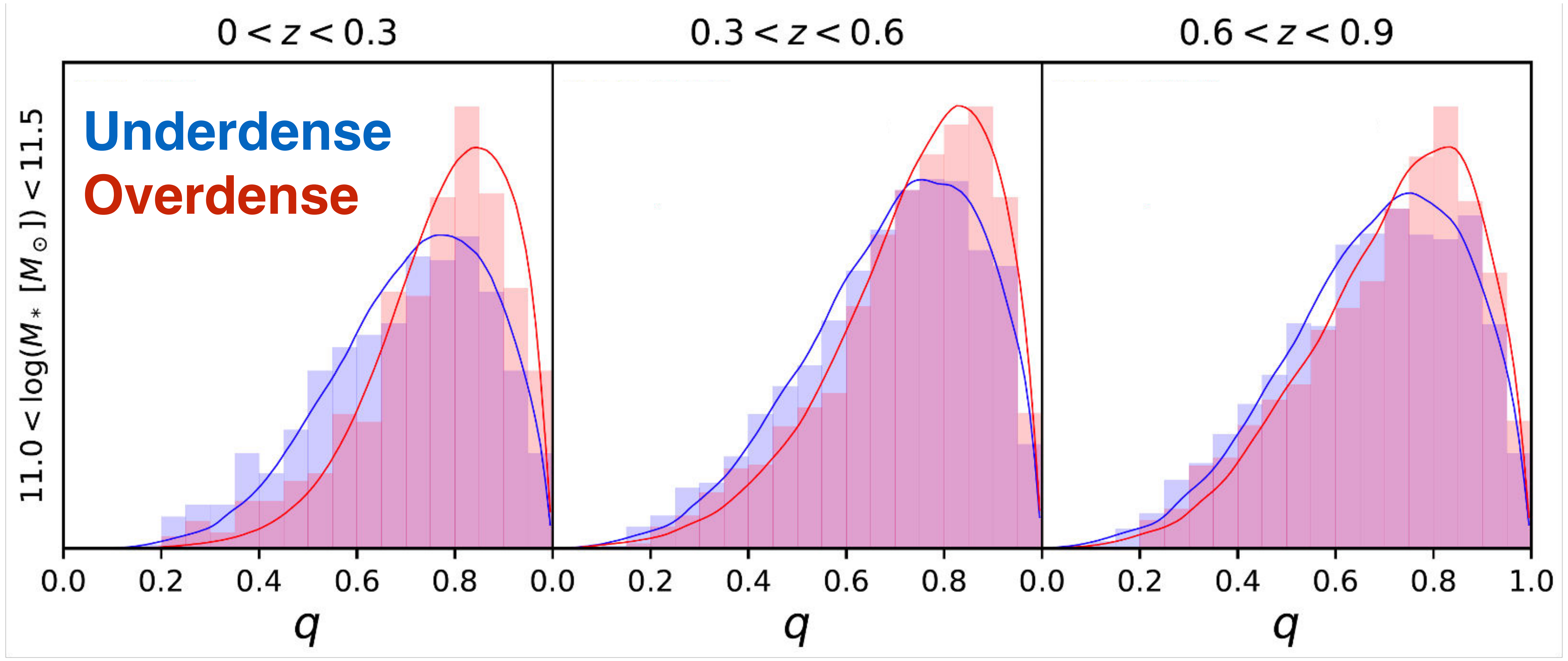

Projected axis ratio

Zhang et al. 2022 (also e.g. van der Wel. 2009; Holden et al. 2012; Satoh et al. 2019)

3D intrinsic shapes - quiescent galaxies

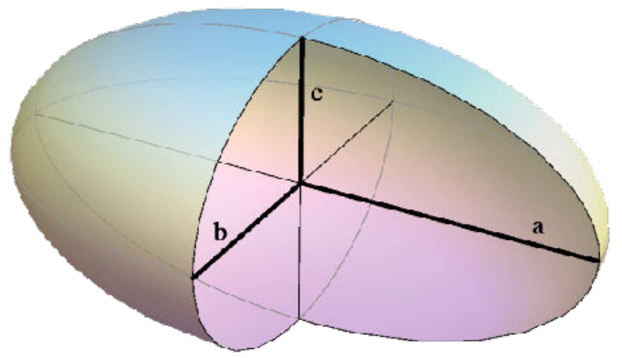

Projected axis ratio

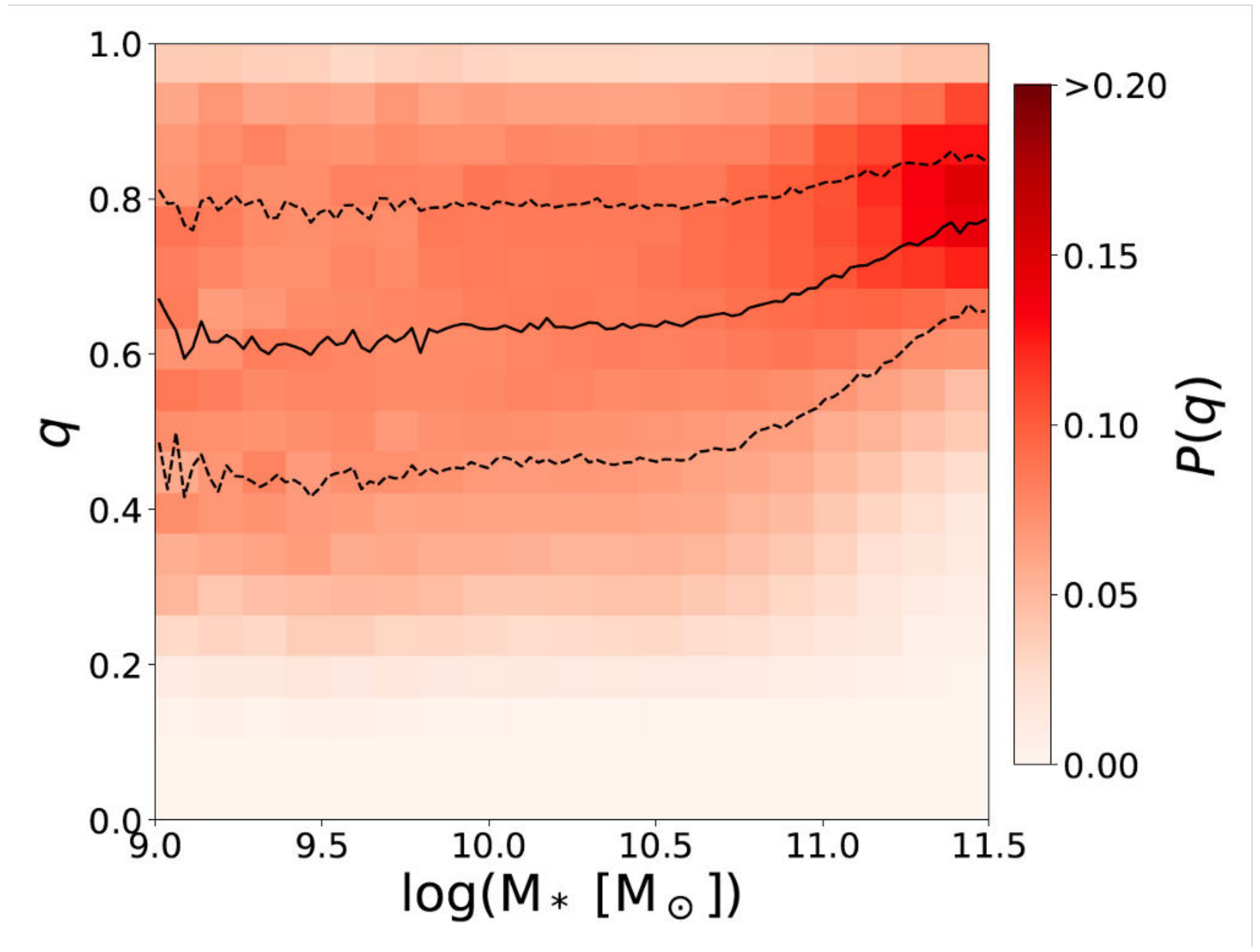

Strong mass- and redshift-independent trend between n_{Sersic} and median q

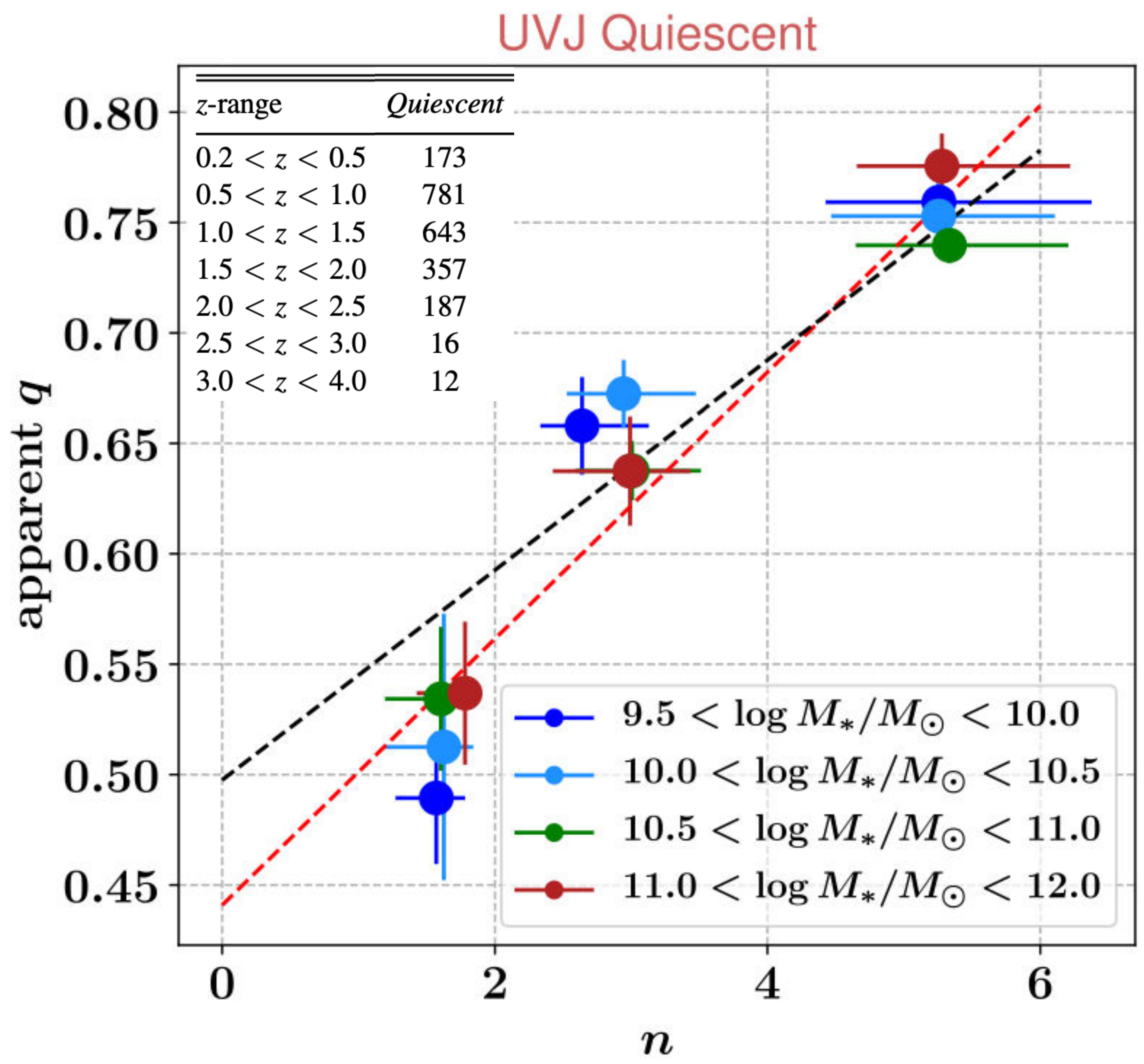

Hill et al. 2019

Zhang et al. 2022 (also e.g. van der Wel. 2009; Holden et al. 2012; Satoh et al. 2019)

3D intrinsic shapes - star-forming galaxies

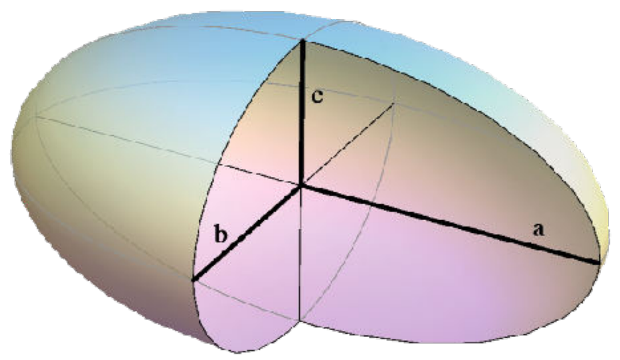

Morphological disk settling:

Flattened axisymmetric systems appearing at high mass first

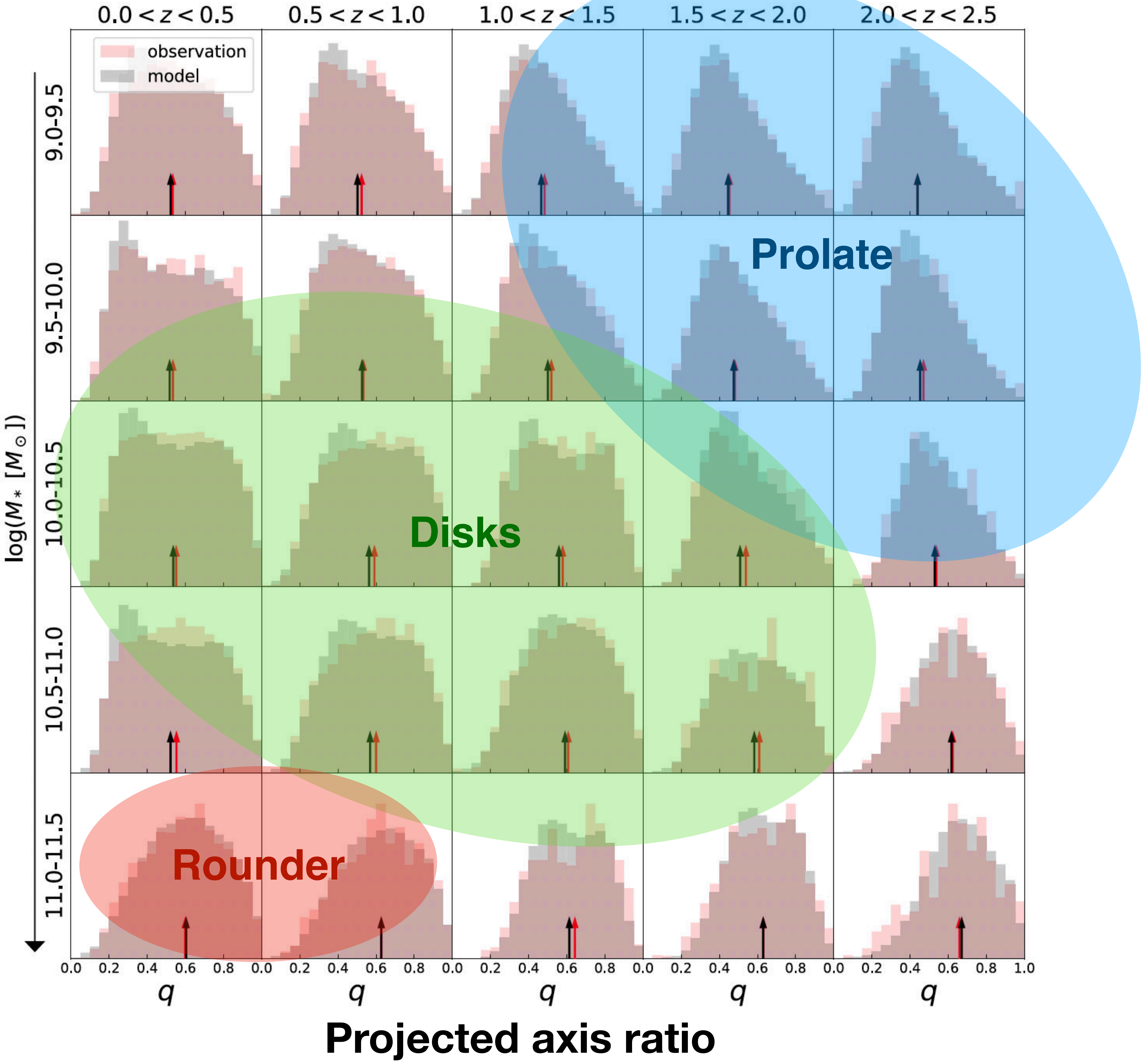

Zhang et al. 2023 (also e.g. van der Wel. 2014; Zhang et al. 2019; Pandya et al. 2023 with JWST)

Star-dust geometry

Mdust↗ with z↗
Re↘ with z↗
A_V does not vary much with z↗
A_V less inclination dependent at high z
⇒ clumpier dust distribution at high z

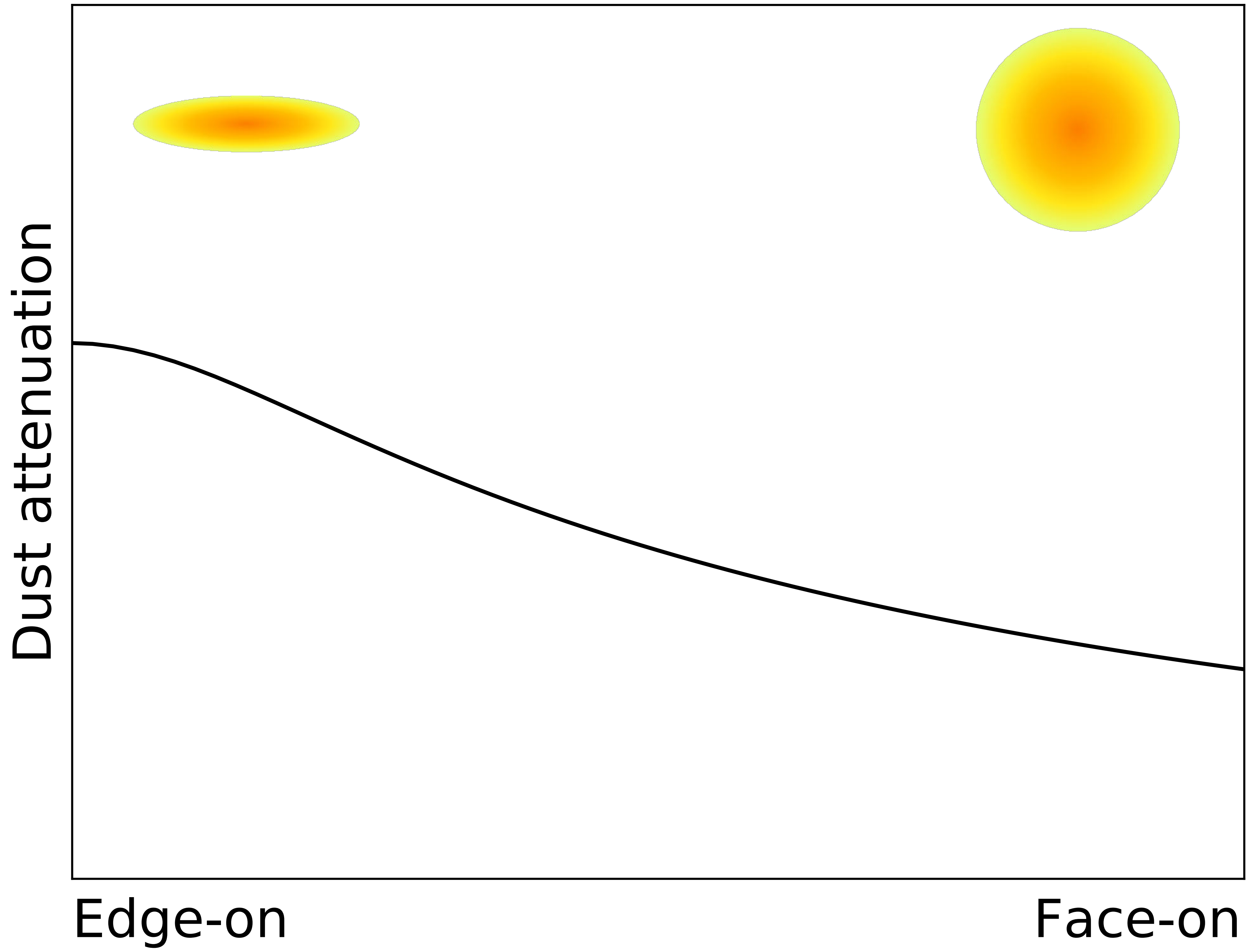

★ median A_V for (M_{star}, z) bin

Zhang,SW+2023; also Patel+2012; Zuckerman+2021; Shapley+2022

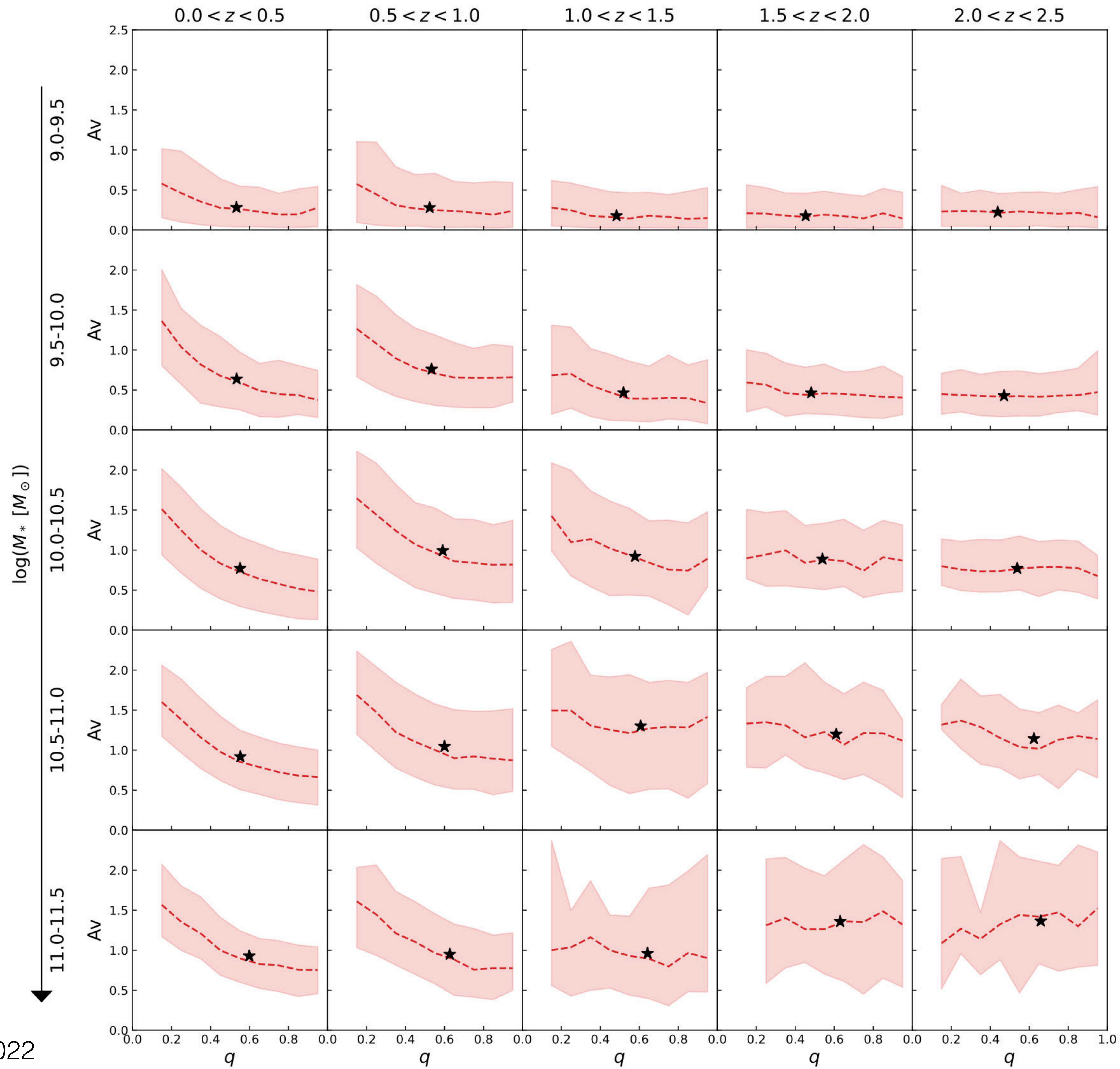

Evolution of morphological types

Sample:

log(M_{star}) > 9
SFGs & QGs

Method:

Convolutional neural networks trained on visual classifications

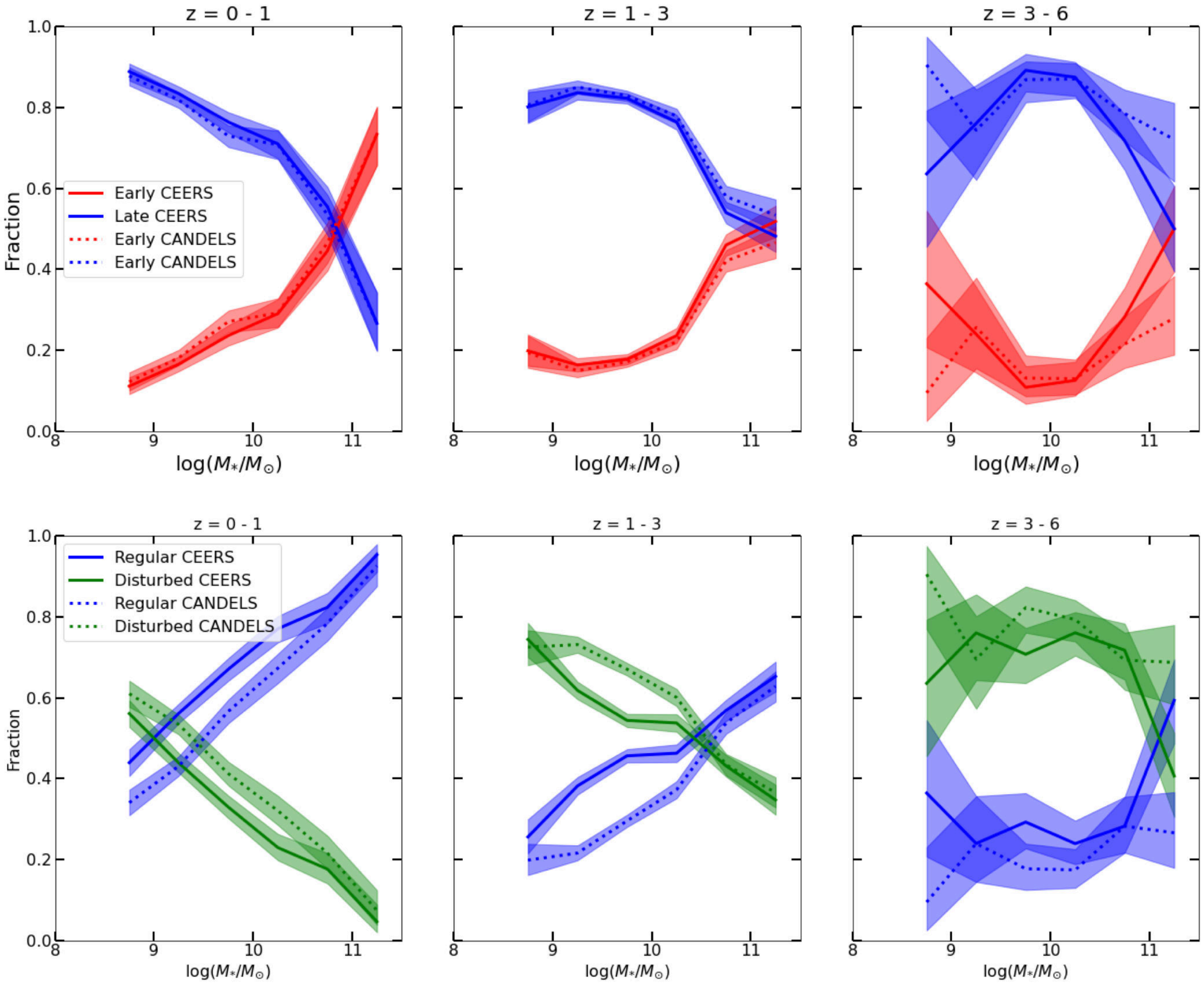

Note:

Disturbed morphology can indicate merger OR in-situ instabilities

Need kinematics to assess!

Huertas-Company et al. 2023

Substructure - bar instabilities at cosmic noon

Cosmic Evolution Early Release Science Survey
CEERS

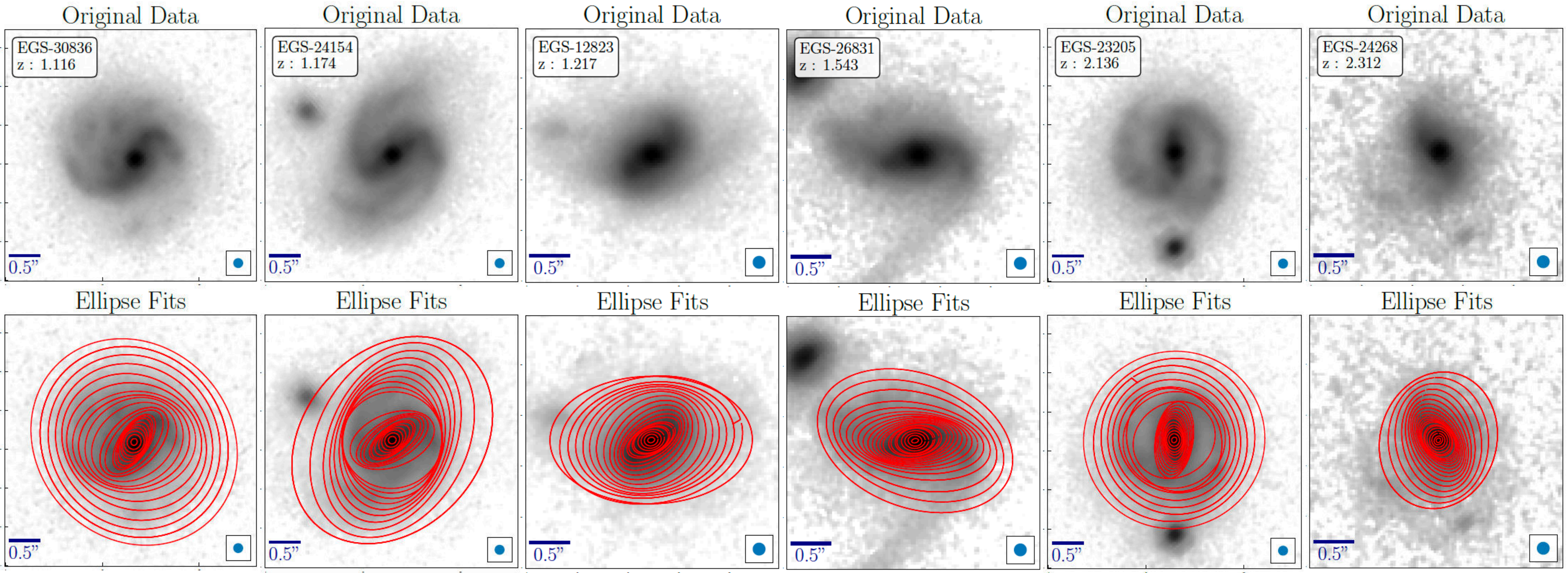

Guo & CEERS team 2023
Costantin & CEERS team 2023, Nature z~3

Substructure - star-forming clumps

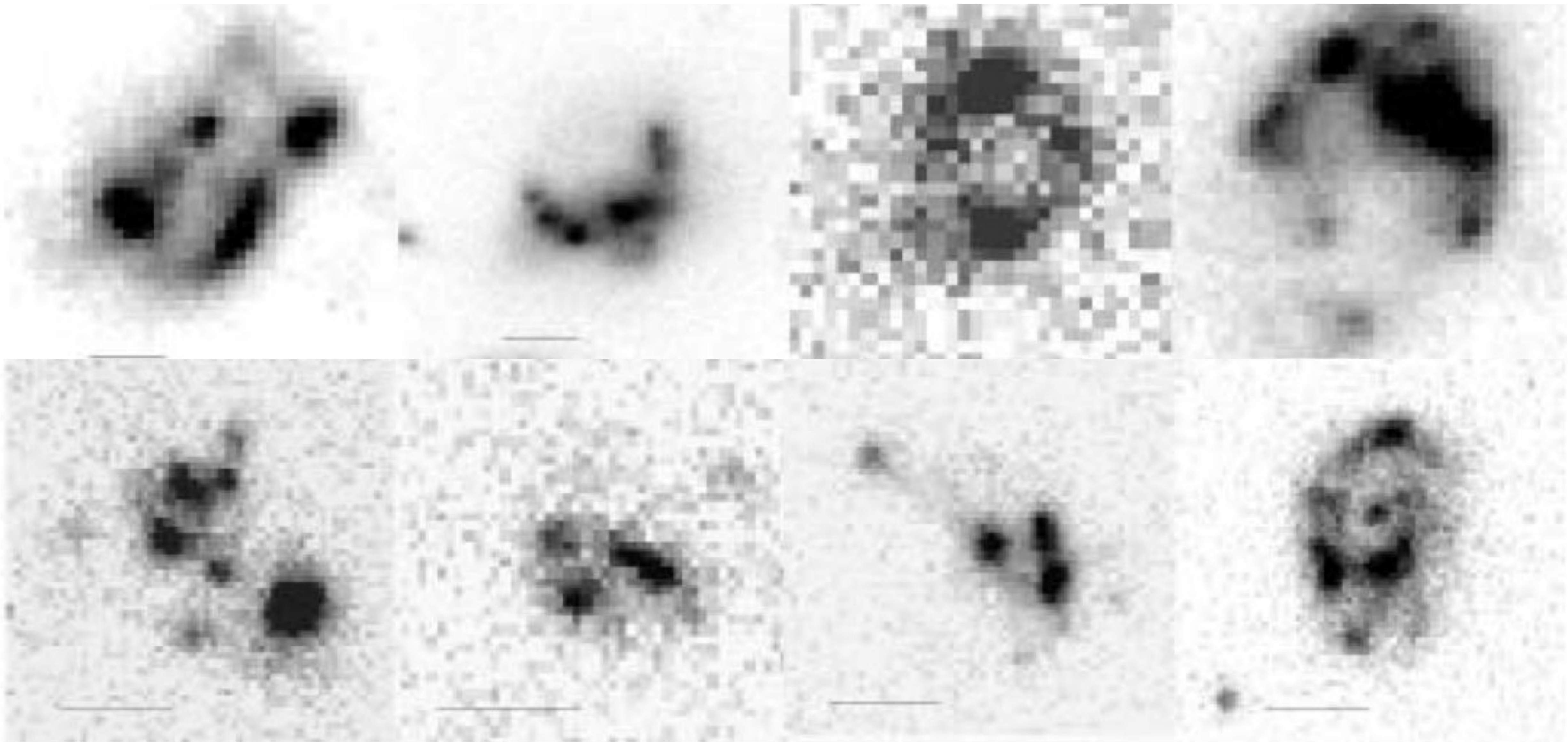

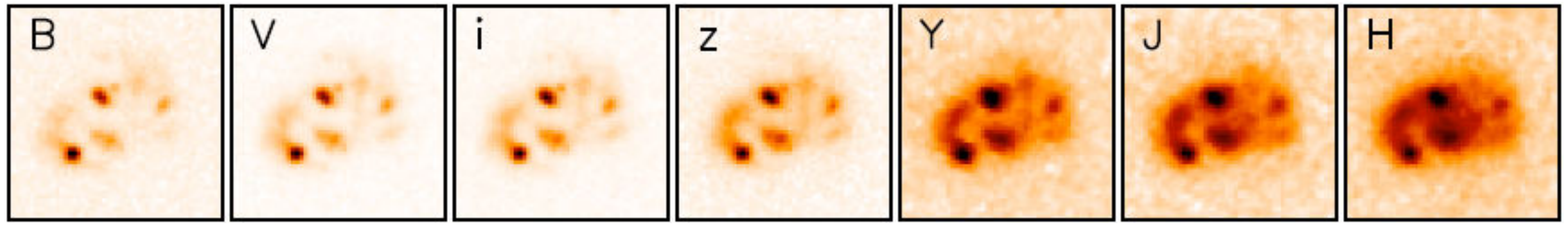

WFC3 (imaging+grism) → Resolved SED modelling for sizeable samples
Wuyts+2012,2013; Guo+2015,2018; Zanella+2019; Huertas-Company+2020; Ginzburg+2021

Incidence of clumpy galaxies

Properties of UV-selected clumps:

* blue colors, high Hα EW → low M/L ratios, enhanced sSFR, young ages
* low Hα/UV → reduced dust attenuation
* modest contribution to UV > contribution to SFR > contribution to Mstar

Elmegreen+2005,2007; Genzel+2011; Förster Schreiber+2011; Wisnioski+2011
rest-UV, Hα (aided by velocity channels) + some initial NICMOS rest-optical

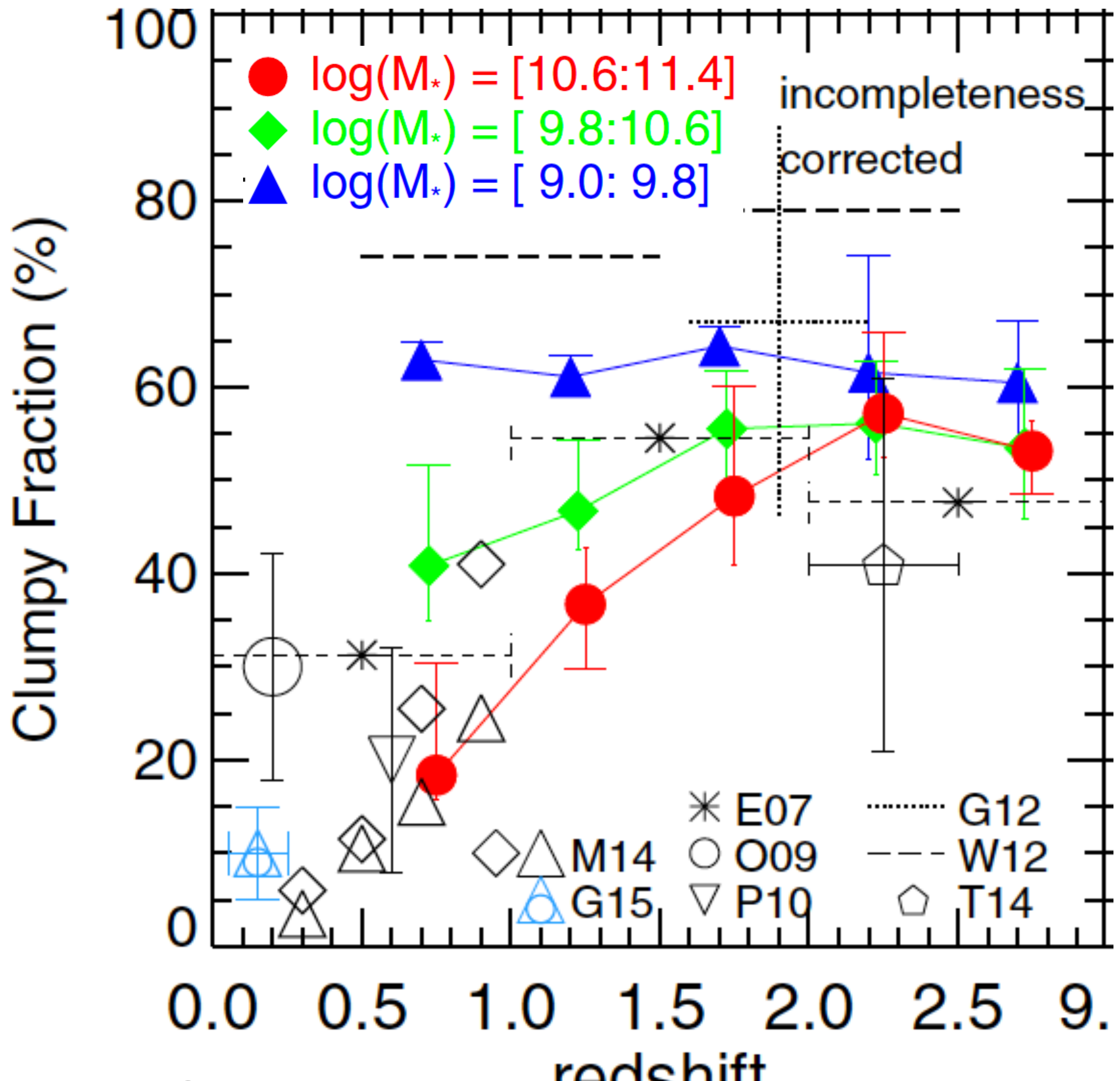

Guo+2015

Substructure - star-forming clumps

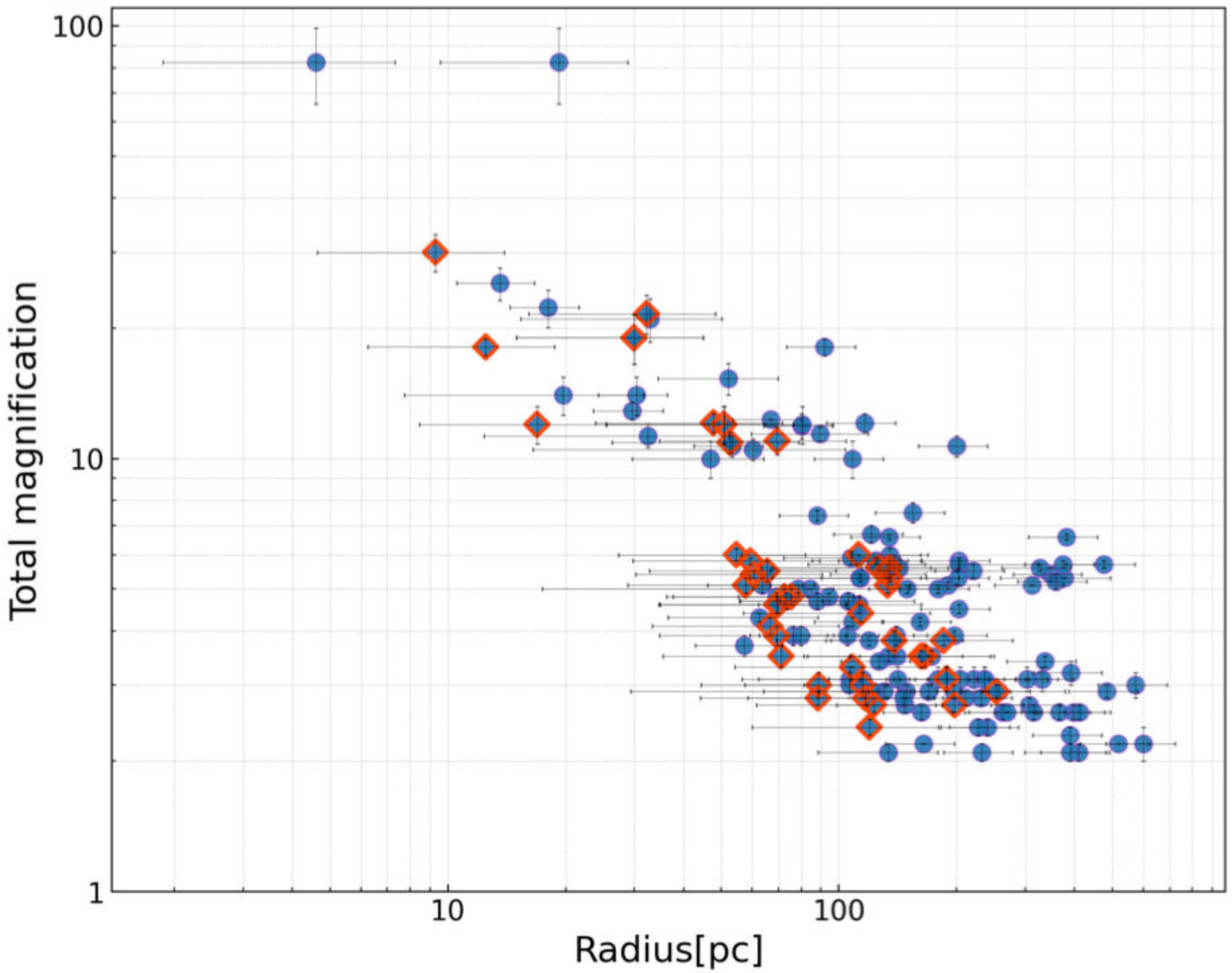

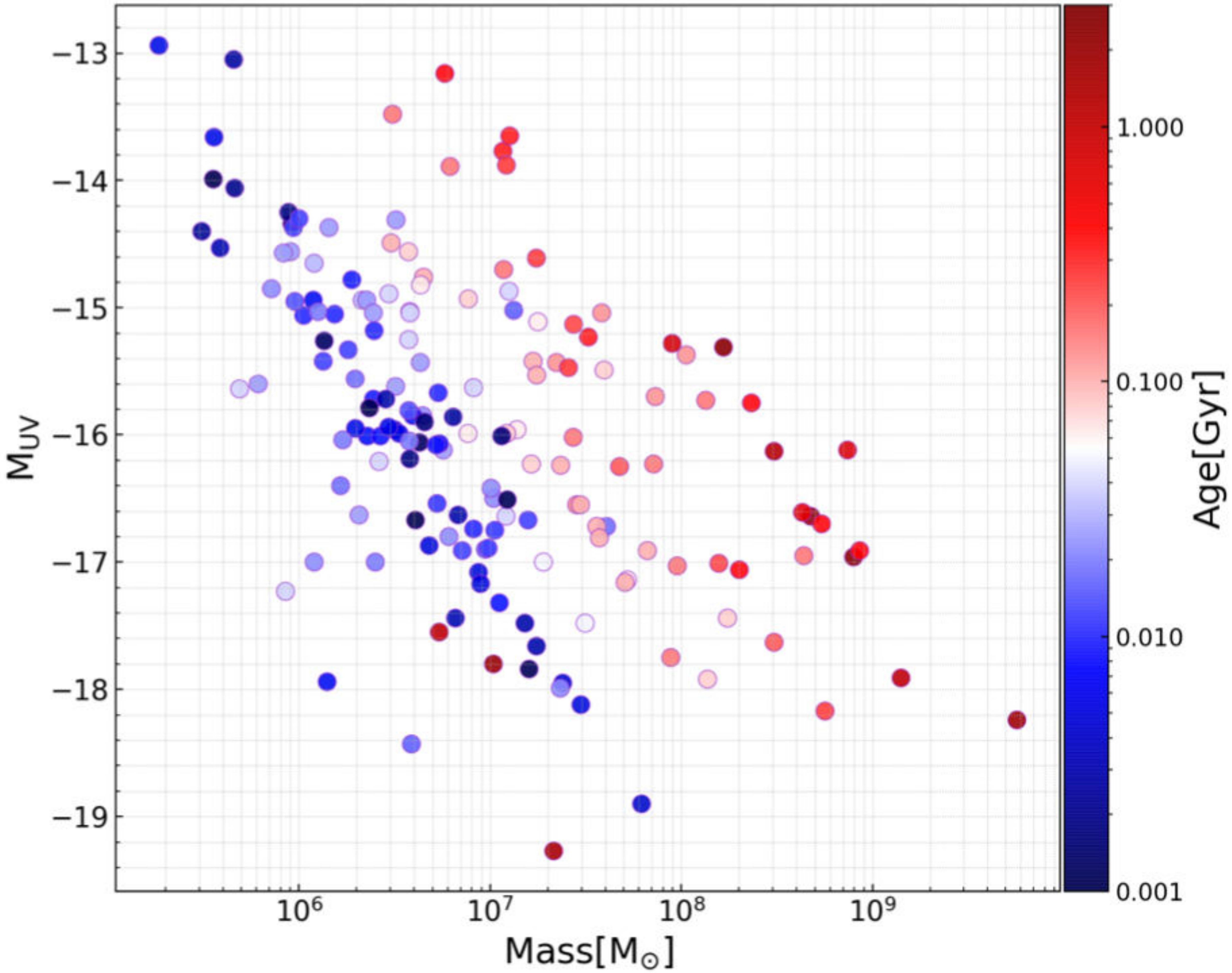

Mestric+2022 166 clumps at z ~ 2 - 6.2 (magnification 2 < μ < 82) behind lensing cluster MACS-J0416 → low clump masses & small (resolution-dependent) sizes

see also Livermore+2012,2015; Dessauges-Zavadsky+2017; Rigby+2017; Cava+2018

also in simulations resolution-dependent clump sizes: Tamburello+2015,2017; Faure+2021 (+ see Huertas-Company+2020 for 3D vs 2D clumps)

Resolved studies of cosmic noon SFGs

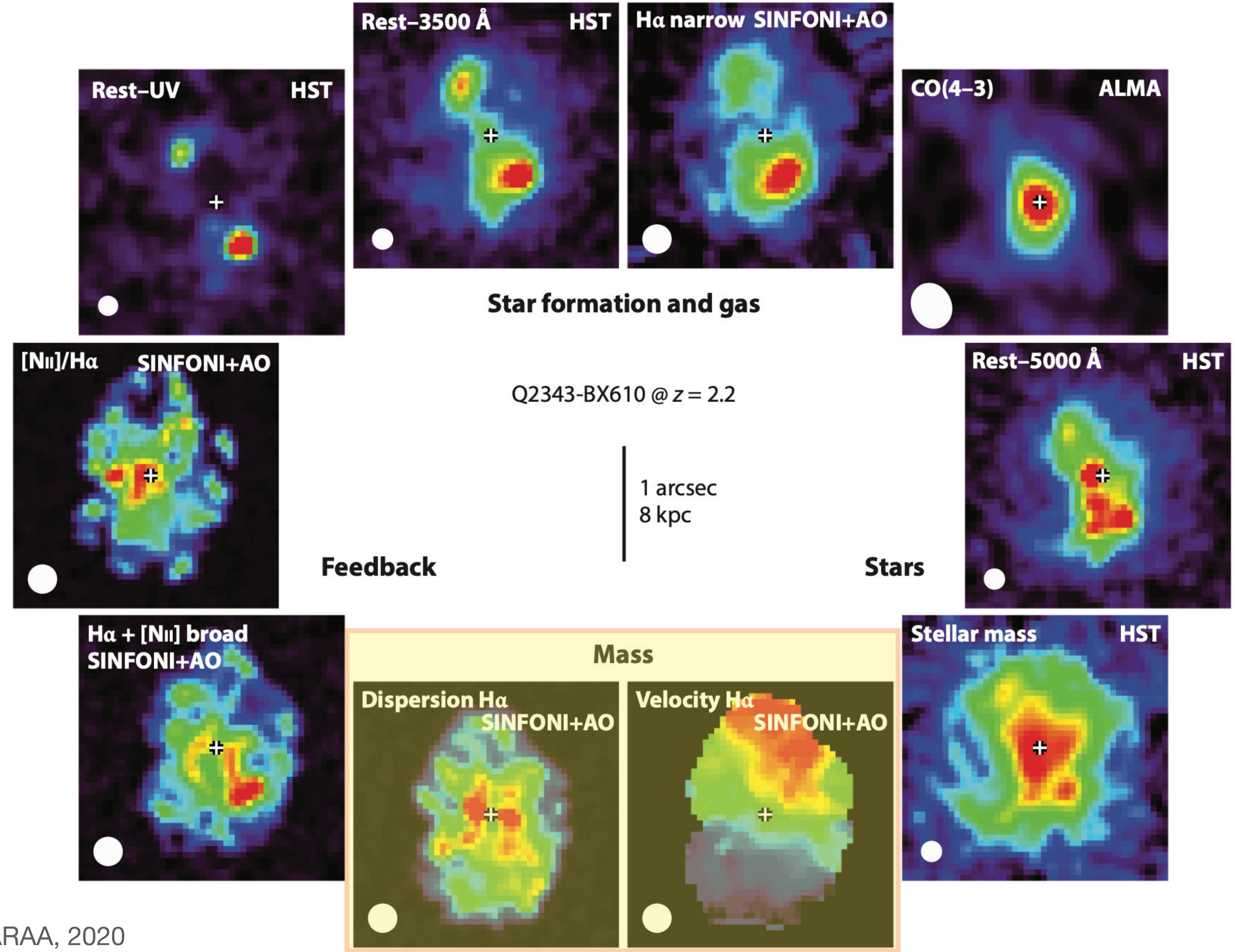

Förster Schreiber & Wuyts, ARAA, 2020

Dynamics - settling of turbulent disks

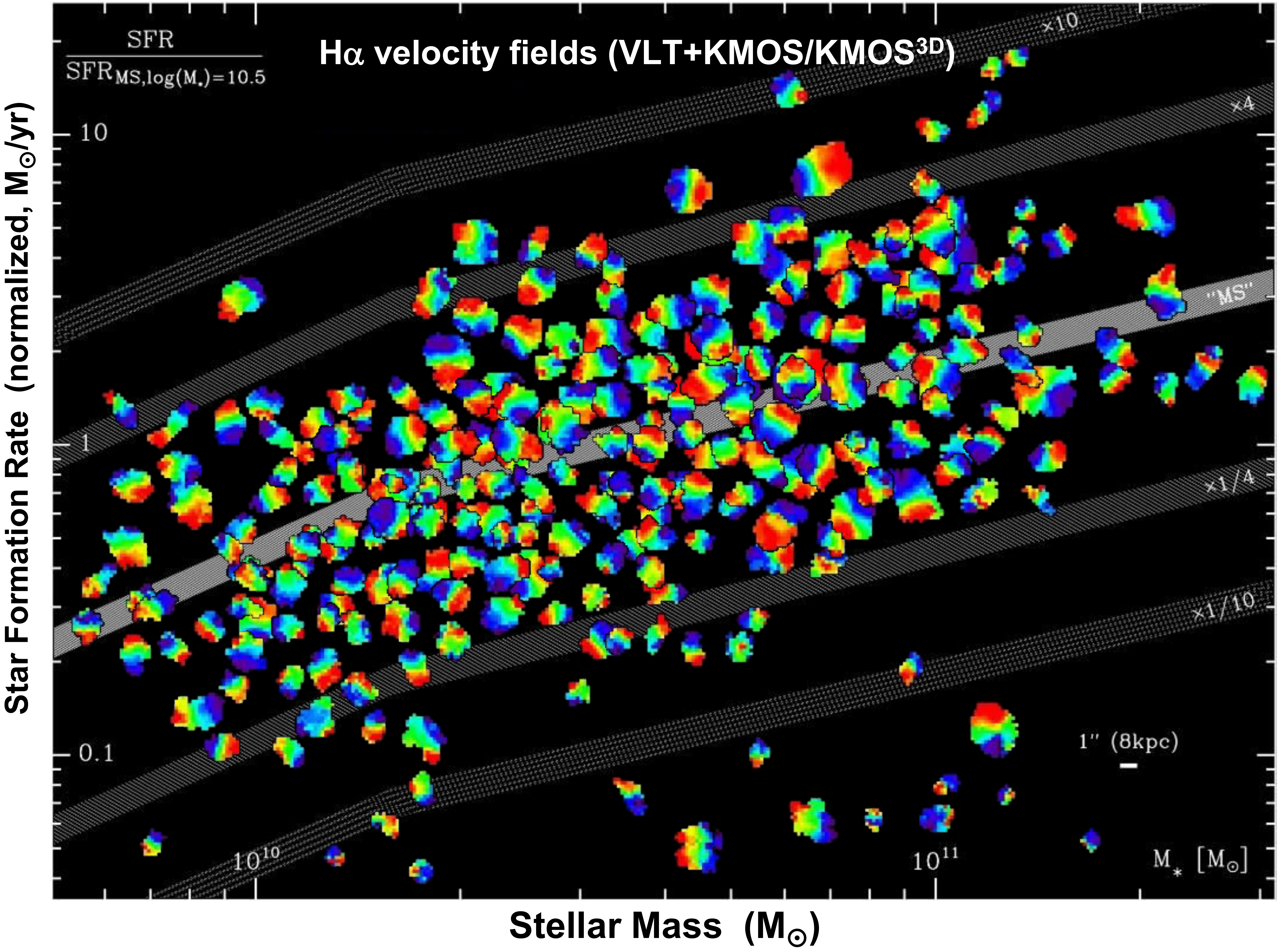

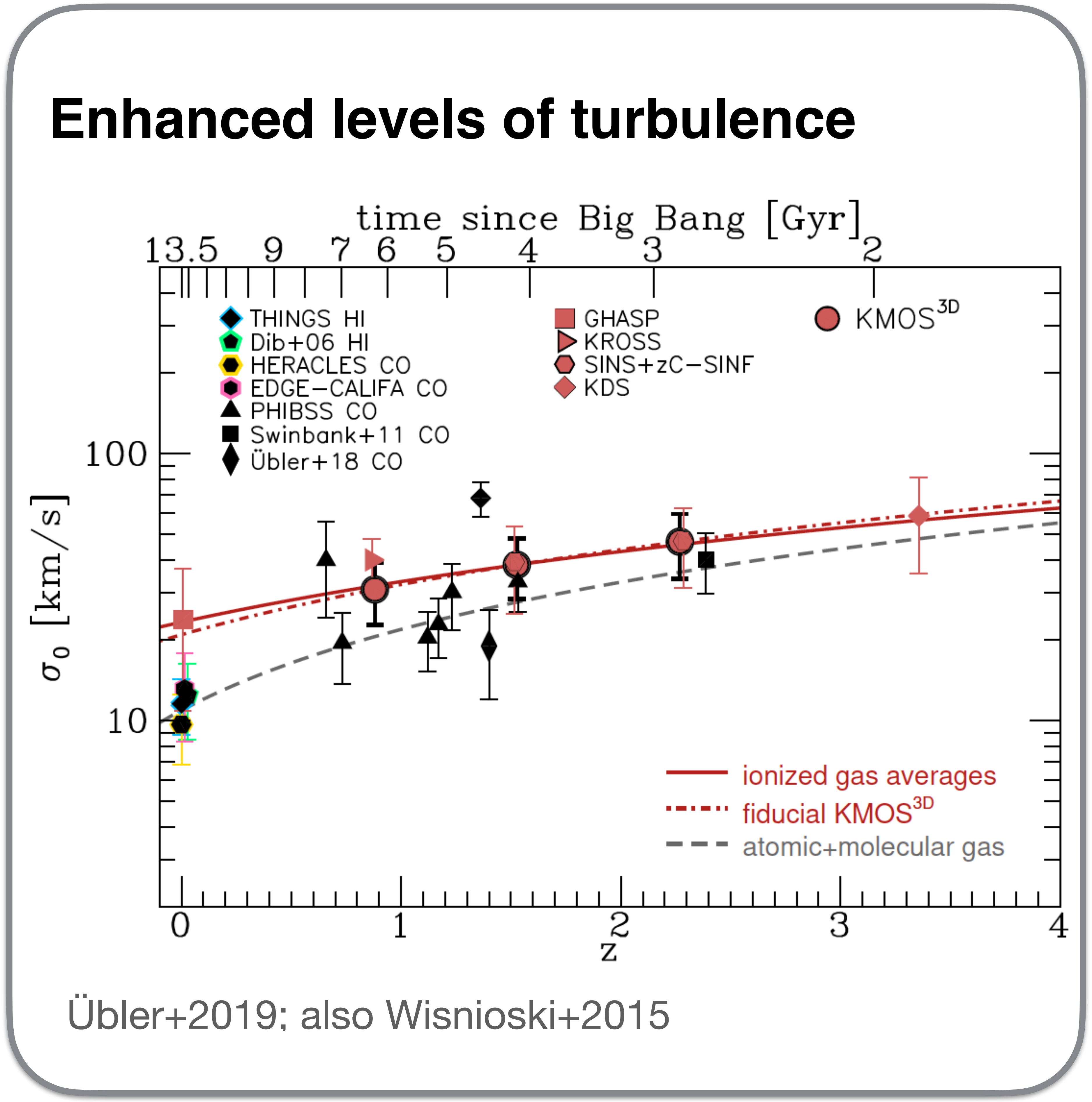

Förster Schreiber & Wuyts, ARAA, 2020; also e.g. Glazebrook+2013; Wisnioski+2015, 2019; Stott+2016; Harrison+2017

Dynamics - settling of turbulent disks

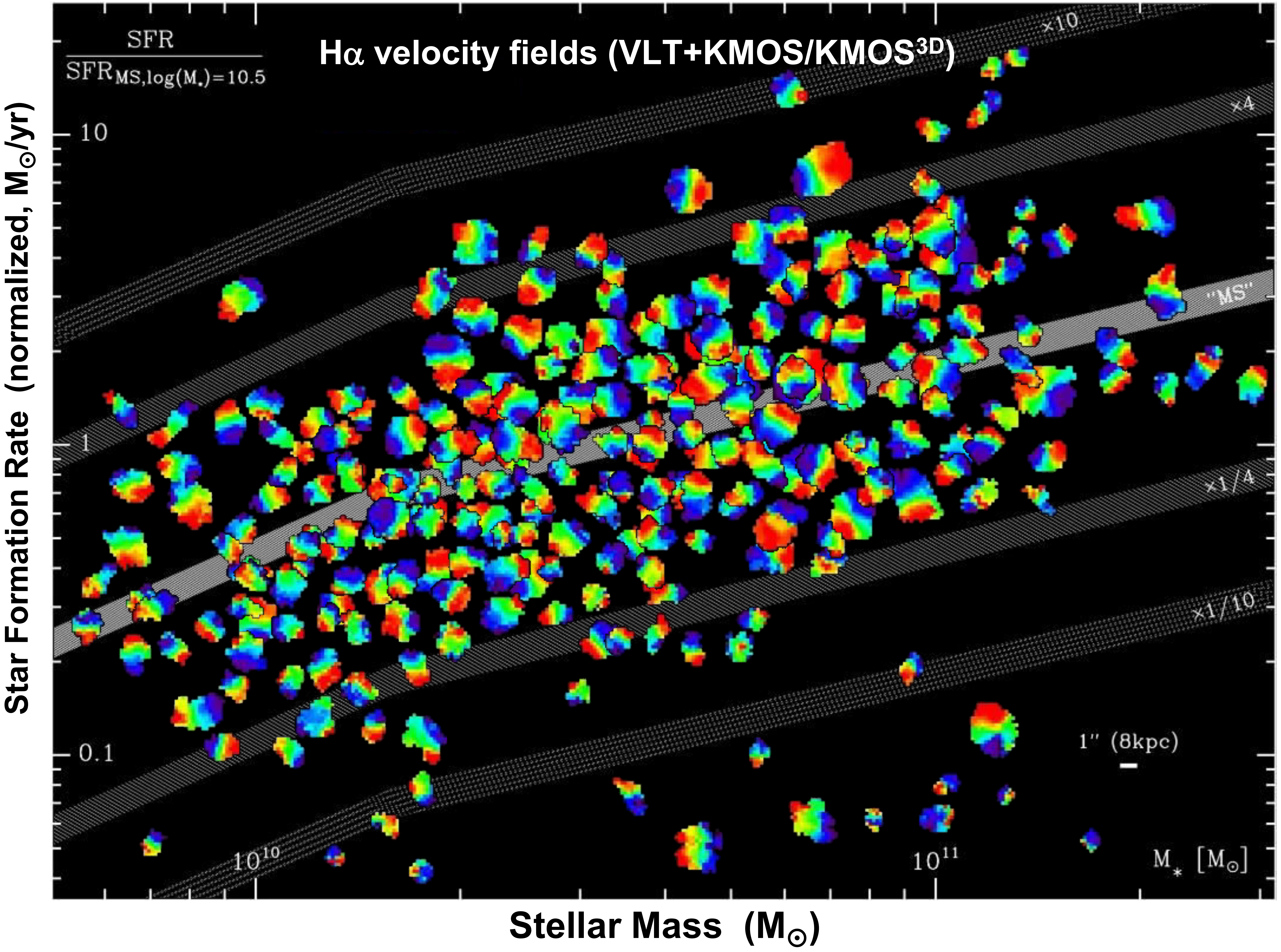

Enhanced levels of turbulence

Disk settling of massive galaxies

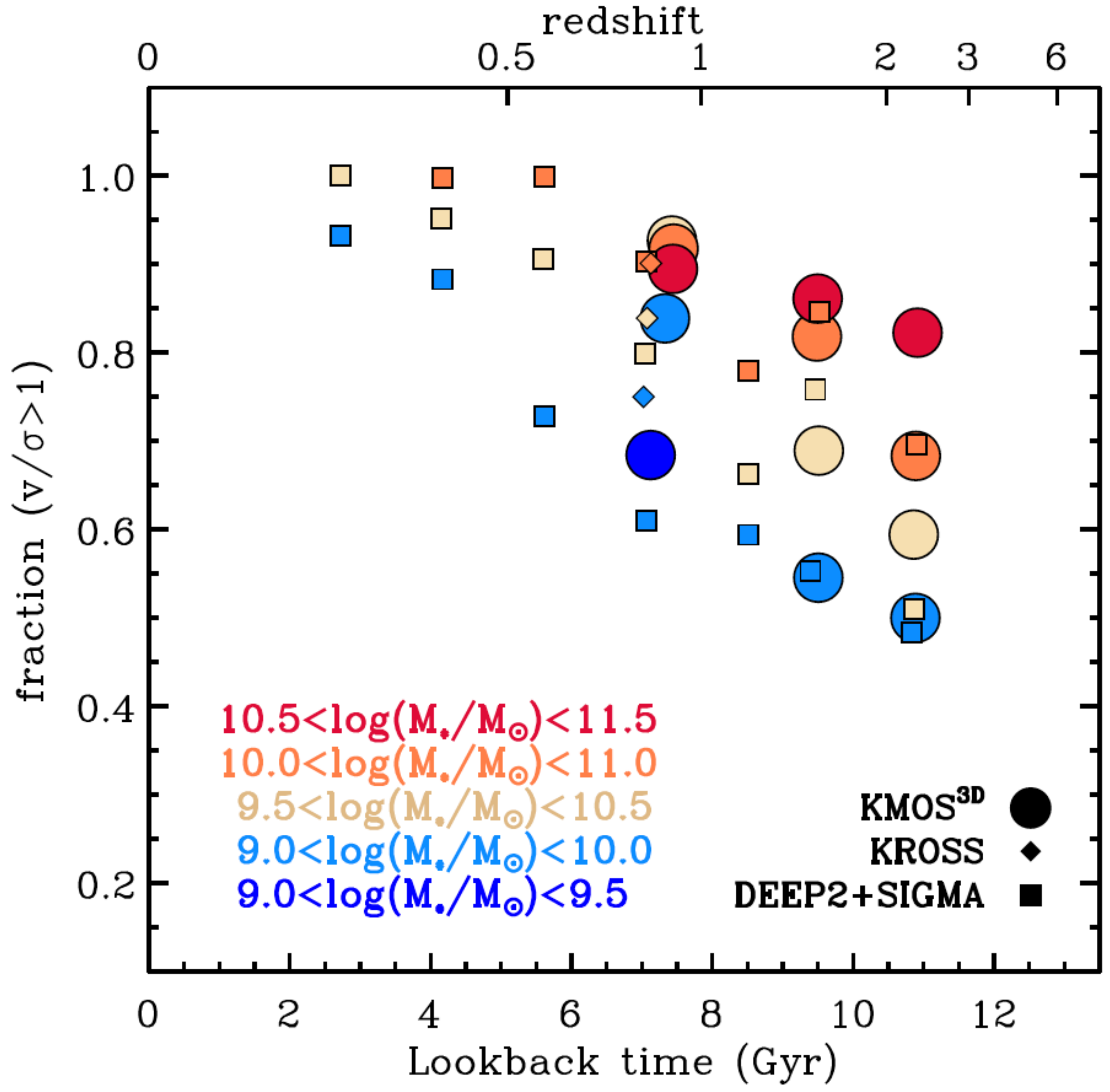

Wisnioski+2019; also Kassin+2012; Simons+2017; Turner+2017; Tiley+2021

Förster Schreiber & Wuyts, ARAA, 2020; also e.g. Glazebrook+2013; Wisnioski+2015, 2019; Stott+2016; Harrison+2017

Dynamics - forward modeling of disk rotation

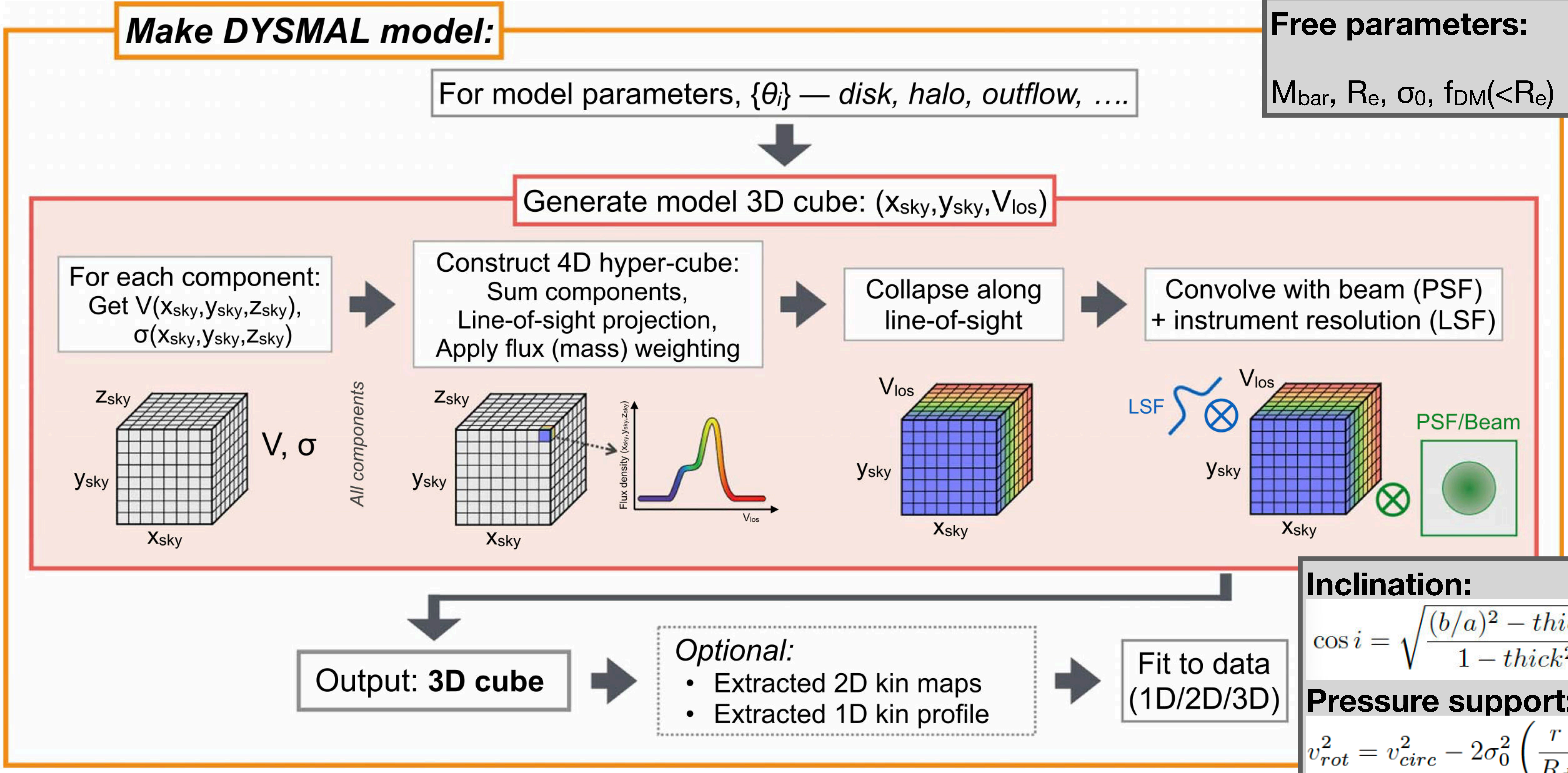

Free parameters:

M_{bar}, R_e, σ_0, $f_{DM}(<R_e)$

Inclination:

$$\cos i = \sqrt{\frac{(b/a)^2 - thick^2}{1 - thick^2}}$$

Pressure support:

$$v_{rot}^2 = v_{circ}^2 - 2\sigma_0^2 \left(\frac{r}{R_d}\right)$$

Price et al. 2021 (also Cresci+09, Davies+11, Wuyts+16, Genzel+17; Übler+18; other codes: Galpak3D Bouché et al. 2015; 3DBAROLO Di Teodoro & Fraternali 2015)

Dynamics - forward modeling of disk rotation

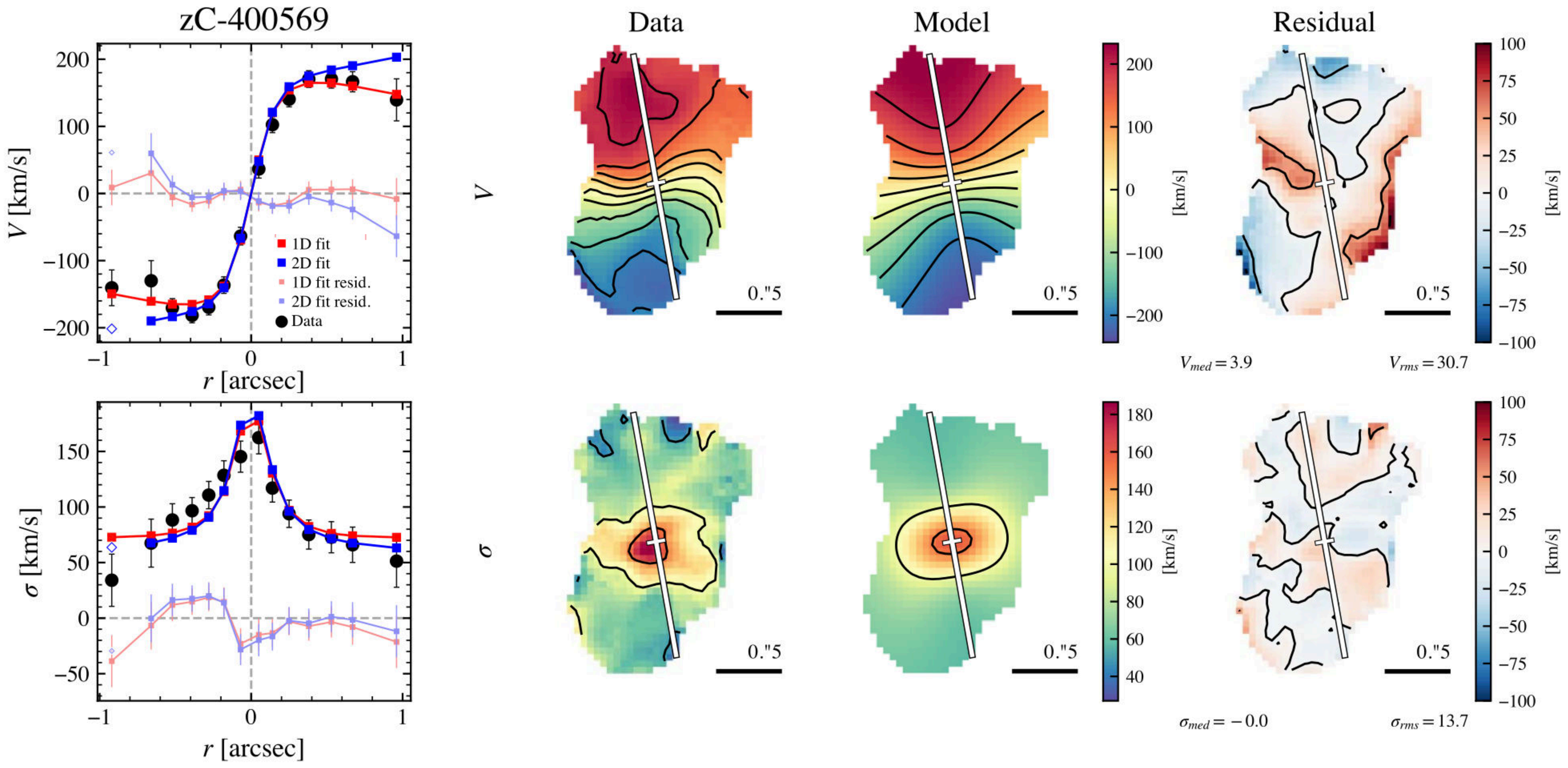

Price et al. 2021

Dynamics - forward modeling of disk rotation

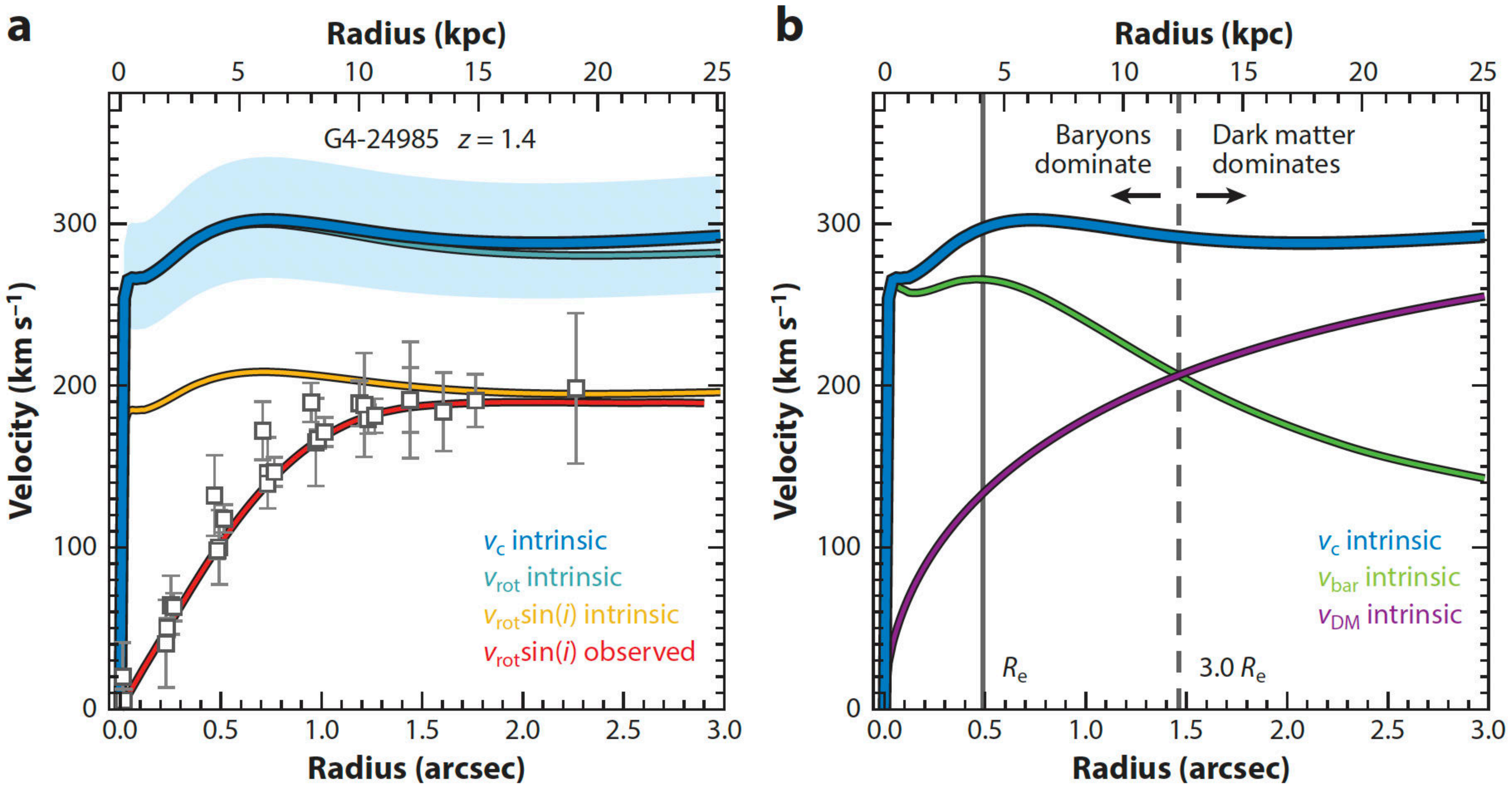

Förster Schreiber & Wuyts, ARAA, 2020

Baryon dominance within R_e for high Σ_{bar} disks

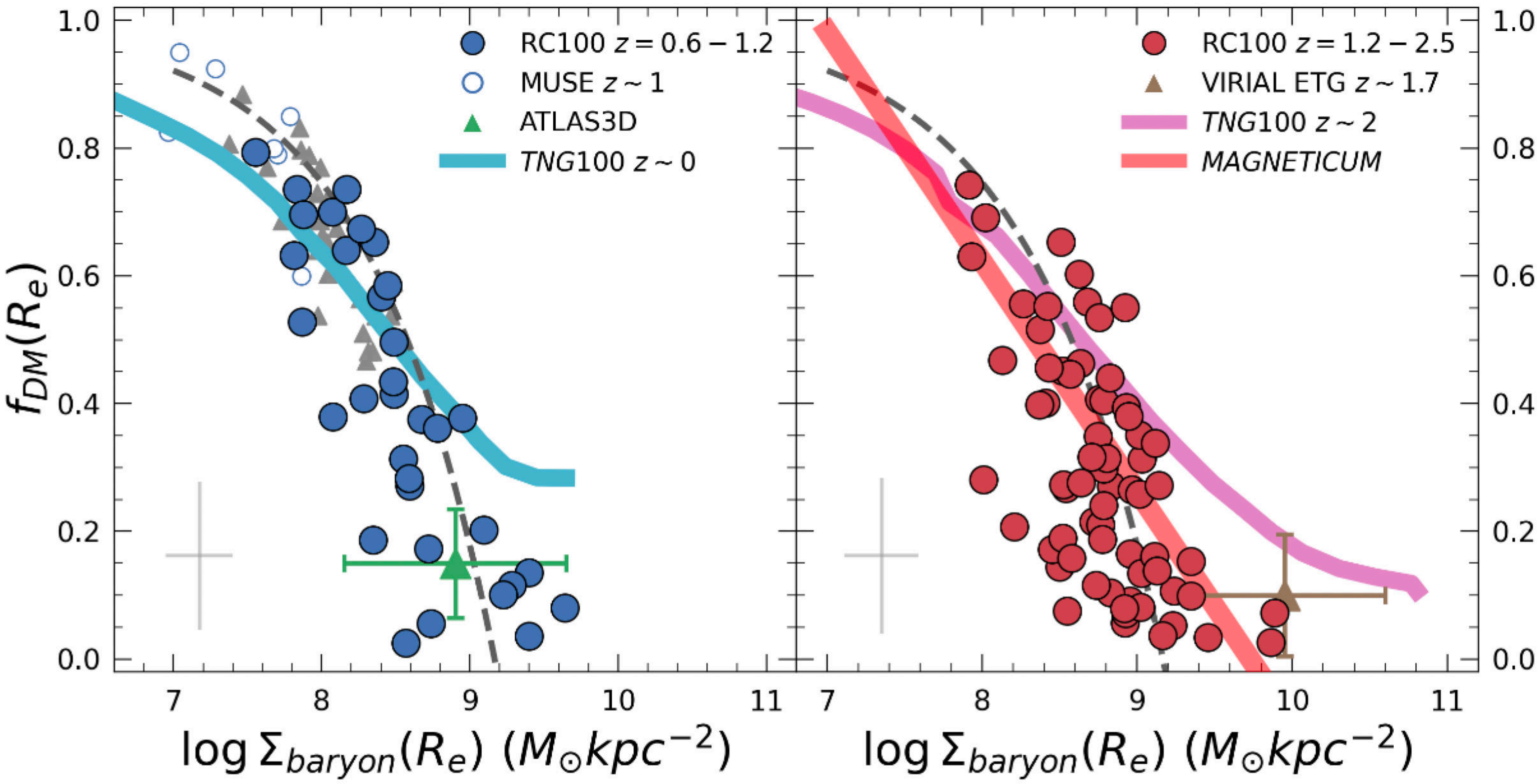

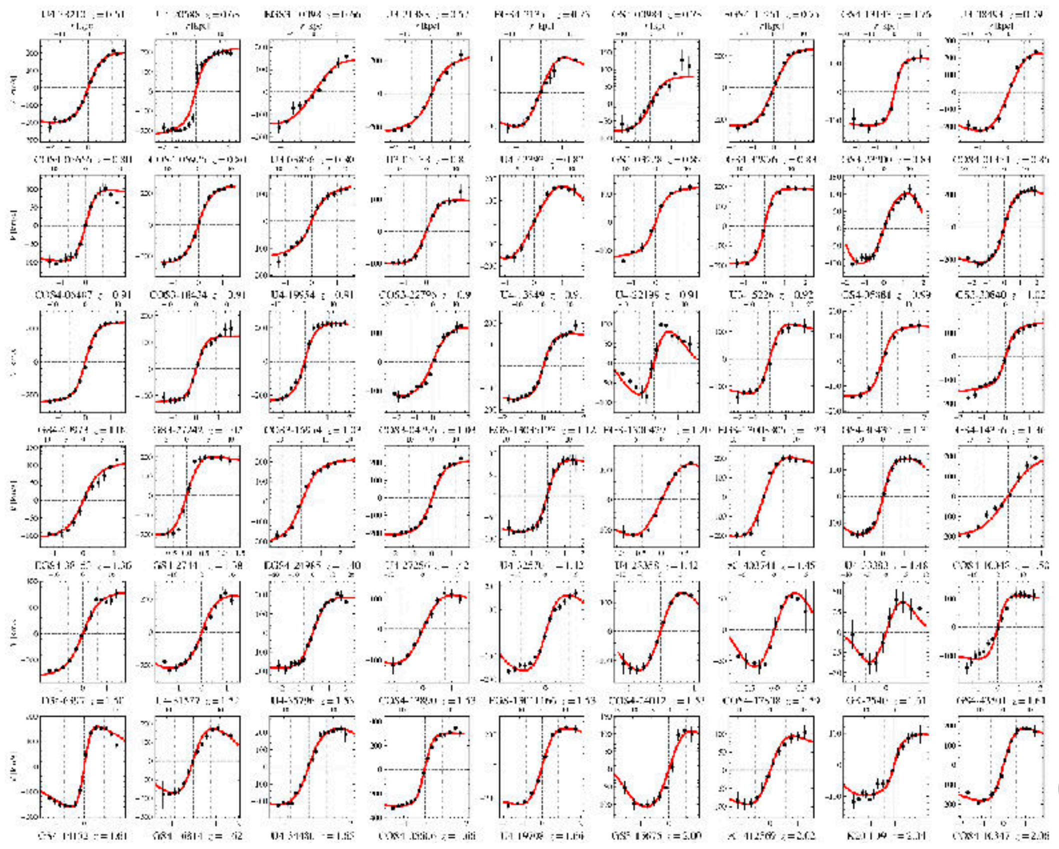

(54% of sample shown)

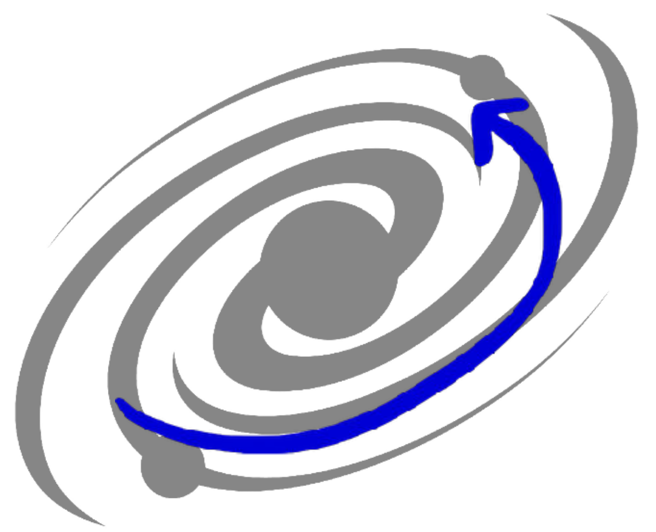

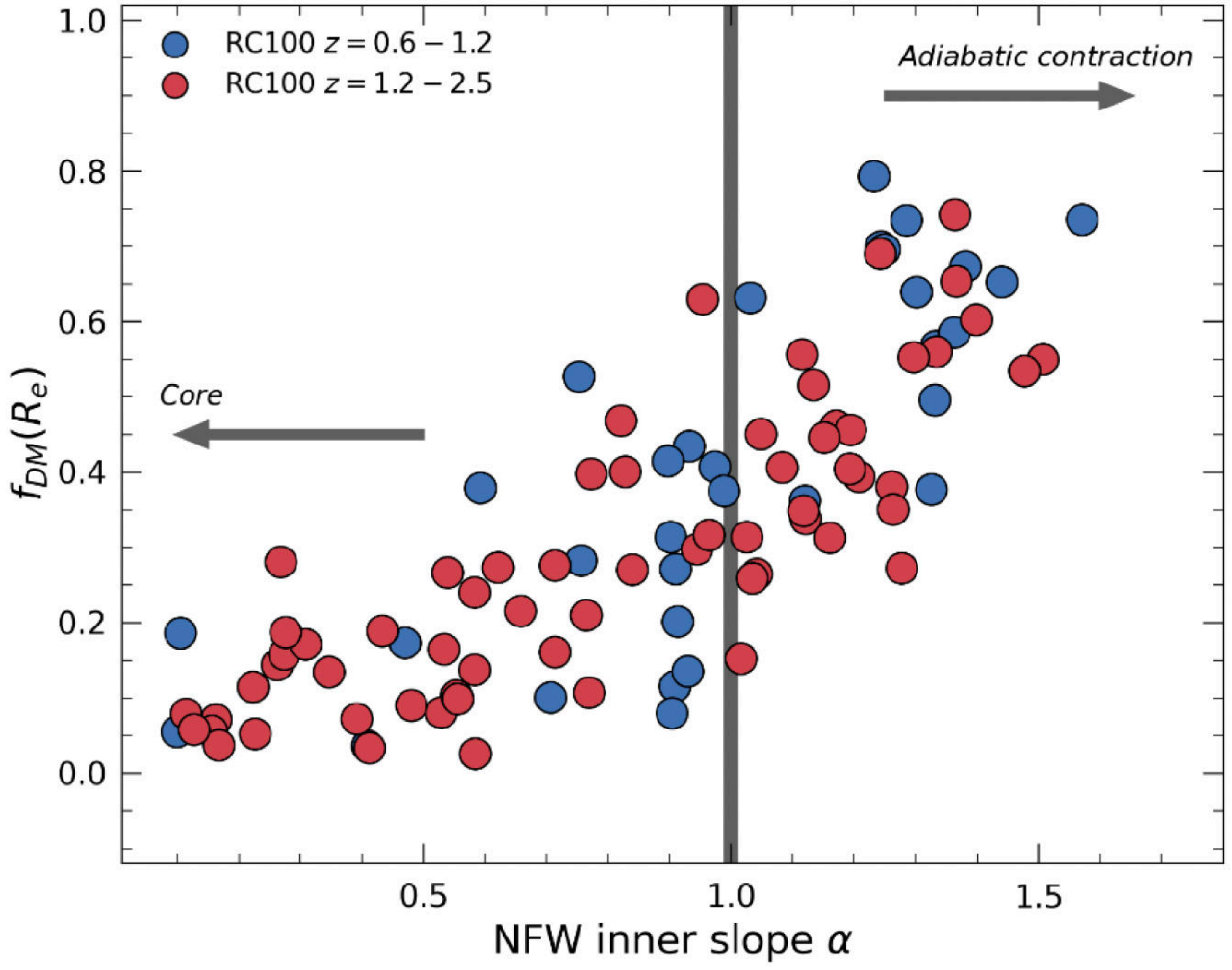

Nestor Shachar+23; also Wuyts+16; Genzel+17,22; Lang+17; Mendel+20; Price+21
See Bouché+2022 for cores in low-M, DM-dominated galaxies at z~1

Theory: Lovell+2018; Dekel+2021; Übler+2021

Further observational perspectives: Tiley+2019; Sharma+2021; Lelli+2021

Dynamics - non-circular motions

Price+2021; also Genzel+2023

Kinematics - feedback

M82: blue-white: optical/near-infrared; red: ionized hydrogen gas

Galactic outflows

Drivers:
Star formation and/or AGN

Method:
Broad velocity components to emission lines or absorption lines (MgII, NaD)

For AGN, distinguish from Broad Line Regions (BLRs): presence broad components in forbidden lines & spatially resolve

Location:
Star-forming clumps and/or nucleus

Incidence:
Above MS (SF)
High-mass end (AGN)

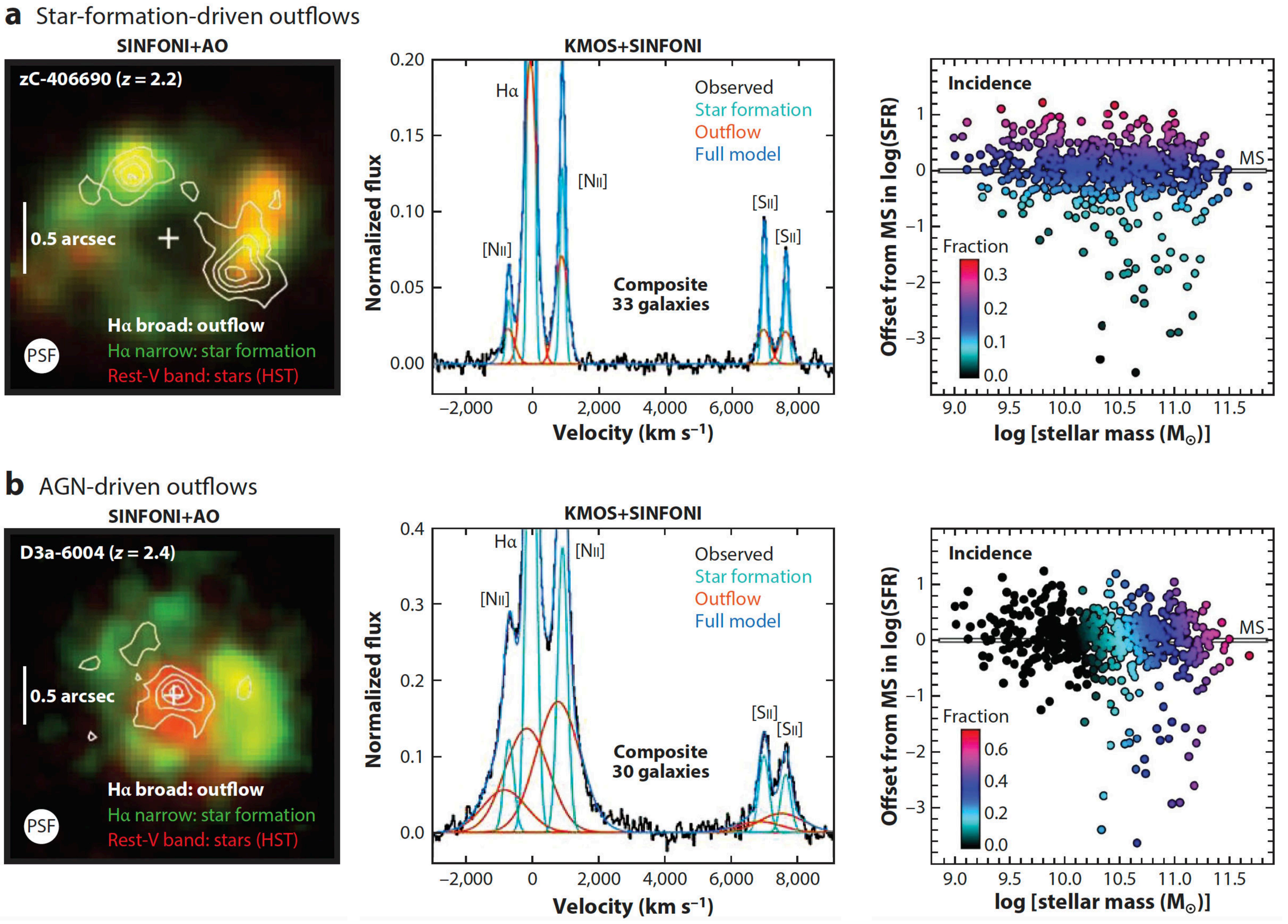

Förster Schreiber & Wuyts, ARAA, 2020
also Newman+2012; FS+14,19; Swinbank+2019; Leung+2019; Herrera-Camus+2019; Davies+19,20; Spilker+2020; Kakkad+2020; Weldon+2022; Concas+2022

Galactic outflows - incidence

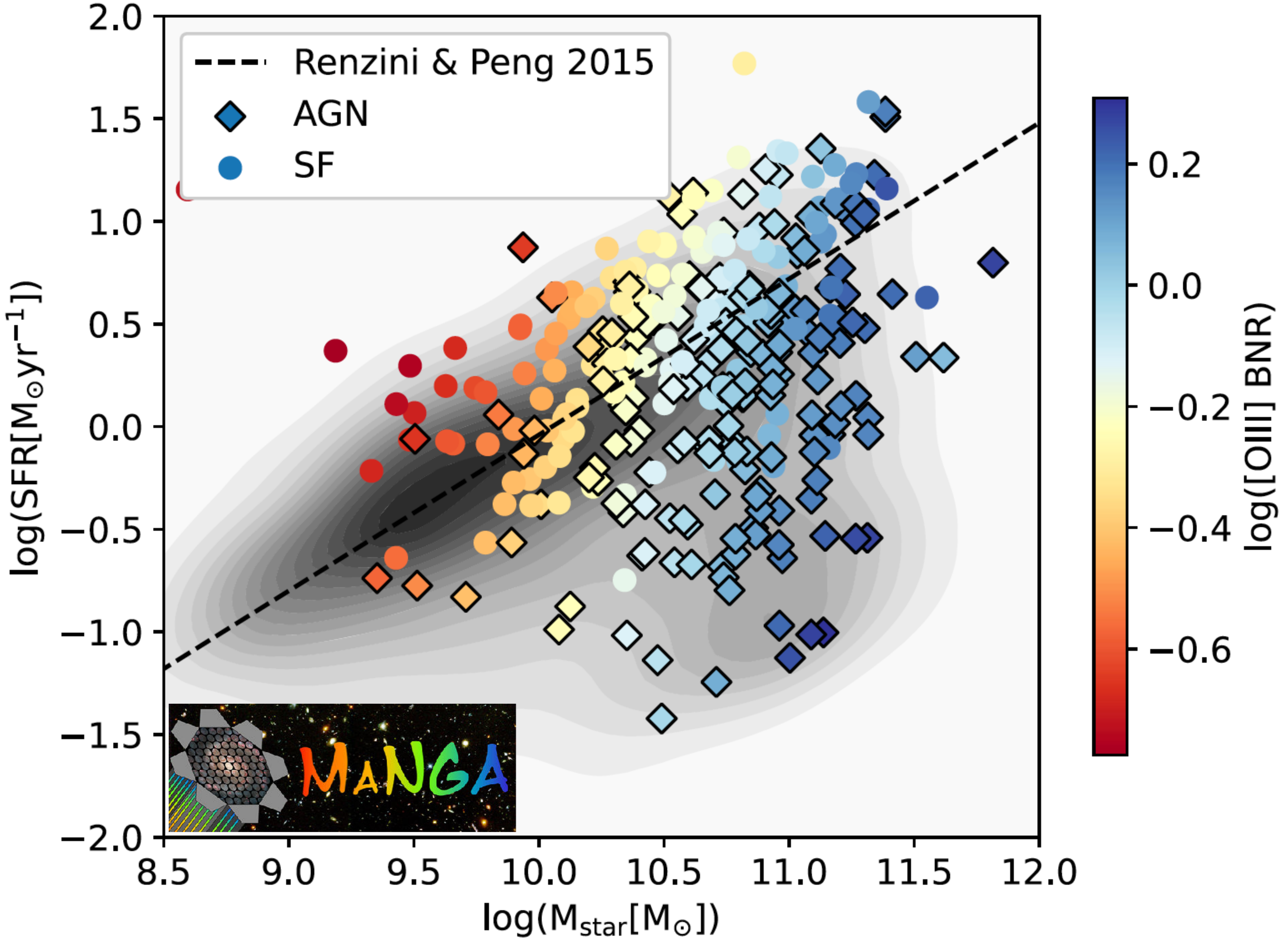

Avery, SW et al. 2021,2022

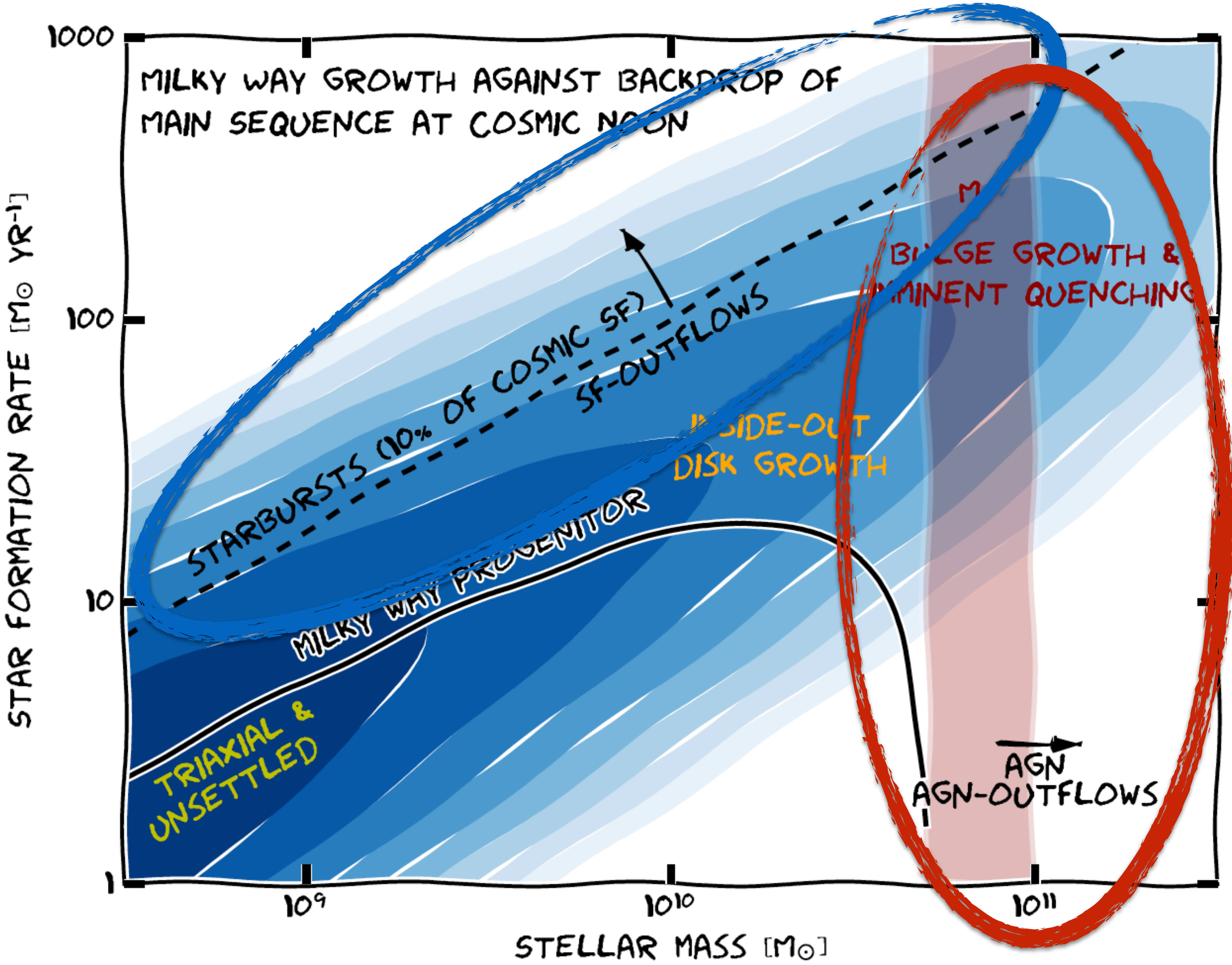

Förster Schreiber & Wuyts 2020, ARAA

Winds from normal nearby galaxies
Ionized & neutral gas phase
Incidence, scaling relations & nature

also Roberts-Borsani & Saintonge 2019 + MEGAFLOW e.g. Langan+2023 for CGM-scale flows
High-z counterpart: Förster Schreiber+2019; Swinbank+2019; Concas+2022

Galactic outflows - physics & scaling relations

$v_{out} = |\Delta v_{broad} - 2\ \sigma_{broad}|$ "outflow velocity"

$M_{out} \propto L_{broad} / n_{e,out}$ with n_e from [SII] doublet ratio

$\dot{M}_{out} = M_{out} \times (v_{out} / R_{out})$ where R_{out} requires AO "mass outflow rate"

$\eta = \dot{M}_{out} / SFR$ "mass loading"

$\dot{E}_{out} = \frac{1}{2} \dot{M}_{out} v_{out}^2$ "energy injection rate"

$\dot{p}_{out} = \dot{M}_{out} v_{out}$ "momentum injection rate"

Förster Schreiber & Wuyts, ARAA, 2020
also Newman+2012; FS+14,19; Swinbank+2019; Leung+2019; Herrera-Camus+2019; Davies+19,20; Spilker+2020; Kakkad+2020; Weldon+2022; Concas+2022

Galactic outflows - physics & scaling relations

$v_{out} = |\Delta v_{broad} - 2\ \sigma_{broad}|$ "outflow velocity"

$M_{out} \propto L_{broad} / n_{e,out}$ with n_e from [SII] doublet ratio

$\dot{M}_{out} = M_{out} \times (v_{out} / R_{out})$ where R_{out} requires AO "mass outflow rate"

Challenges: geometry; stacking; multi-phase (ionized/atomic/molecular); launching vs escaping

Opportunities: towards outflow scaling relations

See Avery+21,22 for a local benchmark on incidence, multi-phase detectability, and scaling relations for winds from normal nearby galaxies augmented with Arribas+2014; Fluetsch+2019 for more extreme (U)LIRGS

Star-forming galaxies at cosmic noon

Förster Schreiber & Wuyts 2020, ARA&A, 58, 661

Observational landscape

Axes of progress

Lookback survey design

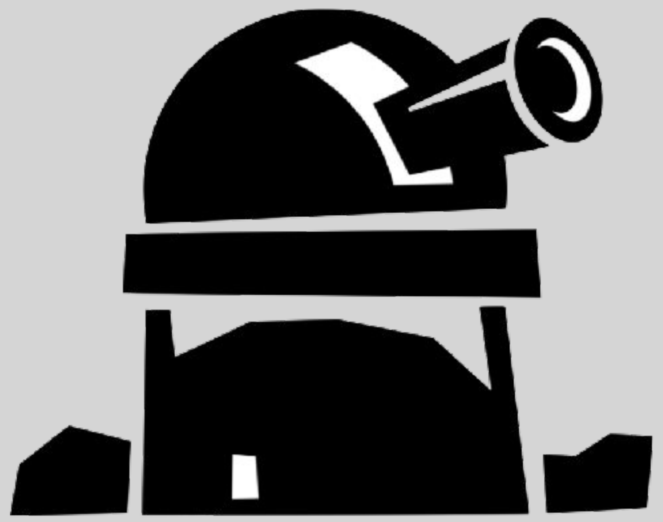

Global

Census

Scaling relations

Evolution

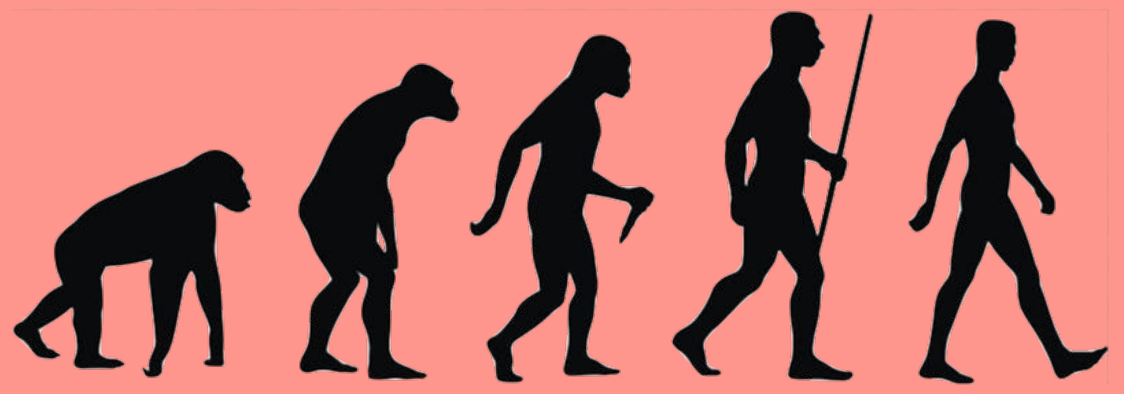

Resolved

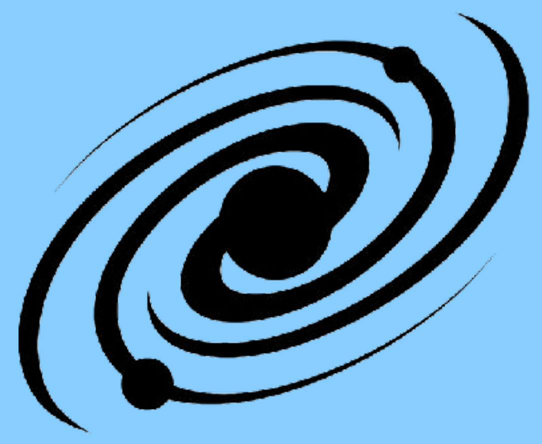

Galaxy sizes

Morphology, shapes & substructure

Disk settling

Kinematics - circular motions

Kinematics - non-circular motions

Kinematics - feedback

Powerful new facilities…

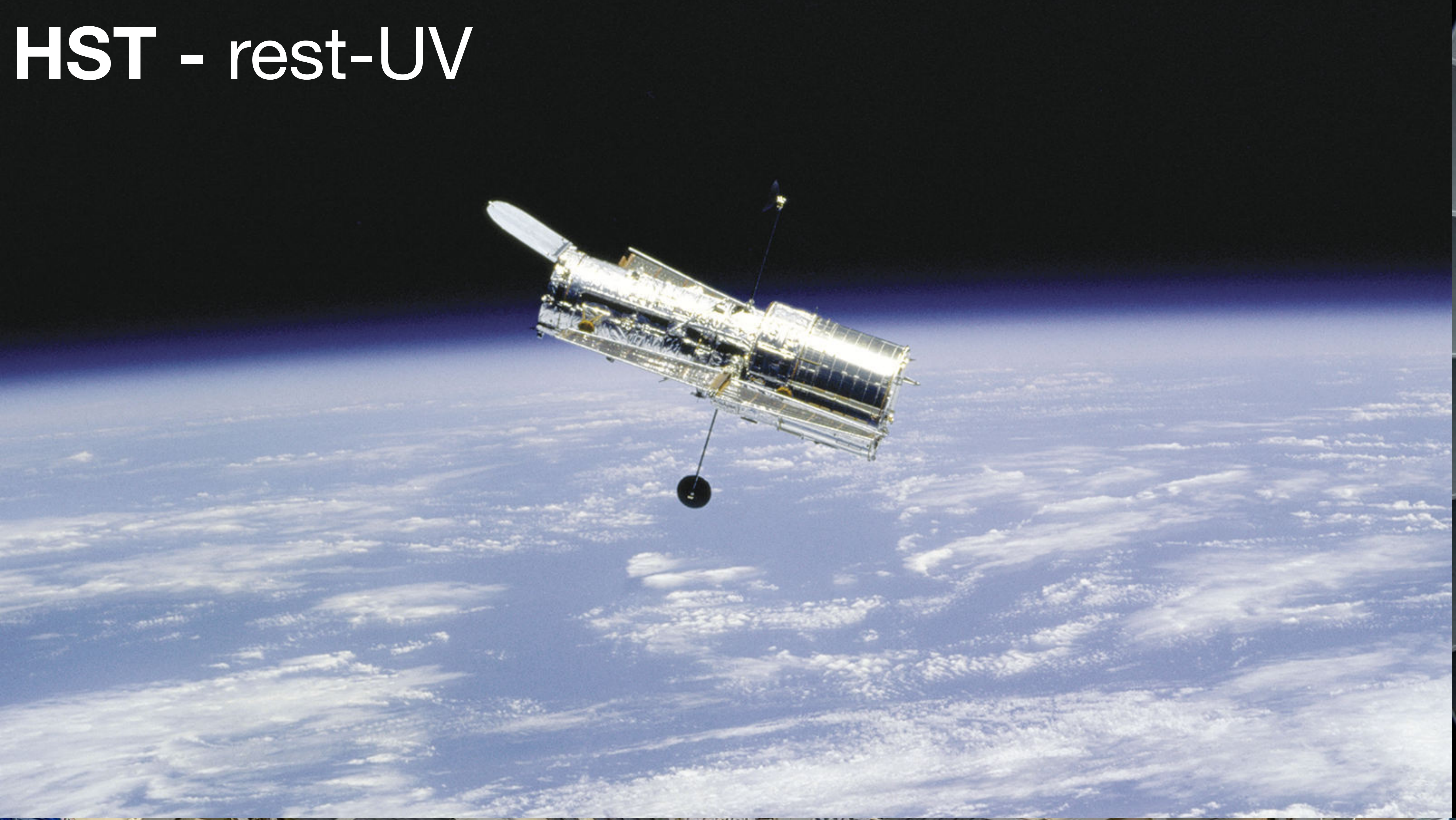
HST - rest-UV


JWST - resolution, sensitivity, longer λ


VLT/ERIS - improved AO & sensitivity IFU

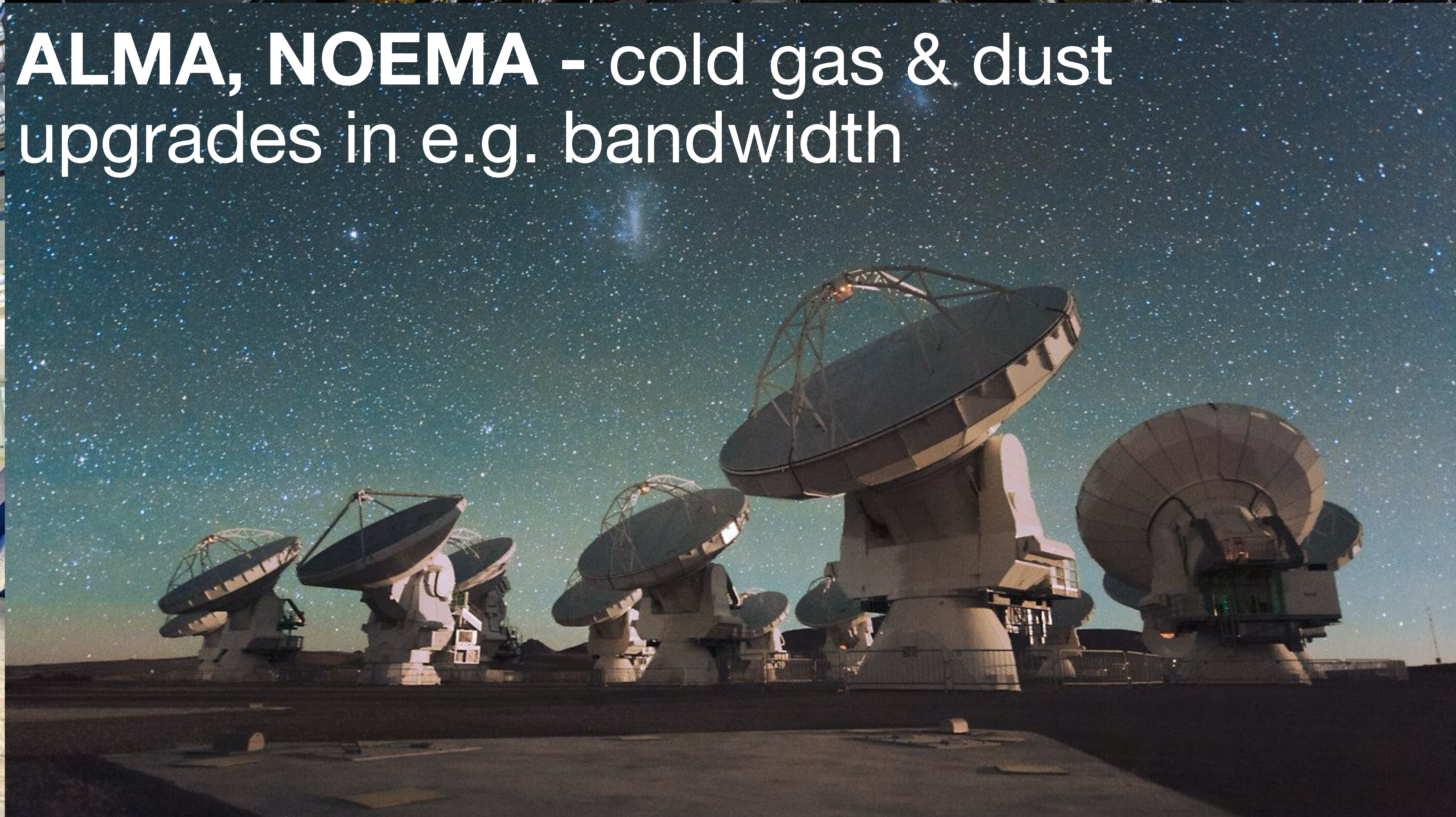
ALMA, NOEMA - cold gas & dust
upgrades in e.g. bandwidth

Extremely Large Telescopes

ELT (39.3m), GMT (25.4m), TMT (30m)

ELT first light instruments:
MICADO - diffraction limited imager
HARMONI - near-infrared integral field spectrograph
2nd generation: MOSAIC - multi-object spectrograph

Förster Schreiber & Wuyts, ARAA, 2020


Vera C. Rubin Observatory (optical imaging)

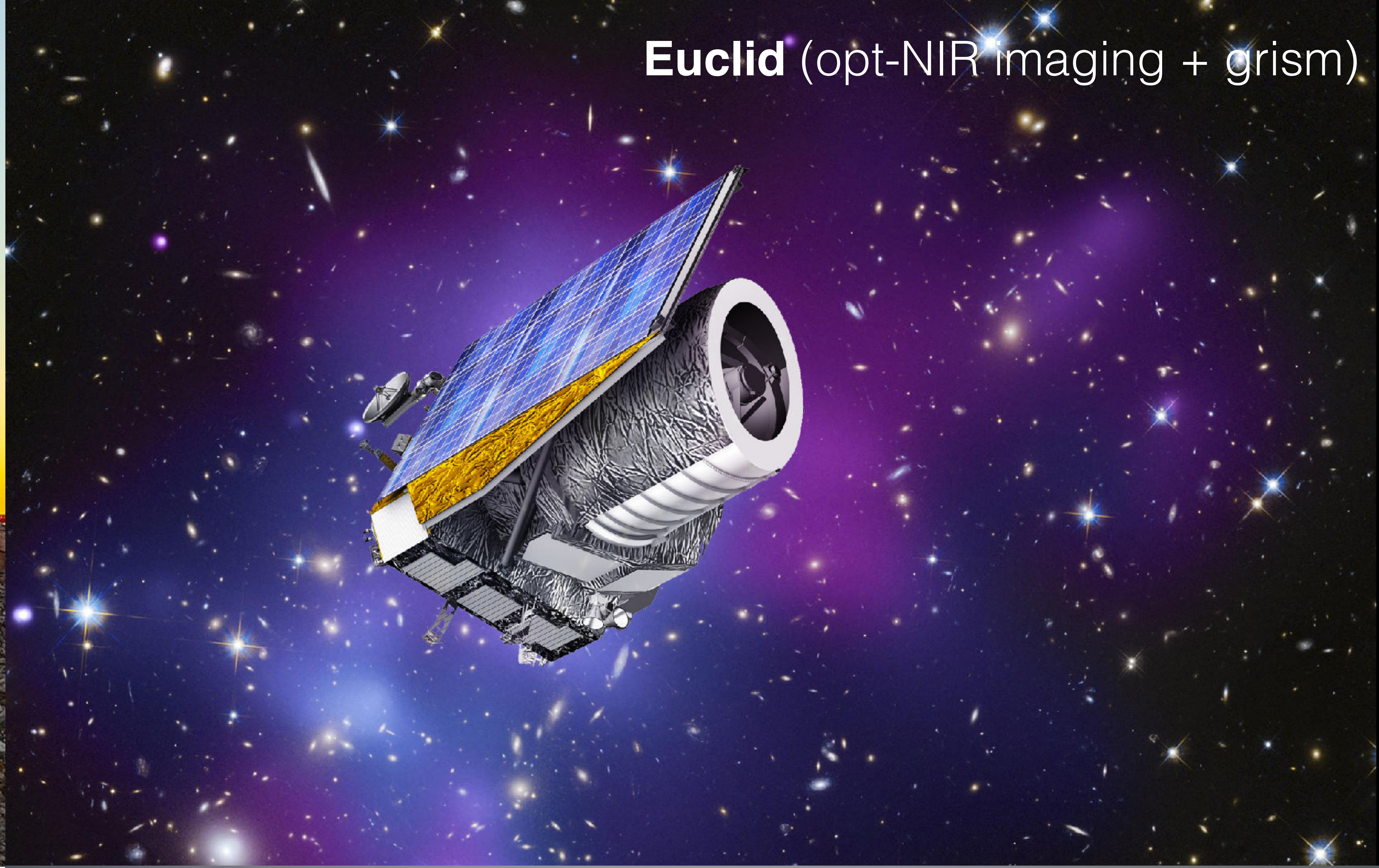
Euclid (opt-NIR imaging + grism)

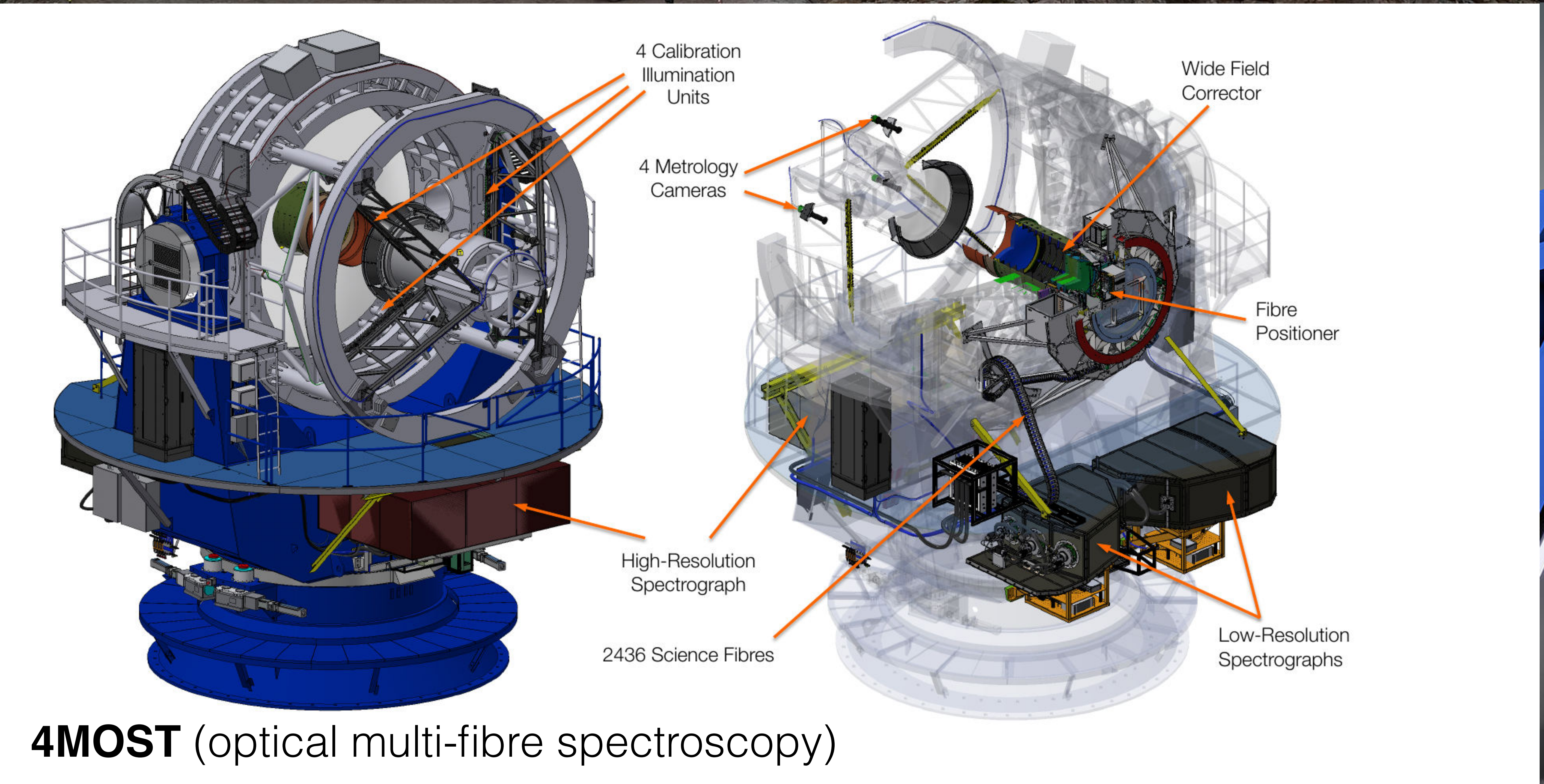
4 Calibration Illumination Units
4 Metrology Cameras
Wide Field Corrector
Fibre Positioner
High-Resolution Spectrograph
2436 Science Fibres
Low-Resolution Spectrographs
4MOST (optical multi-fibre spectroscopy)

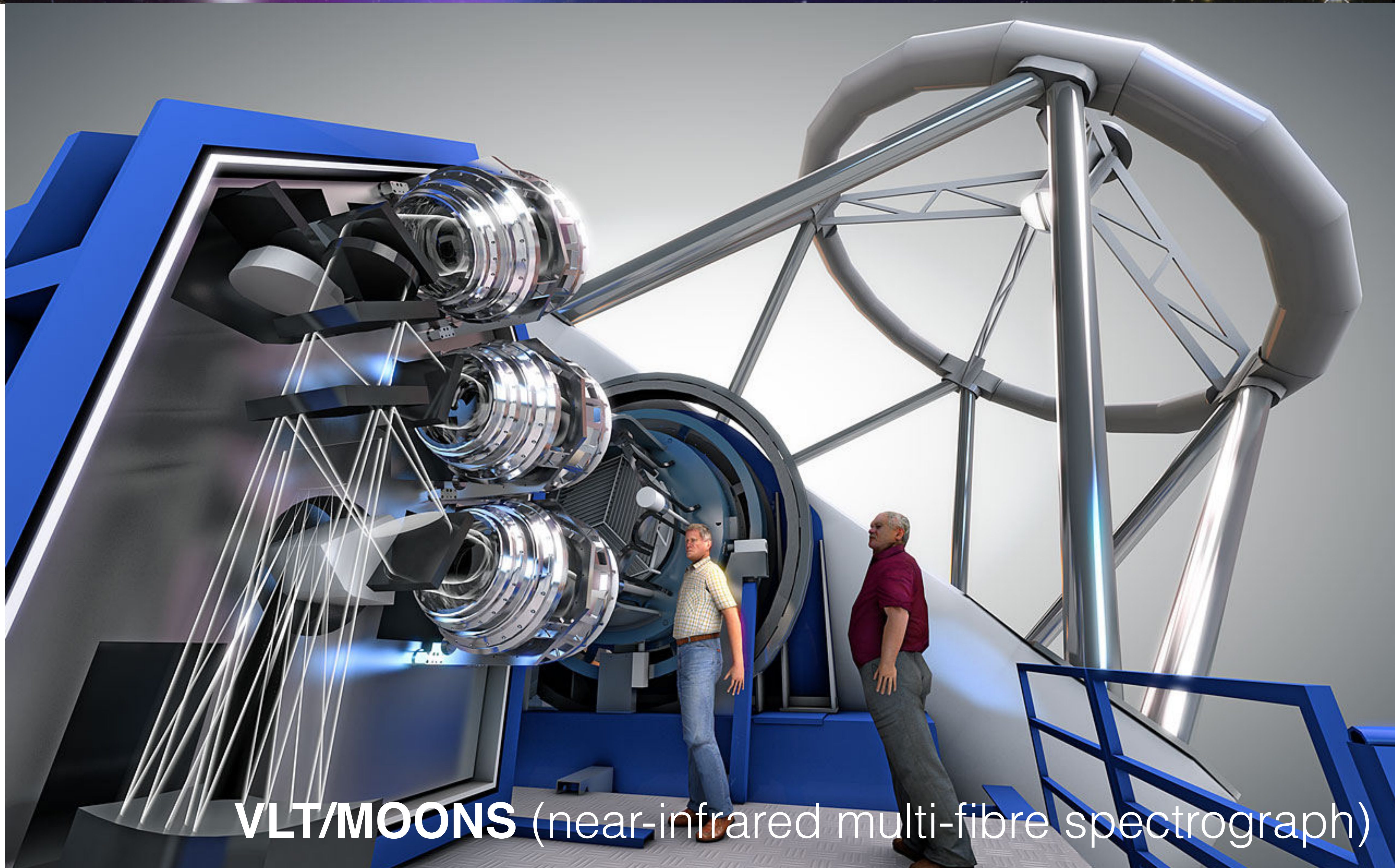
VLT/MOONS (near-infrared multi-fibre spectrograph)

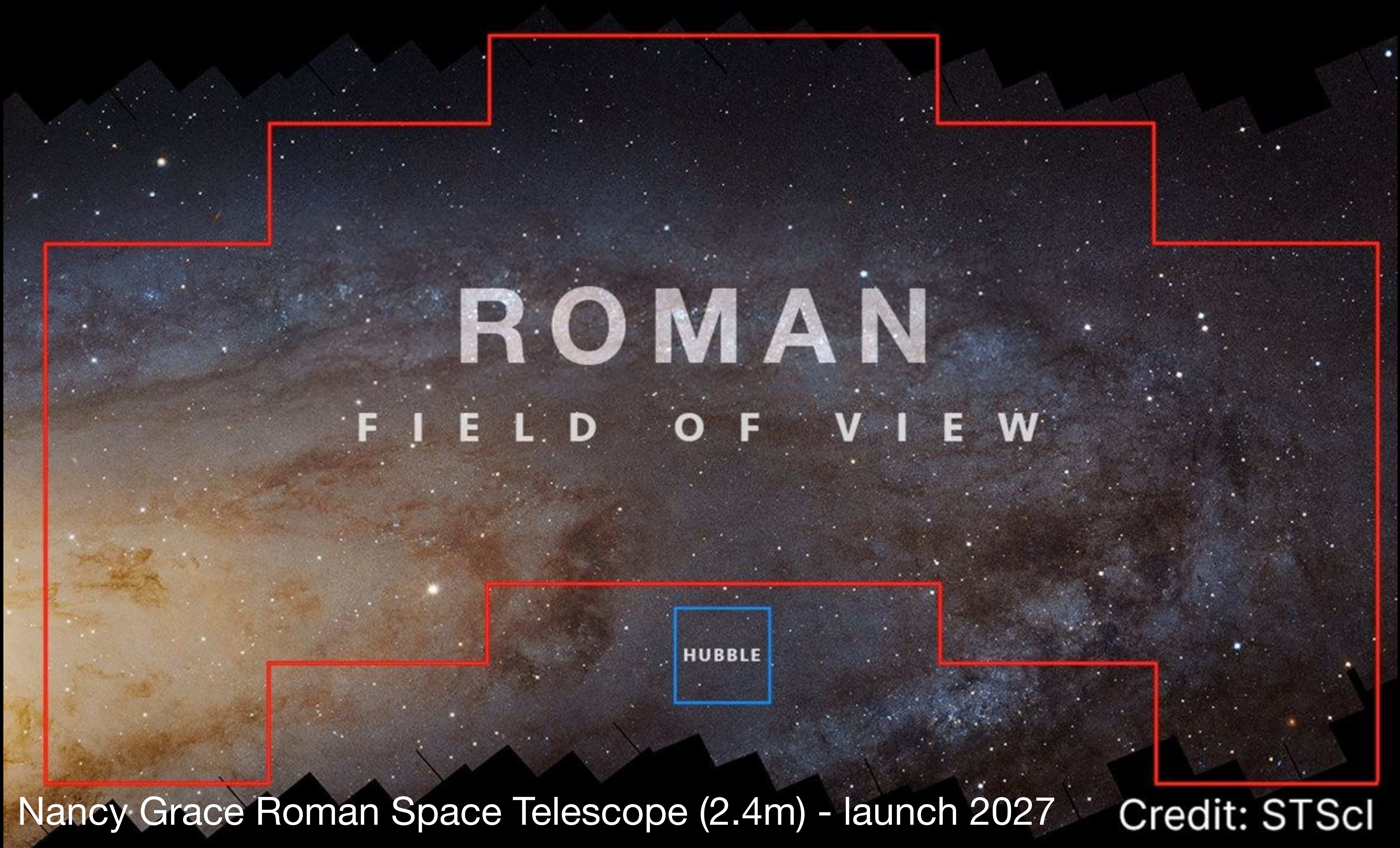

Nancy Grace Roman Space Telescope (2.4m) - launch 2027

Credit: STScI

Building galaxies

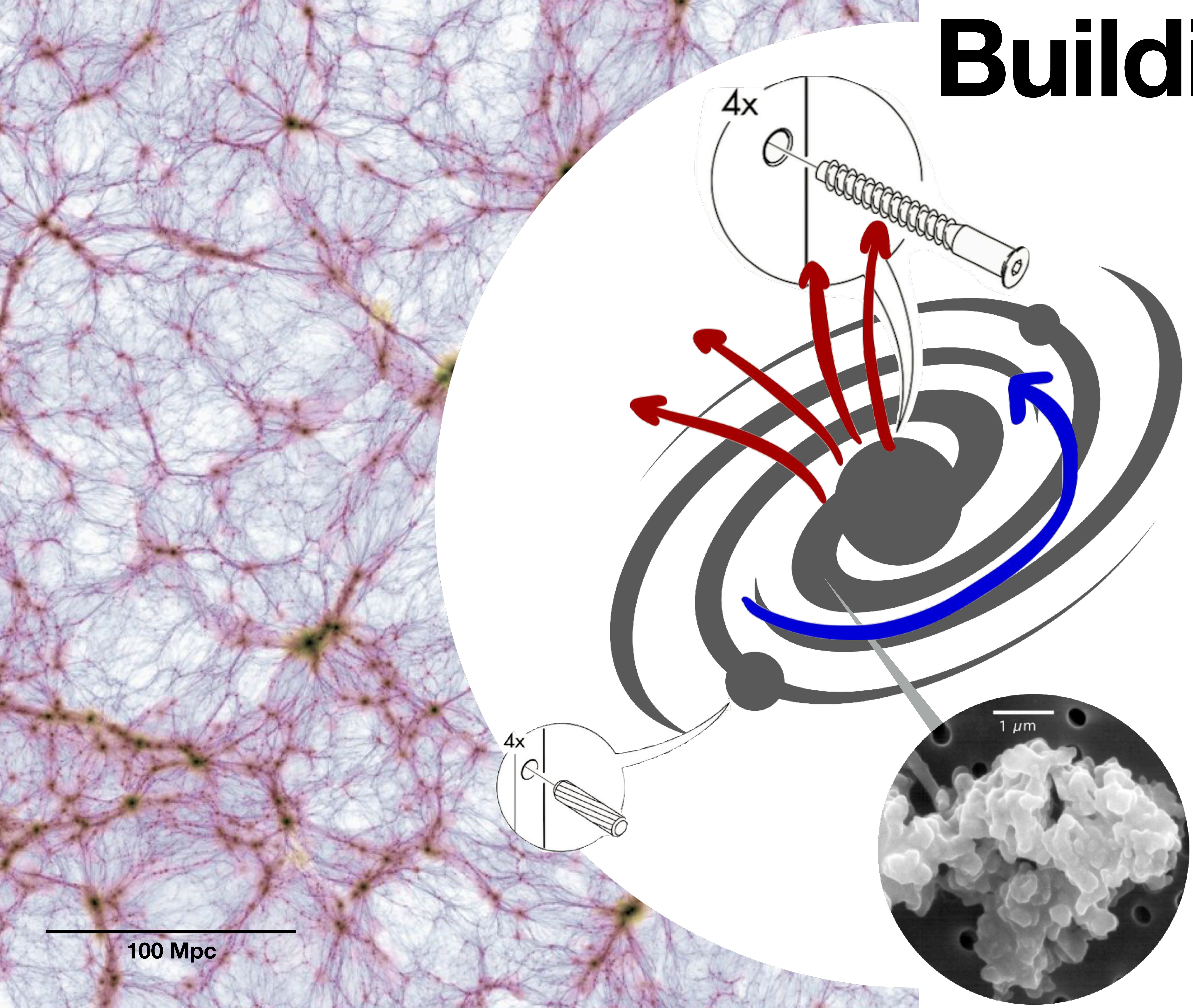

- Multi-scale
- Resolution
- Direct observables
  ≠ physical components